A REFRACTION SEISMIC SURVEY OF MARTINIQUE BEACH: GEOMETRY AND SIGNIFICANCE TO BARRIER BEACH EVOLUTION.

Gordon N. Oakey

Submitted as partial requirement for the completion of an Honours Bachelor of Science Degree in Geology.

Dalhousie University

March,1985

Distribution License

DalSpace requires agreement to this non-exclusive distribution license before your item can appear on DalSpace.

NON-EXCLUSIVE DISTRIBUTION LICENSE

You (the author(s) or copyright owner) grant to Dalhousie University the non-exclusive right to reproduce and distribute your submission worldwide in any medium.

You agree that Dalhousie University may, without changing the content, reformat the submission for the purpose of preservation.

You also agree that Dalhousie University may keep more than one copy of this submission for purposes of security, back-up and preservation.

You agree that the submission is your original work, and that you have the right to grant the rights contained in this license. You also agree that your submission does not, to the best of your knowledge, infringe upon anyone's copyright.

If the submission contains material for which you do not hold copyright, you agree that you have obtained the unrestricted permission of the copyright owner to grant Dalhousie University the rights required by this license, and that such third-party owned material is clearly identified and acknowledged within the text or content of the submission.

If the submission is based upon work that has been sponsored or supported by an agency or organization other than Dalhousie University, you assert that you have fulfilled any right of review or other obligations required by such contract or agreement.

Dalhousie University will clearly identify your name(s) as the author(s) or owner(s) of the submission, and will not make any alteration to the content of the files that you have submitted.

If you have questions regarding this license please contact the repository manager at dalspace@dal.ca.

Grant the distribution license by signing and dating below.

_____ _____

Name of signatory Date

DALHOUSIE UNIVERSITY
Department of Geology
Halifax, N.S. Canada B3H 3J5 Telephone (902) 424-2358 Telex: 019-21863

DALHOUSIE UNIVERSITY, DEPARTMENT OF GEOLOGY

B.Sc. HONOURS THESIS

Author:

Title:

Date: April 4, 1985

Table of Contents

ABSTRACT

During the summer of 1984 a refraction seismic survey was conducted at Martinique Beach using a 12 geophone array and seismic recorder with a hammer plate as the acoustic source. Sixteen sites were occupied along the 3.5 km beach with geophone sounding lines varying in length from 15 m to 50 m in order to examine the stratigraphy and depth of the bedrock. Current theories based upon nearshore marine seismic reflection profiles and coastal barrier coring indicate that barrier beaches on the Eastern Shore of Nova Scotia, such as Martinique Beach, exist at the mouth of Pleistocene channels. These channels resulted from scouring of till and the Meguma Group acoustic basement by glacial ice and meltwater. To date, no seismic measurements on beaches have been made to extend nearshore data shoreward. The present survey was designed to determine whether significant variability in sediment thickness, indicating a bedrock channel, exists at Martinique Beach. From each of the sites, the sound velocity data were analyzed to determine depth to the boundary between unconsolidated sediments and the acoustic basement. Quantitative results presented in this thesis indicate that from Whale Point to the mid-beach outcrop the average bedrock depth is approximately 15 m. From the midbeach outcrop to Flying Point further east, however, results indicate a 20 m deep bedrock channel of less than 0.5 km in width. Such a relatively narrow, deep channel provides strong speculative evidence for differential erosion as a result of glacial processes and is consistent with current theories of the location of beaches such as Martinique.

1: INTRODUCTION

1.1: Applications

Refraction seismic surveying was the first geophysical method used in oil exploration. Advancement in reflection seismic techniques has caused a dramatic decrease in the general use of refraction seismics in the oil industry. Refraction methods have been used recently in deep crustal profiling as well as in civil engineering to measure overburden thicknesses. The field techniques and data processing are generally simple. However, meaningful interpretations from the field data require careful experimental design from an estimation of the site conditions as well as a good understanding of the limitations of refraction methods.

The refraction method involves the measurement of travel times of the compressional waves at known distances from an acoustic source. The times of arrival are measured relative to the "zero-time" of the explosive impulse. Commonly the energy source is a small explosive charge or a mechanical source such as a sledge hammer striking a steel plate. Although the acoustic pulse from a mechanical source is generally much lower in amplitude than an explosive source, repeated shots and stacking of data can remove this problem. The arrival times and distances from the shot point are then manipulated to calculate velocities, depths, and slopes.

1.2: Theory

The propagation of seismic energy through subsurface layers is described by essentially the same rules that govern the propogation of light. The refraction of the sound wave, as described by Snell's Law, depends upon the ratio of the sound velocities in each layer (Fig.1.1).

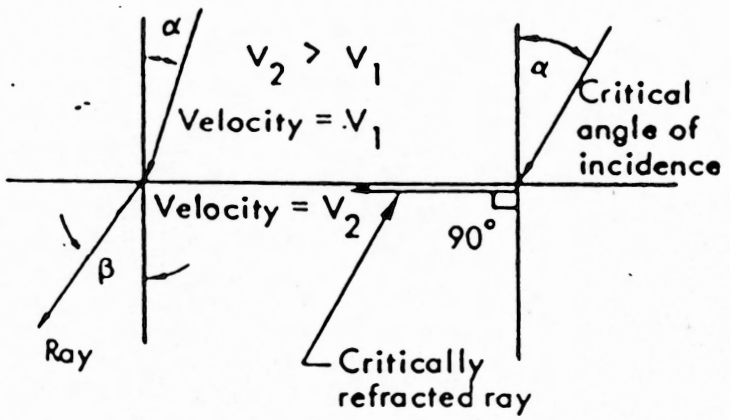

Snell's Law: $\frac{\sin\alpha}{\sin\beta} = \frac{V_1}{V_2}$

Critical incidence occurs when $\beta = 90°$, i.e.,

$\sin\alpha = V_1/V_2$

Figure 1.1 Definition of Critical Angle (Redpath 1973).

Critically refracted rays travel along the interface, producing a wave-front with ray paths travelling upwards at the same critical angle. The arrival times measured are a combination of an acoustic pulse travelling only in the upper layer (direct wave) and a refracted pulse. The arrival times of the direct wave depend on the velocity of sound in the upper layer and the distance from the shot point. The refracted wave is dependent on the critical angle and the depth to the interface. Using graphical techniques for manipulating the data, several values become important (Fig.1.2).

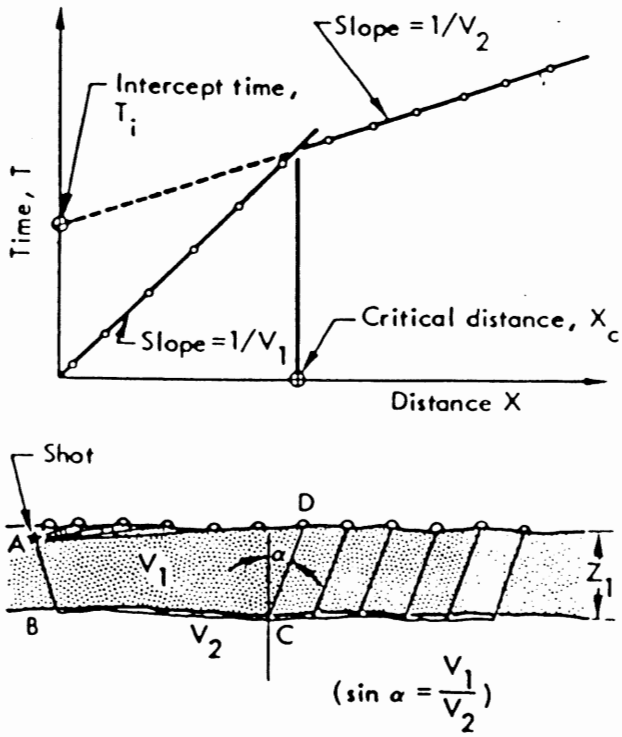

Figure 1.2 Simple two layer model and corresponding time-distance curve (Redpath 1973).

To calculate the thickness of layer 1, the formula, derived from Snell's Law is:

$$Z_1 = \frac{(T_{i2}) V_1}{2 \cos \{ \arcsin (V_1 / V_2) \}}$$

If there are more than two layers, the derivation to calculate thickness becomes more complicated. For a three layer model :

$$Z_2 = \frac{\left[T_{i3} - T_{i2} \dfrac{\cos \{ \arcsin (V_1 / V_3) \}}{\cos \{ \arcsin (V_1 / V_2) \}} \right] . V_2}{2 \cos \{ \arcsin (V_2 / V_3) \}}$$

where Z_J is the thickness of layer J,

V_J is the velocity in layer J,

and T_{iJ} is the intercept time for velocity J,

where J = 1,2,3 .

- Dipping Interface

In most real situations, interfaces parallel to the surface are uncommon. Therefore using the dipping interface model is a more realistic approach to processing the data (Fig.1.3).

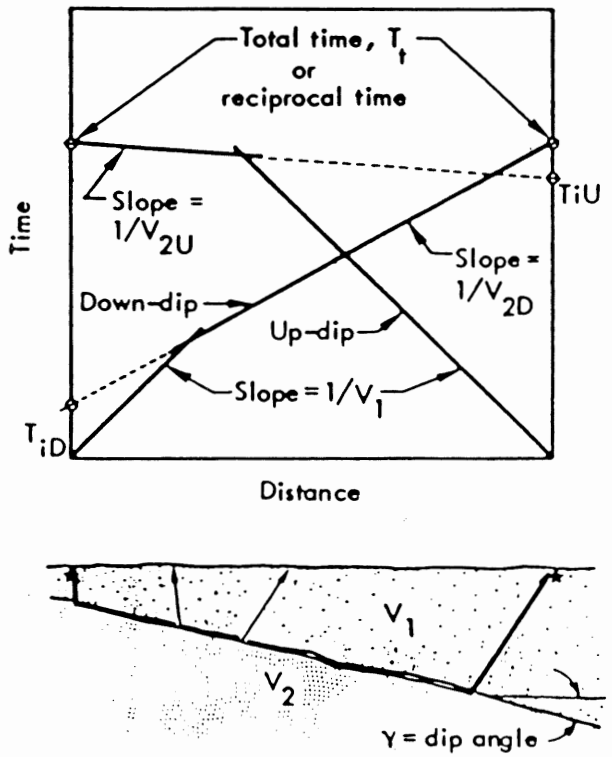

Figure 1.3 Dipping Interface. Reversed line showing different 'apparent velocities' (Redpath 1973).

If the shot point were placed at both ends, calculated values for V_2 would be quite different, resulting in erroneous depth calculations. To remove this problem, the dip of the interface must be calculated and a corrected velocity determined. The following formulae are used :-

$$DIP = (1/2).[\ ARCSIN\ (\ V_1\ /\ V_{2D}\ )\ -\ ARCSIN\ (\ V_1\ /\ V_{2U}\ )]$$

$$V_2 = \frac{2\ V_{2U}\ V_{2D}}{V_{2U} + V_{2D}}\ COS\ (\ DIP\ )$$

where the velocities V_J are defined in Fig.1.3. Using the true velocity, V_2, obtained above, the depths calculated from each end of the line are now the true perpendicular distances from the interface to each of the shot points.

1.3: Problems and Limitations

-Irregular surfaces:

The most apparent problem using refraction seismics is the scatter of data due to irregularities in the topography or non-linear interfaces (Fig.1.4).

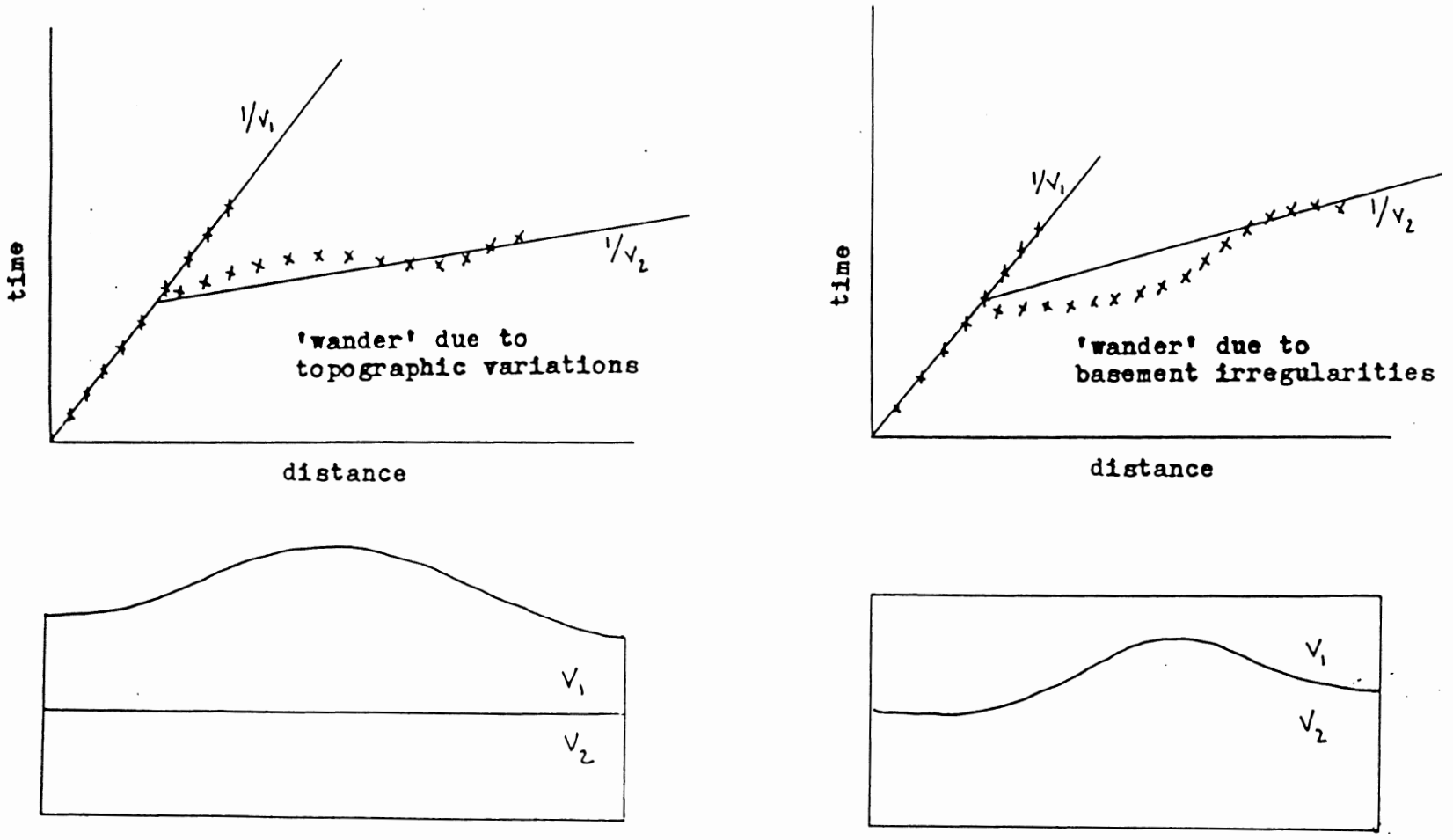

Figure 1.4 Effects of irregular surfaces on time-distance curves.

In this experiment, topograhpic changes are roughly zero, as all geophones were placed at the high tide line. Irregularities in the bedrock/sand interface are inherent and explain some isolated scatter. However, this interface is generally quite uniform and causes little problem.

-Low Velocity Zone:

One limitation of a refraction seismic survey is the detection of a Low Velocity Zone (Fig.1.5). The wave pulse, when hitting this layer, will not be critically refracted and will completely travel through the Low Velocity Layer. If a higher velocity layer is encountered, a wave pulse will return to the surface. If the thickness of this layer is great enough, a 'shadow zone' or data gap may occur before subsequent first arrivals are seen.

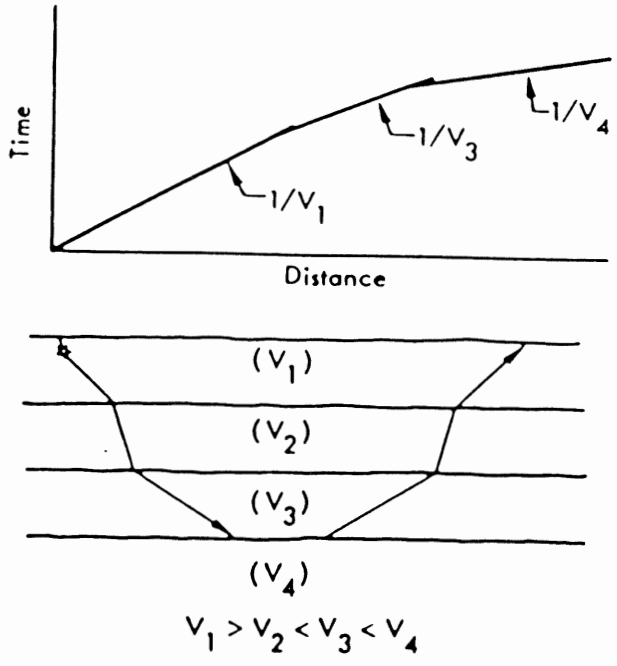

Figure 1.5 Effects of Low Velocity Zone (Redpath 1973).

-Thin Layer:

A second and more significant limitation to refraction seismics is the ability to detect a thin layer. This 'blind zone' or hidden layer is usually a medium velocity layer with an underlying high velocity layer (Fig.1.6).

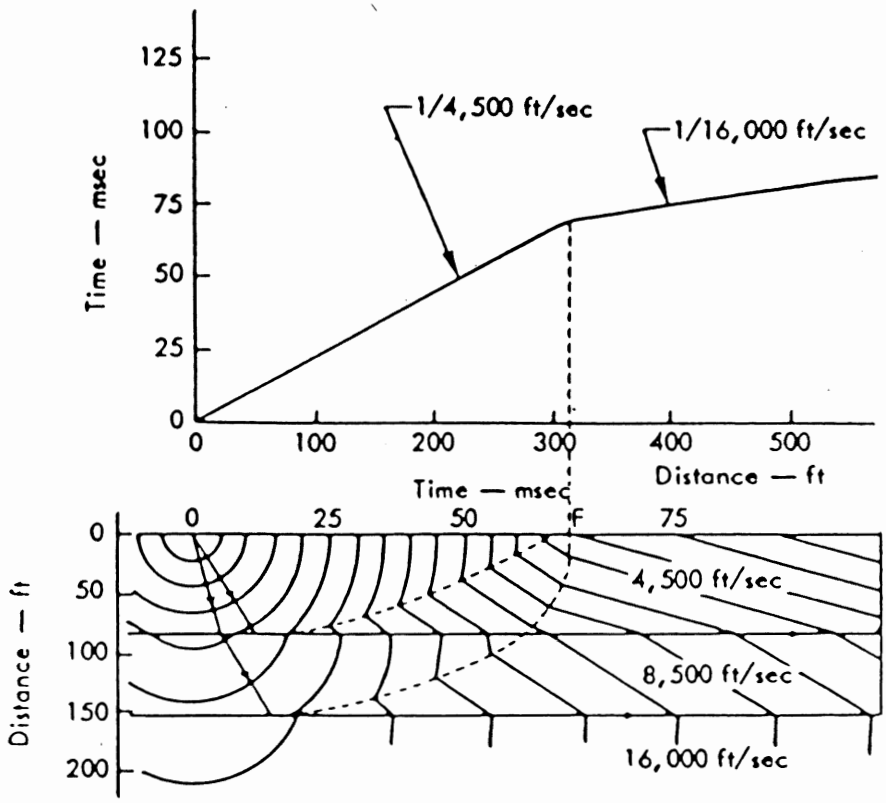

Figure 1.6 Occurence of a thin layer and the effects on time-distance curves (Redpath 1973).

A thickness calculated for the upper layer by standard techniques is a maximum, ignoring the possibility of a hidden layer. If the velocity contrast observed is great, and a hidden layer suspected, the following procedure may be used to calculate the maximum thickness of this undetected hidden layer.

The maximum thickness of layer ONE, $Z_1(max)$, is calculated using the time-distance plot. An assumption of the velocity (V_2) for the hidden layer must be made. A sound velocity value half-way between that of the upper and lower value is a good approximation, though several values may be tried. The following parameters are calculated.

$$A_{23} = \text{ARCSIN} (V_2/V_3)$$

$$A_{13} = \text{ARCSIN} (V_1/V_3)$$

$$A_{12} = \text{ARCSIN} (V_1/V_2)$$

$$S = \text{TAN} (A_{23}) / \text{TAN} (A_{13})$$

The values of A_{23}, A_{13} and A_{12} are plotted on the curves (Fig.1.7) to obtain a value of R. From the parameters $Z_1(max)$, A_{13}, A_{23}, S, and R the maximum thickness of layer TWO and the minimum thickness of layer ONE can be calculated. If these values are combined, a maximum total thickness can be obtained.

$$Z_2(max) = Z_1(max) \times (R \times S) / (R + S)$$

$$Z_1(min) = Z_2(max) / R$$

The maximum total thickness can be much greater than the thickness calculated for $Z_1(max)$. This drawback can seriously affect the reliability of a refraction seismic survey and can only be resolved by drilling.

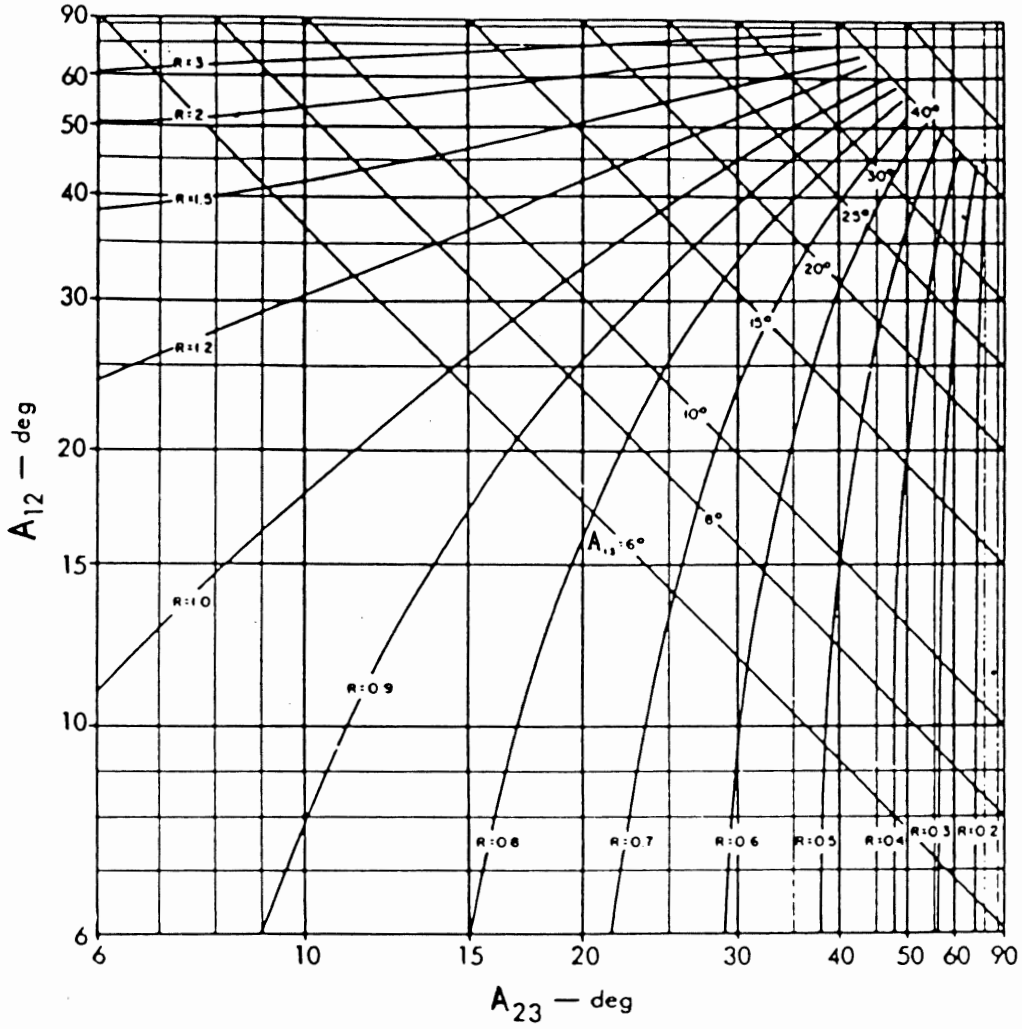

Figure 1.7 Curves used to calculate maximum thickness of Hidden Layer (Redpath,1973).

2: FIELD PROCEDURES

Martinique Beach is roughly 3.5 km in length from Whale Point in the west to Flying Point in the east (Fig.2.1). There is a minor point along the beach called the mid-beach outcrop. The width of the beach varies from roughly one hundred metres to several hundred metres near Whale Point where extensive estuarine tidal flats meet the main beach. Basement is outcropping at each of the headlands. The 1982 field-work at Martinique Beach by Yin Wang (1983) involved the placement of marked stakes at 100 m intervals starting with number one at Flying Point and ending with number thirty-two at Whale Point. Most of these stakes are still in situ though some have been burned by a grass fire. Sixteen stations were chosen with line centers approximately 200 m apart (Fig.2.2) with the aid of these stakes, physical measurements, and the use of air photos. Seven days of field-work were required to complete data collection at these stations. Due to the spacing of the stations and the length of the lines, no lines were run to measure the variations in the depth to bedrock with the beach width. This has been found to be reasonable as variation along the length of the beach is quite regular.

While doing such a survey, one was faced with the problem of using a suitable geophone spread for each station. To be able to substantiate internal detail within the sediment column, a high density of data is needed. This results in the necessity of a closely spaced line. From

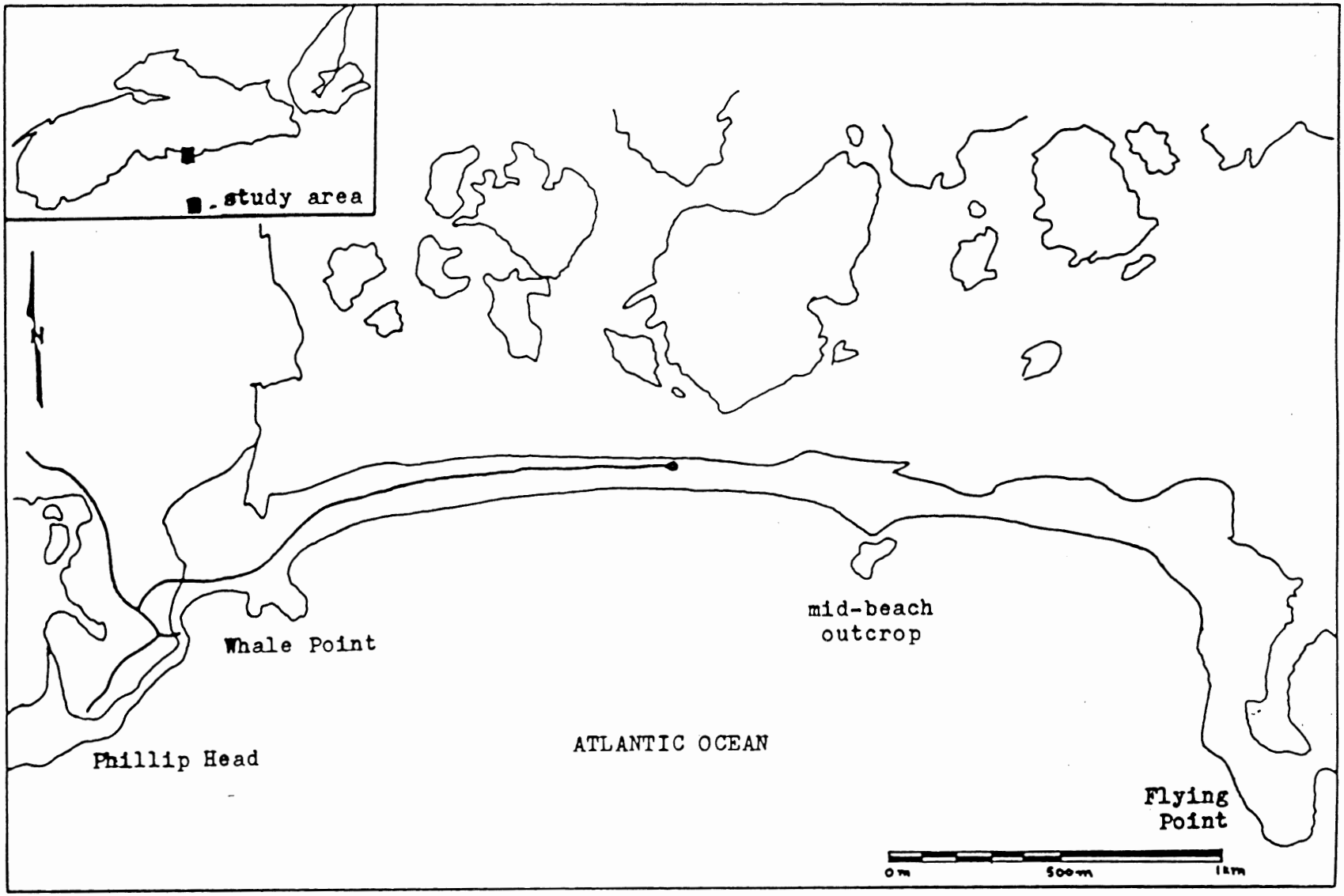

Figure 2.1 Martinique Beach

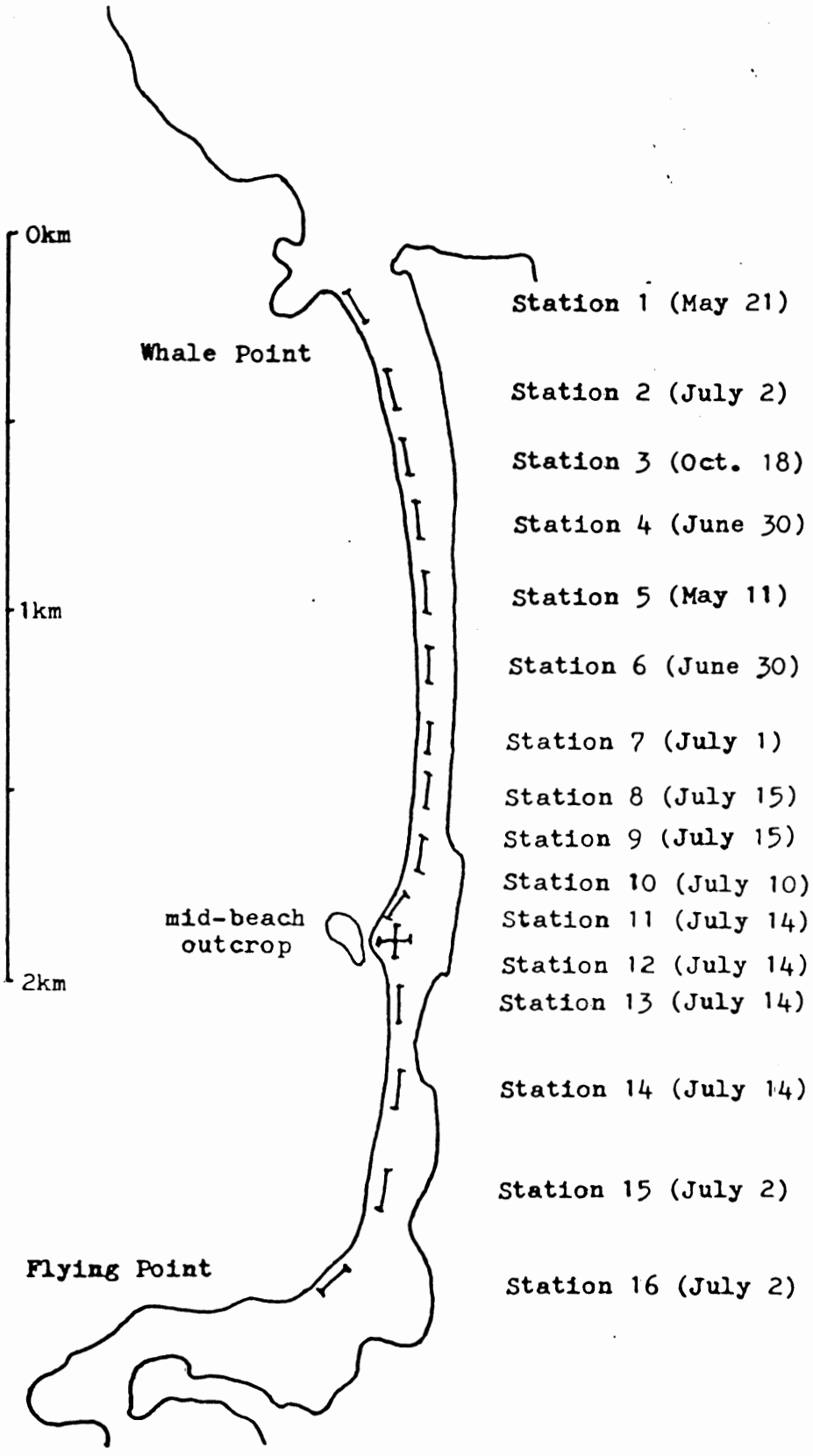

Figure 2.2 Position of stations on Martinique Beach as part of this investigation.

early lines, it was found that the sediment column is too homogeneous with respect to velocity characteristics to measure internal detail. Thus the primary field objective was to accurately determine the depth to bedrock yet still use a small geophone spread to retain high density data. Assuming that there were no great variations in depth to bedrock over short lateral distances, line lengths were shorter near the headlands and increased towards the center of the beach.

Two styles of data acquisition were used. Each has its own merit. The first procedure takes longer and the resulting data, although useful as a control, was of unnecessary detail for the required results.

2.1: Procedure 1

The geophones were placed at a 4 m to 6 m spacing. Shot points were located at both ends, usually at 5 m and 15 m. This allowed for the measurement of the gross sediment velocity as well as the basement velocity. Then the geophone spacing was changed to 1 m and shot points were at .5 m at both ends. This allowed for accurate determination of velocities within the upper few metres of sediment. However, only three unique velocity layers were measureable: a low velocity layer; a medium velocity layer (occupying the bulk of the sediment column); and the acoustic basement. From early trials, it was found that the upper low velocity layer was uniform in terms of velocity and thickness. As continuous measurement of this layer served no purpose, a second procedure was proposed.

2.2: Procedure 2

One line was used with a geophone spread varying from 3 m to 6 m. Shot points were placed at 5 m to 15 m from each end and a third shot point was placed in the middle of the line. This mid-line shot point allowed control over the velocity determination of the medium velocity layer. This is essential for such a refraction survey, as the accuracy of the upper layer velocities will control the accurate determination of the bedrock depth.

2.3: Equipment and Data Acquisition

All data were measured with an EG&G Geometrics Nimbus ES-1210F multichannel signal enhancement seismograph. This is a 12-channel digital seismograph which stacks successive shots until readable output has been obtained. The sound source used was a 15 pound sledge hammer hitting a steel plate. Several soundings had to be made for each trial. The data were recorded on a hard-copy printout after visual inspection of the video display.

Noise levels on the beach were quite high: waves, wind,and people being responsible for most of this. As the seismograph has variable gain for each channel, a null-noise level was obtained while still increasing the gain with distance from the shot point.

Seismic velocities vary with frequency. A standard of 100 Hz was used for all measurements (in the range of 30 Hz to 300 Hz). This frequency was originally recommended and was continued for consistency of the data.

A second factor in recording was the 'mode'. The seismograph has five 'modes': high pass, low pass, band pass, all pass, and band reject. These all have a corner frequency (as set by the frequency dial) and different acceptance 'windows'. For this experiment, a high pass mode was used, as there appeared to be an excess of low frequency noise (Fig.2.3).

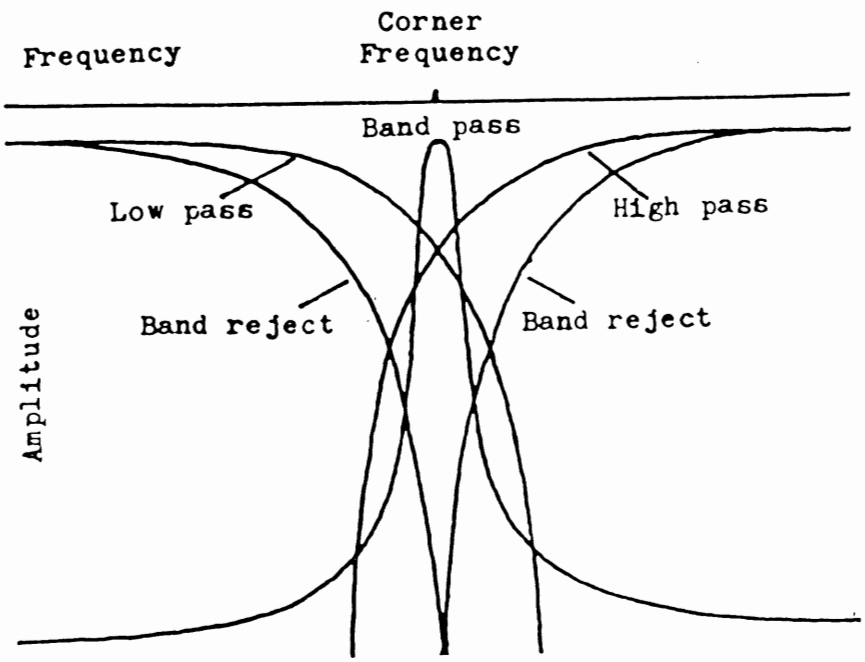

Figure 2.3 Amplitude of accepted signal as set by Mode and Corner Frequency.

3: DATA AND DATA PROCESSING

3.1: Defining of Points Picked from Printouts

During each trial a video display was used to monitor the quality of the data. Once first arrivals were apparent, a hard-copy of the data was produced. The hard-copy showed a poor resolution whereas the resolution of the display is significantly better. The printouts were marked, showing the first arrivals with aid of the video display.

In most trials, a 200 ms sweep time was used and printed on an extended printout. The values used for processing were visually picked from the printouts. The error in reading is roughly 0.5 ms.

Accurate reading of the printouts is critical for meaningful results. Generally, first arrival times are chosen, as they represent the arrival of the refracted wave front. Unfortunately, due to the physical characteristics of the signal wave, the first arrival is often quite low in amplitude and hard to pick out. Because of this, second arrivals or first rarefaction peaks may be used if accurately converted to first arrival times.

3.2: Quality of Data

-Repeatability:

Once problems of noise had been eliminated, the repeatability was very good. Compared data from repeated trials shows an error of roughly 0.1 ms (Fig.3.1). The error in picking the data points is higher than this, thus possible errors in repeatability are ignored.

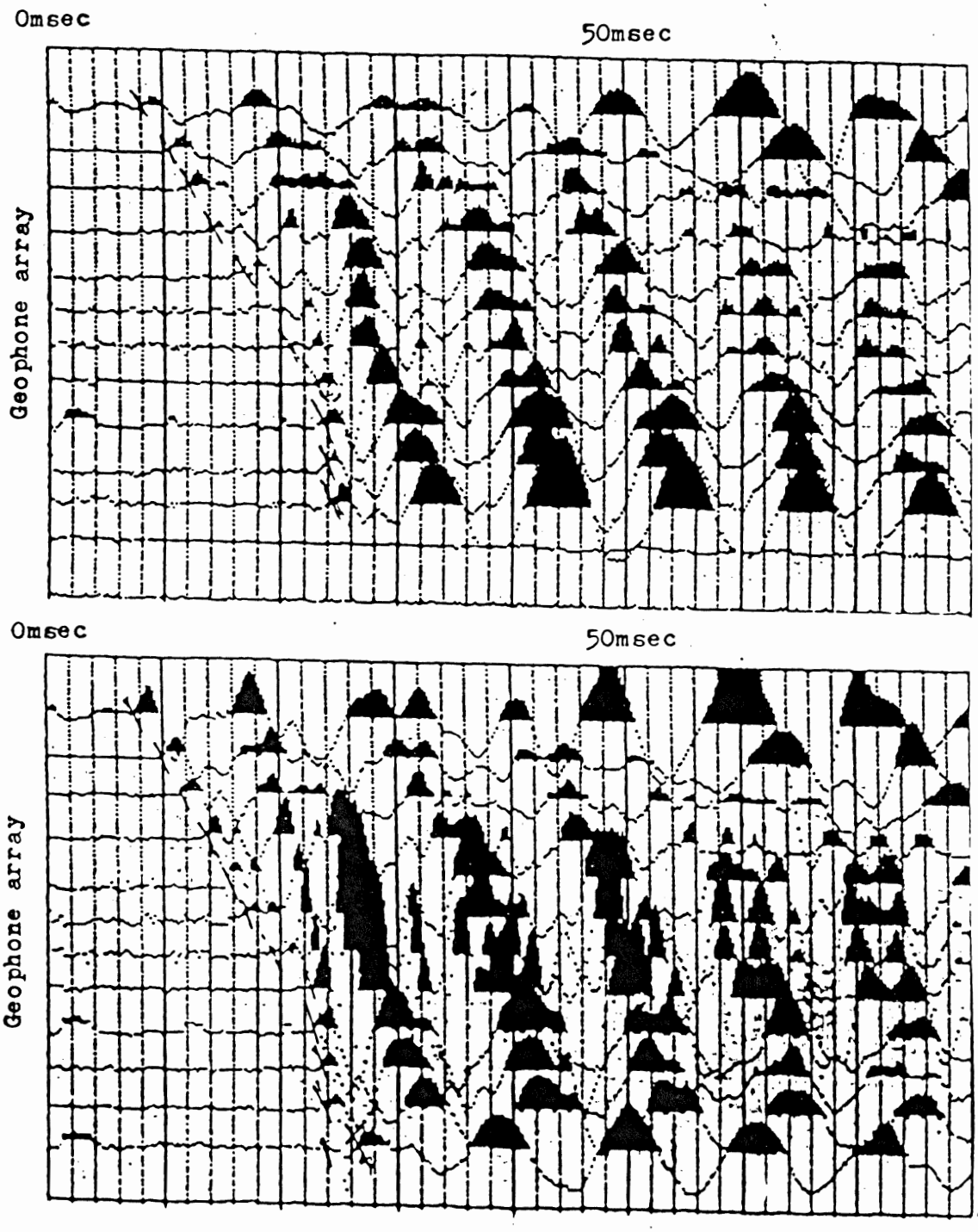

Figure 3.1 Repeated trials showing quality of data.

-Equipment Error:

Calibration of the seismograph using an external time source shows a sweep-time error of 5.6% (Fig.3.2) (values in Appendix 1). This time-error has been applied to the data set.

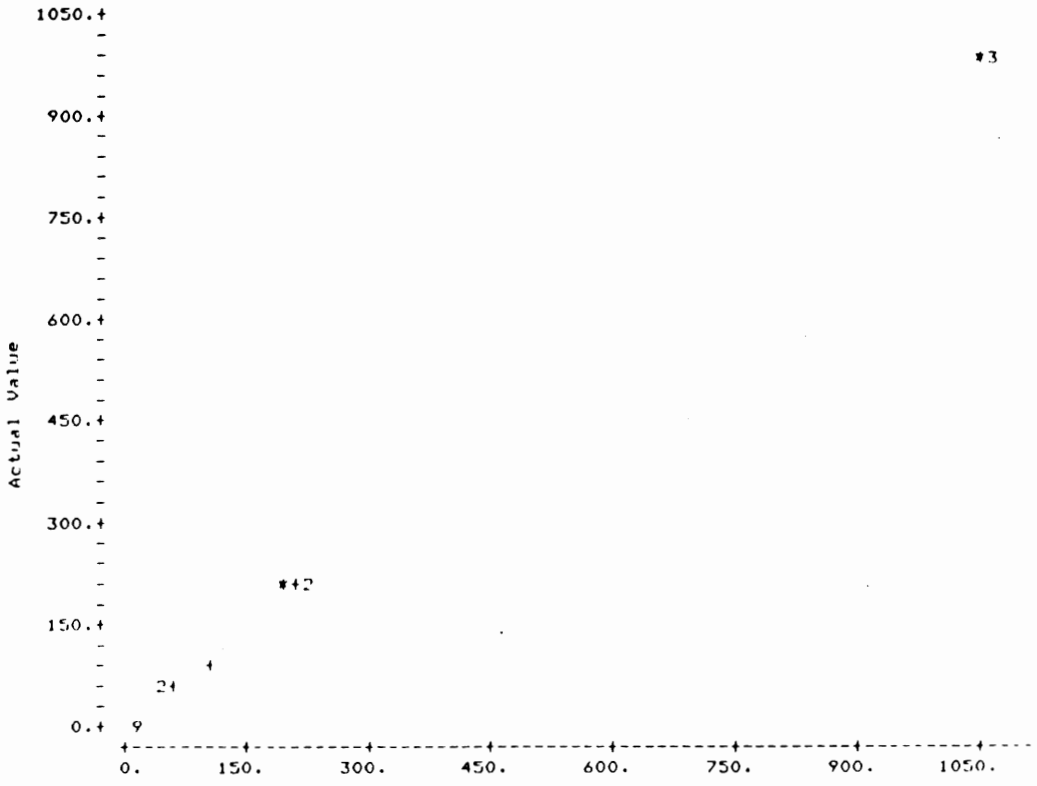

THE REGRESSION EQUATION IS
Y = .329 + 1.06 X1

	COLUMN	COEFFICIENT	ST. DEV. OF COEF.	T-RATIO = COEF/S.D.
	--	0.3290	0.4949	0.66
X1	C3	1.05718	0.00169	627.32

THE ST. DEV. OF Y ABOUT REGRESSION LINE IS
S = 3.042
WITH (55- 2) = 53 DEGREES OF FREEDOM

R-SQUARED =100.0 PERCENT
R-SQUARED =100.0 PERCENT, ADJUSTED FOR D.F.

ANALYSIS OF VARIANCE

DUE TO	DF	SS	MS=SS/DF
REGRESSION	1	3640734	3640734
RESIDUAL	53	490	9
TOTAL	54	3641225	

Figure 3.2 Plot of calibration data and output from regression program showing sweep error.

3.3: Data Formatting

Digital values taken from the printouts were converted to a standard format:

```
16      1     10.0  4.0  24.0  0.0123  2
 :      :      :     :     :     :     :
 :      :      :     :     :     :     layer
 :      :      :     :     :     :
 :      :      :     :     :     time
 :      :      :     :     :
 :      :      :     :     distance
 :      :      :     :
 :      :      :     spread
 :      :      :
 :      :      shot point distance
 :      :
 :      position (east-west)
 :
 station
```

Using this format, all data are stored in one file for processing (Appendix 2).

3.4: Data Processing

The data were processed using MINITAB on the Dalhousie CYBER. Plots of the data were produced for visual inspection (Appendix 3) and the slopes and the intercepts were calculated using regression. With calculated velocities and intercepts (Table 1) for each station, a program was written to calculate depths to interfaces (Table 2).

Table 1

Station	V2E	V2W	V3E	V3W	I1E	I1W	I2E	I2W
1	1323.	1685.	3068.	3925.	.00591	.00733	.01033	.00978
2	1498.	1930.	3727.	4348.	.00855	.00964	.02517	.03349
4	1542.	1565.	4078.	2136.	.01755	.01782	.03349	.02104
5	1394.	1944.	4907.	4616.	.01694	.01782	.02649	.02435
6	1513.	1595.	5173.	4686.	.01107	.01118	.02637	.02489
7	1705.	1533.	2778.	3486.	.01393	.01320	.02270	.02967
8	1736.	1636.	4409.	6839.	.00927	.00881	.02103	.02539
9	1235.	1935.	2862.	5089.	.00851	.01069	.01730	.02177
10	1450.	1520.	5362.	4615.	.00801	.00851	.01989	.01788
11	1800.	1623.	3125.	5750.	.00496	.00472	.01034	.01662
13	1581.	2027.	6154.	3609.	.00522	.00733	.02328	.01755
15	1789.	1584.	5263.	5627.	.00894	.00854	.02552	.02890
16	1489.	1420.	4677.	3125.	.00875	.00759	.03142	.02019

Table 2

Station	V2	V3	Z1E	Z1W	Z2E	Z2W
1	1482.	3438.	.7	.9	4.9	4.1
2	1686.	4011.	1.1	1.2	16.0	21.9
4	1553.	2741.	2.2	2.2	15.8	7.7
5	1623.	4757.	2.1	2.2	13.7	11.7
6	1553.	4917.	1.4	1.4	15.3	14.2
7	1614.	3085.	1.7	1.7	10.8	15.8
8	1685.	5348.	1.2	1.1	13.1	16.7
9	1507.	3634.	1.1	1.3	8.9	11.2
10	1484.	4959.	1.0	1.1	11.2	9.6
11	1707.	4011.	.6	.6	6.1	11.0
13	1776.	4522.	.7	.9	16.9	11.3
15	1680.	5439.	1.1	1.1	16.8	19.6
16	1454.	3733.	1.1	1.0	18.1	10.9

where :

V = velocity
I = intercept
Z = thickness
E = East
W = West

4: RESULTS

4.1: Velocity Model

Two dominant interfaces result in the measurement of three distinct velocity layers. This three layer model is consistent throughout the length of Martinique Beach.

-Layer 1, the upper unit, is characterized by a velocity of 247 m/s determined using the combined data of all trials where a short (1 to 2m spacing) spread was used (Fig.4.1). From the combined data of all the relevent trials this velocity was determined with minimal error. Within a velocity table this velocity lies within the region of loose dry soils. The beach surface, several centimeters of loose dry sand, may be acoustically similar to that of dry soil, and would explain this velocity layer. Calculations of the thickness of this layer do not give a true representation of a uniform slab with this velocity, and only truly represents the depth to the next strong acoustic interface.

-Layer 2 is bounded on its upper surface by the tidal water level and is characterized by velocities ranging from 1300 m/s to 1700 m/s and falls within the range of water saturated sediments. This layer constitutes the bulk of the sediment thickness of the beach profile and is generally considered to have a uniform velocity throughout. It is between this layer and the acoustic basement that the presence of a hidden layer may be found.

-Layer 3, the acoustic basement, is a high velocity layer characterized by a large range of velocities (2500 m/s to 6000 m/s). Although this is a high range, the variation can be explained by the lack of data in some trials and by irregularities in the bedrock topography. The beach profile shows three bedrock highs, where Meguma Group bedrock is outcropping at each Point and the mid-beach outcrop. Between Whale Point and the mid-beach outcrop, the sediment thickness is about 12-15 m. Between the mid-beach outcrop and Flying Point, there is a deeper bedrock depression with approximately 20m of overburden (Fig. 4.2).

4.2: Reliability

As described in section 1, two potential sources of error in interpreting refraction seismic data are the presence of a low velocity zone or a hidden layer. For Martinique Beach, described by the above three layer model, these two effects are shown to cause little error.

A low velocity zone, found within this profile might be accounted for by lagoonal material buried as coastal regression occurred. This layer would likely be found within the layer of the refraction model but not be thick enough to produce any noticeable effects. A thickness of 1-2 meters is a reasonable estimate of such a layer, and would not introduce a substantial error in the calculated sediment thickness.

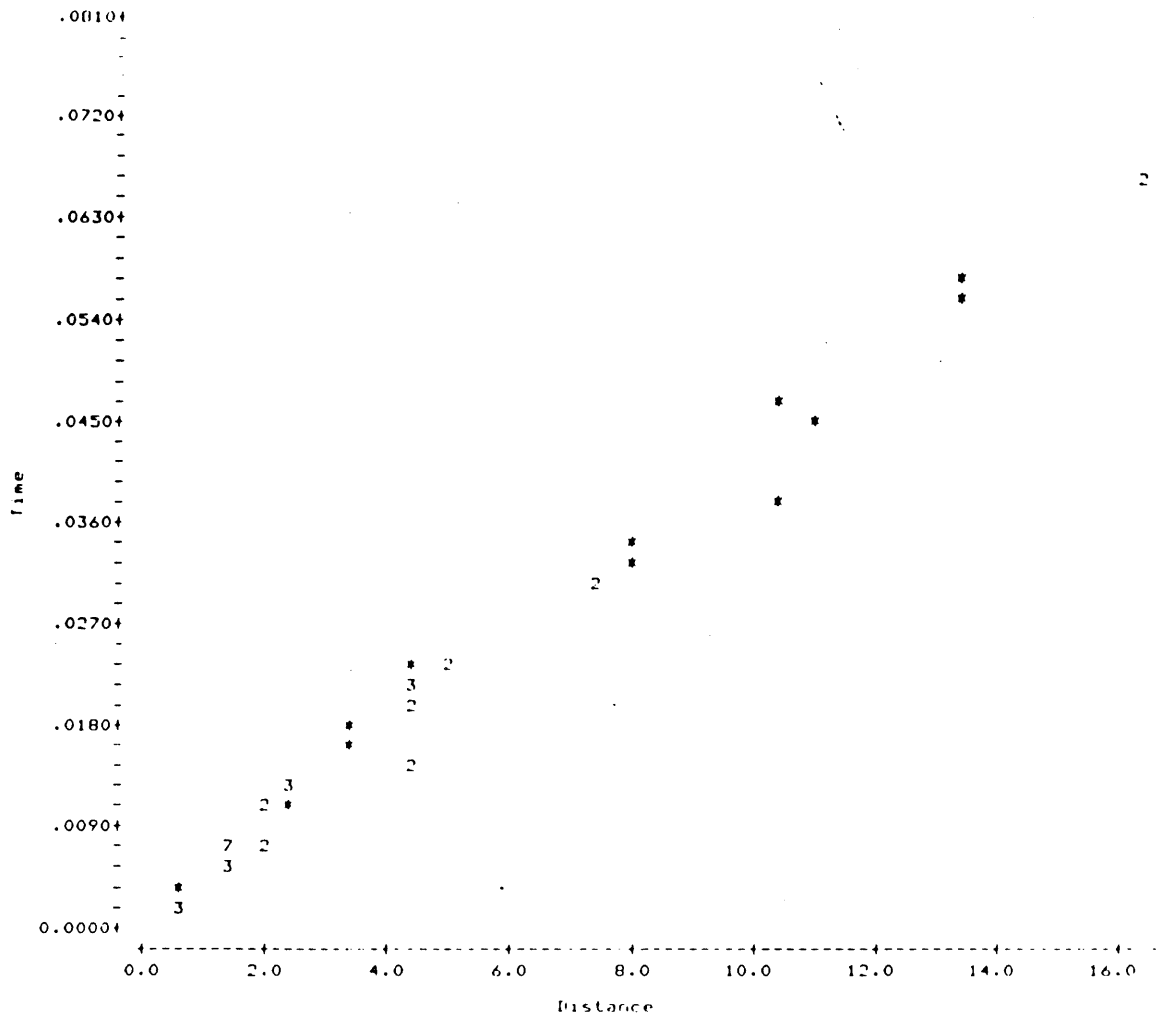


```
MTB > REGRESS C1 1 C2

THE REGRESSION EQUATION IS
Y =     .283 +  247. X1

                                        ST. DEV.     T-RATIO =
      COLUMN      COEFFICIENT          OF COEF.     COEF/S.D.
      --             -0.2826            0.1166         -2.42
X1    C2            247.448             4.436          55.78

THE ST. DEV. OF Y ABOUT REGRESSION LINE IS
S =  0.5044
WITH (  45-  2) =  43 DEGREES OF FREEDOM

R-SQUARED = 98.6 PERCENT
R-SQUARED = 98.6 PERCENT, ADJUSTED FOR D.F.

ANALYSIS OF VARIANCE

 DUE TO      DF            SS          MS=SS/DF
REGRESSION    1       791.7047          791.7047
RESIDUAL     43        10.9398            0.2544
TOTAL        44       802.6444
```

Figure 4.1 Calculation of velocity for layer ONE.

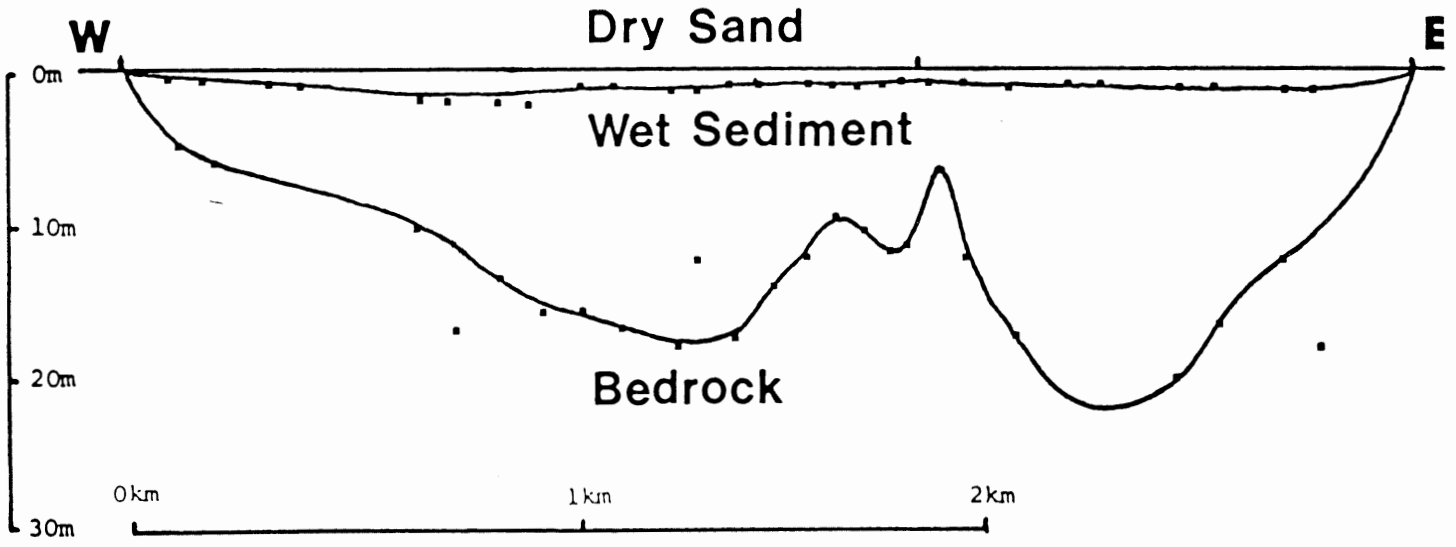

Figure 4.2 Profile of Martinique Beach.

A hidden layer may be postulated to exist between the wet sediment and the bedrock. The composition of this unit would likely be water saturated glacial till which would have an acoustic velocity (1800 m/s) only slightly greater than that of sand. From the procedure described in chapter one, an estimated thickness of this unit can be calculated. Using layer 2 having a velocity of 1500 m/s and a thickness of 12 m, and layer 3 having a velocity of 4000 m/s, the maximum possible thickness of this layer is 10 m , yielding a minimum thickness for layer 2 as 6.5 m and increasing the total sediment column by 1.5 m. The inability to measure detail is unfortunate, yet for this model results in minimal error in calculating the depth to bedrock.

4.3: Profiles

Four marine reflection seismic lines have been run close to Martinique Beach (Fig. 4.3). Profiles from these lines (Fig 4.4a & 4.4b) show the bedrock topography and the sediment overburden. The sediment overburden in this area is ablation till, estuarine sediment, and reworked coastal sand. The sediment cover thins seaward and is found primarily within bedrock 'lows'. The gross bathymetry is strongly controlled by the bedrock topography.

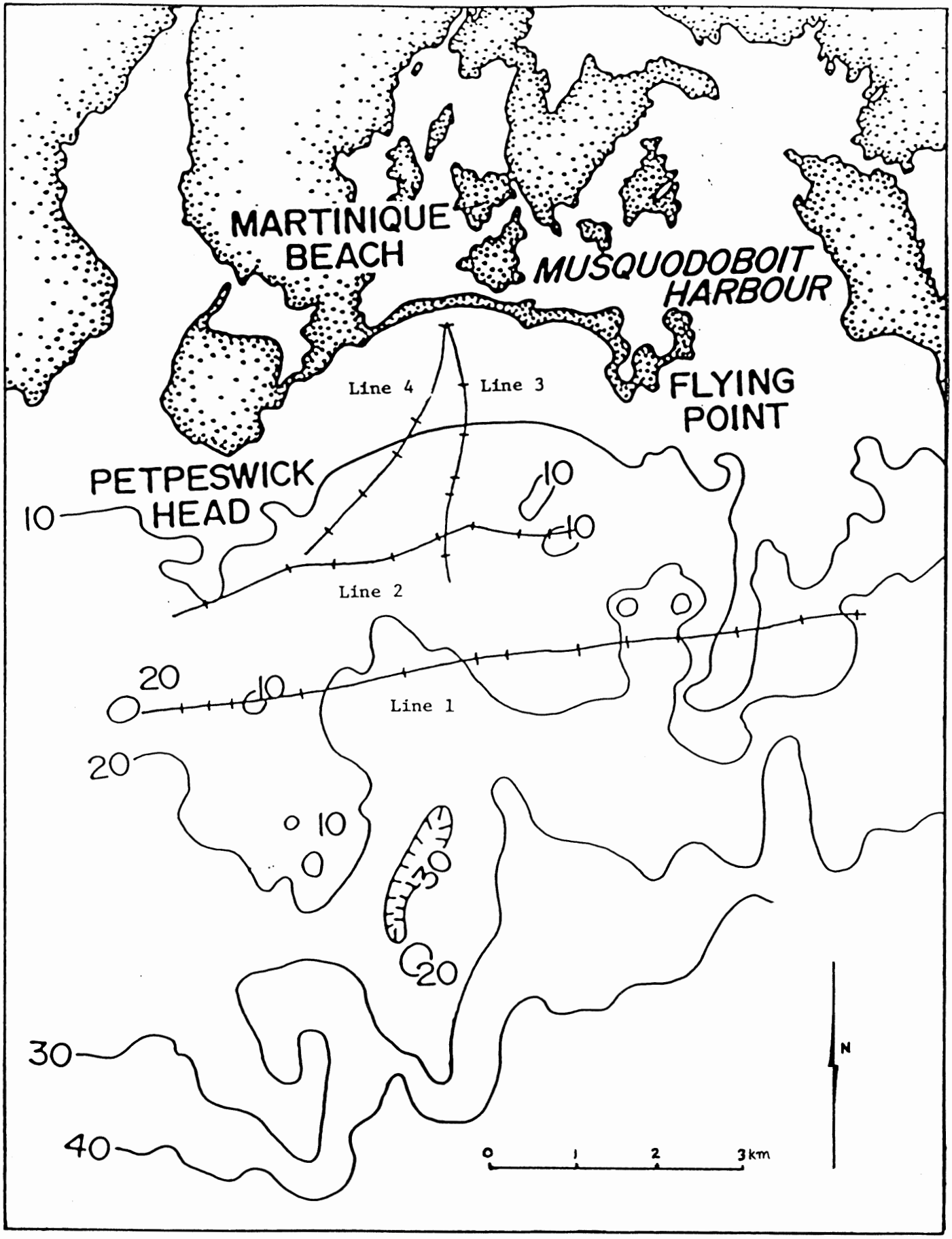

Figure 4.3 Position of marine reflection seismic lines.

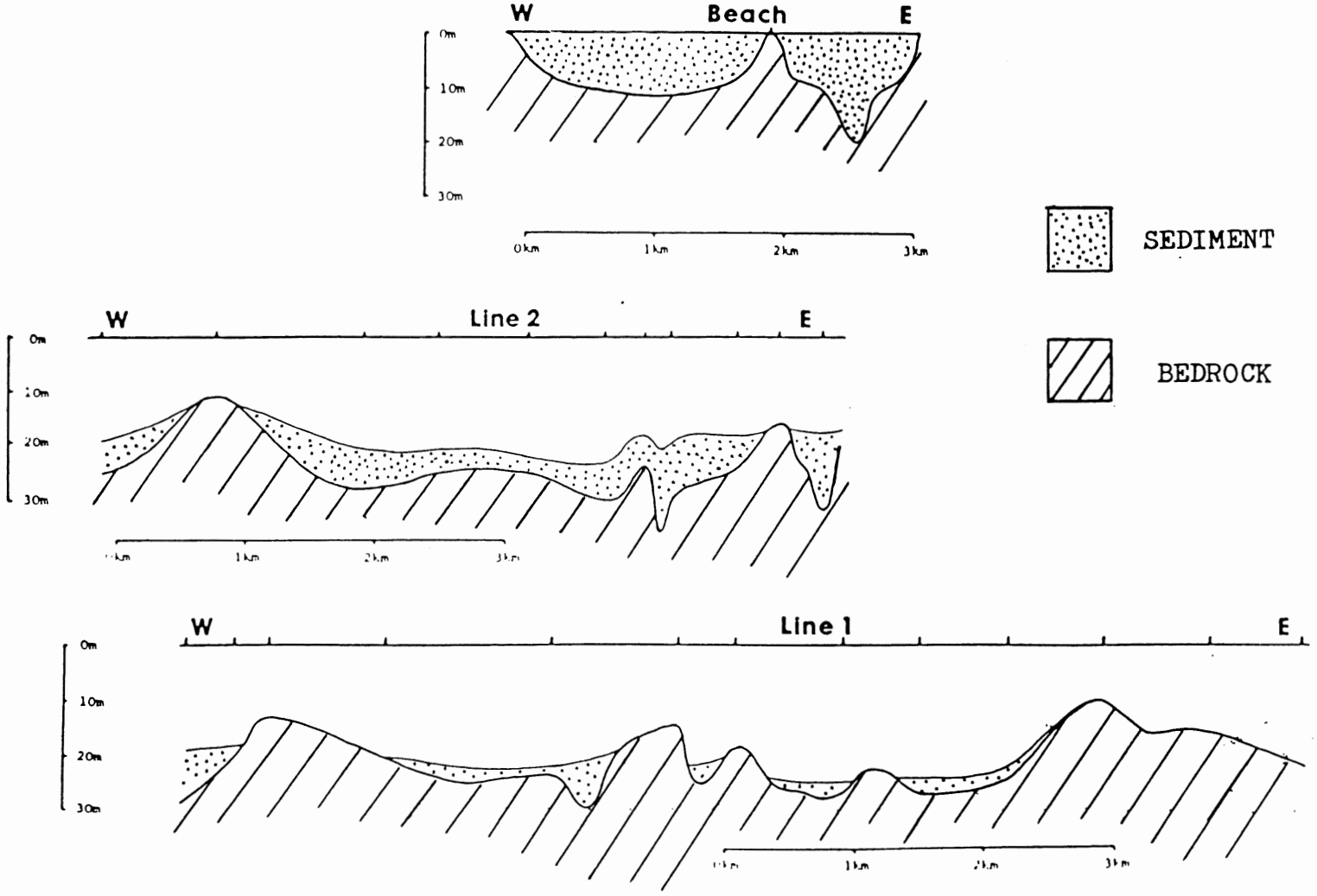

Figure 4.4a Marine seismic profiles parallel to Martinique Beach.

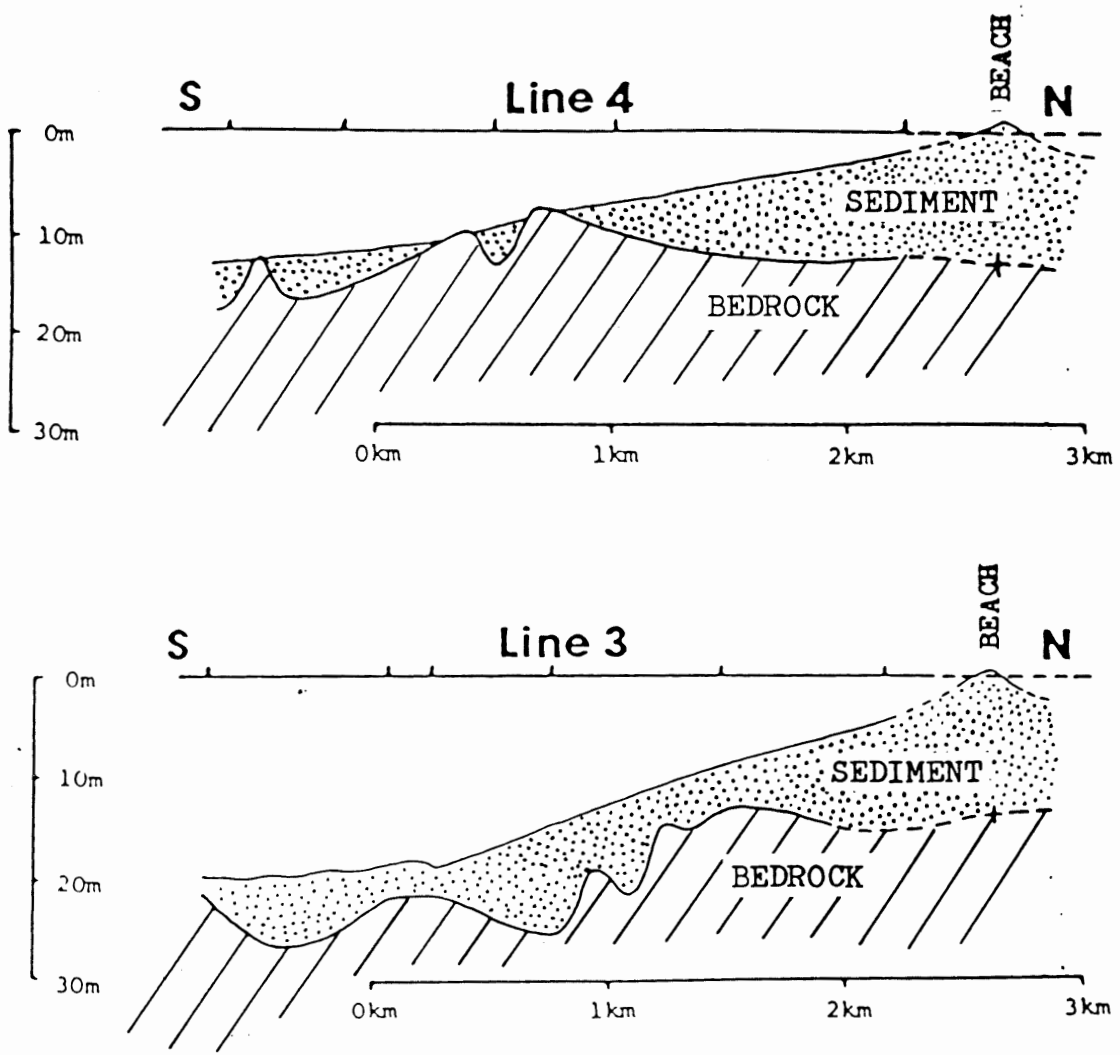

Figure 4.4b Marine seismic profiles perpendicular to Martinique Beach.

5: DISCUSSION

5.1: Environmental Setting

The Eastern Shore of Nova Scotia is a glacially influenced coastline presently experiencing a sealevel transgression. A six stage model (Fig.5.1) has been proposed to describe the genesis and evolution of the beaches found along the Eastern Shore (Boyd et. al. 1984).

-Stage 1 Several phases of glacial advance and retreat occurred during the Wisconsinan Period. The advancement of this ice sheet resulted in extensive scouring of bedrock due to localized differential erosion. Along the Eastern Shore of Nova Scotia, the bedrock is Meguma Group metasedimentary rock. The scour features are preferentially elongated Southeast parallel to the direction of ice movement. These features, generally one to five kilometers in width, have smaller internal topographic variations (scour channels) which are also parallel to the direction of ice movement.

During periodic glacial retreat, sheets of till were deposited as well as large fields of drumlins. These deposits were reworked by ice during periods of advancement and by meltwaters during periods of retreat.

The regional effect of this glacial ice mass was dramatic. It caused the depression of the continental crust under the ice and the production of a peripheral bulge. The effects of the migration of this glacial forebulge have been an important mechanism in the evolution of coastal processes.

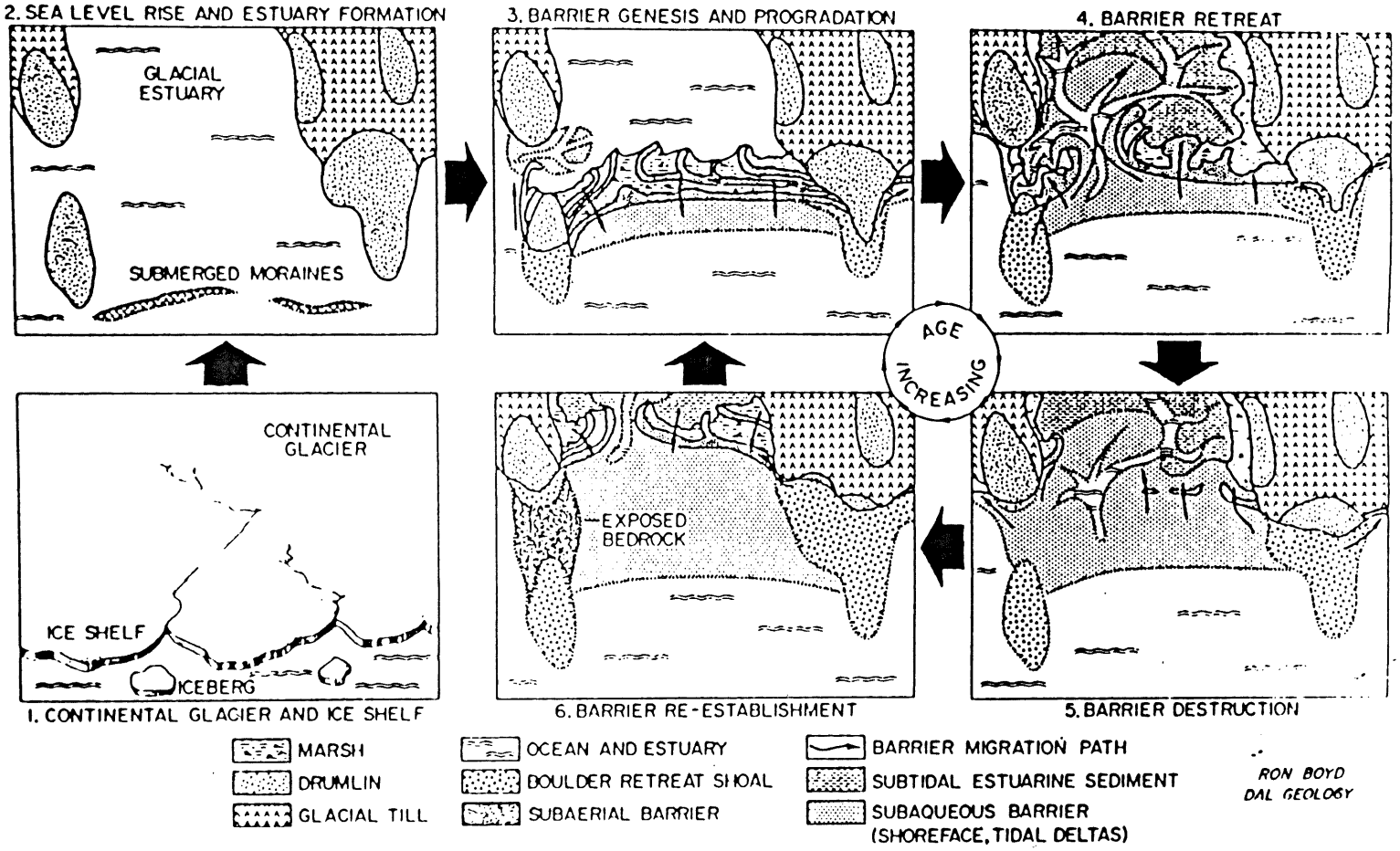

Figure 5.1 Six stage model describing the genesis and evolution of Barrier Beaches such as Martinique Beach (boyd et. al. in print).

-Stage 2 The removal of the ice mass caused the continental crust to rebound isostatically. The glacial forebulge moved shoreward causing an initial drop of relative sea level (RSL) followed by a rising RSL as the forebulge moved past the coastal area.

-Stage 3 The stability of these barrier beaches depends on the rate of sediment supplied compared to the rate of rising RSL and coastal wave energy. These conditions have changed over the last five thousand years causing repeated stages of barrier retreat, destruction, and re-establishment.

While RSL was rising, drumlins and ablation till were being quickly eroded by coastal processes. Large quantities of sediment were being deposited in the glacial estuaries where they were reworked by tidal, wave and wind action to form barrier beaches. When the rate of sediment input exceeds the effects of erosion, the barrier beaches prograde seaward producing advancing dunes or several dune ridges. Commonly the ends of the barrier beaches are anchored to drumlins, a local sediment source, or bedrock 'highs' which may once have been drumlins.

-Stage 4 When the rate of sediment input drops and is unable to sustain the beach, landward migration will occur as the beach is eroded, infilling the estuary with floodtide delta, tidal channels, and marsh sediments.

-Stage 5 The RSL continues to rise increasing the rate of barrier retreat.The large scale retreat of the barrier beach eventually leads to the destruction of the beach.

-Stage 6 The remnant beach, seen as intertidal shoals will stabilize further inland when drumlins or bedrock outcrop can anchor a new beach. The completion of the evolutionary cycle of the beach is reached as new sediment supplies combine with reworked remnants of the previous barrier system to produce a new beach.

5.2: Site Conditions

Martinique Beach has been used as a type example in describing barrier beaches. It is a double barrier beach anchored by Whale Point, the mid-beach outcrop, and Flying Point. The Musquodobit Harbour, one of the larger estuaries on the Eastern Shore, skirts the beach, running between Flying Point and Jeddore Head as bedrock outcrops at each of the headlands and several locations behind the beach within the marsh area. These bedrock outcrops can also be used to map bedrock topography and extrapolate its distribution from lines off shore to the beach profile (Fig.5.2). These trends show local variation of glacial scouring and eventually define the position of the barrier beach and the most stable position for drainage through the remnant glacial estuary.

There are three bedrock 'highs' extending seaward from Martinique Beach: one from Flying Point, another from the mid-beach outcrop, and a third from Whale Point. These

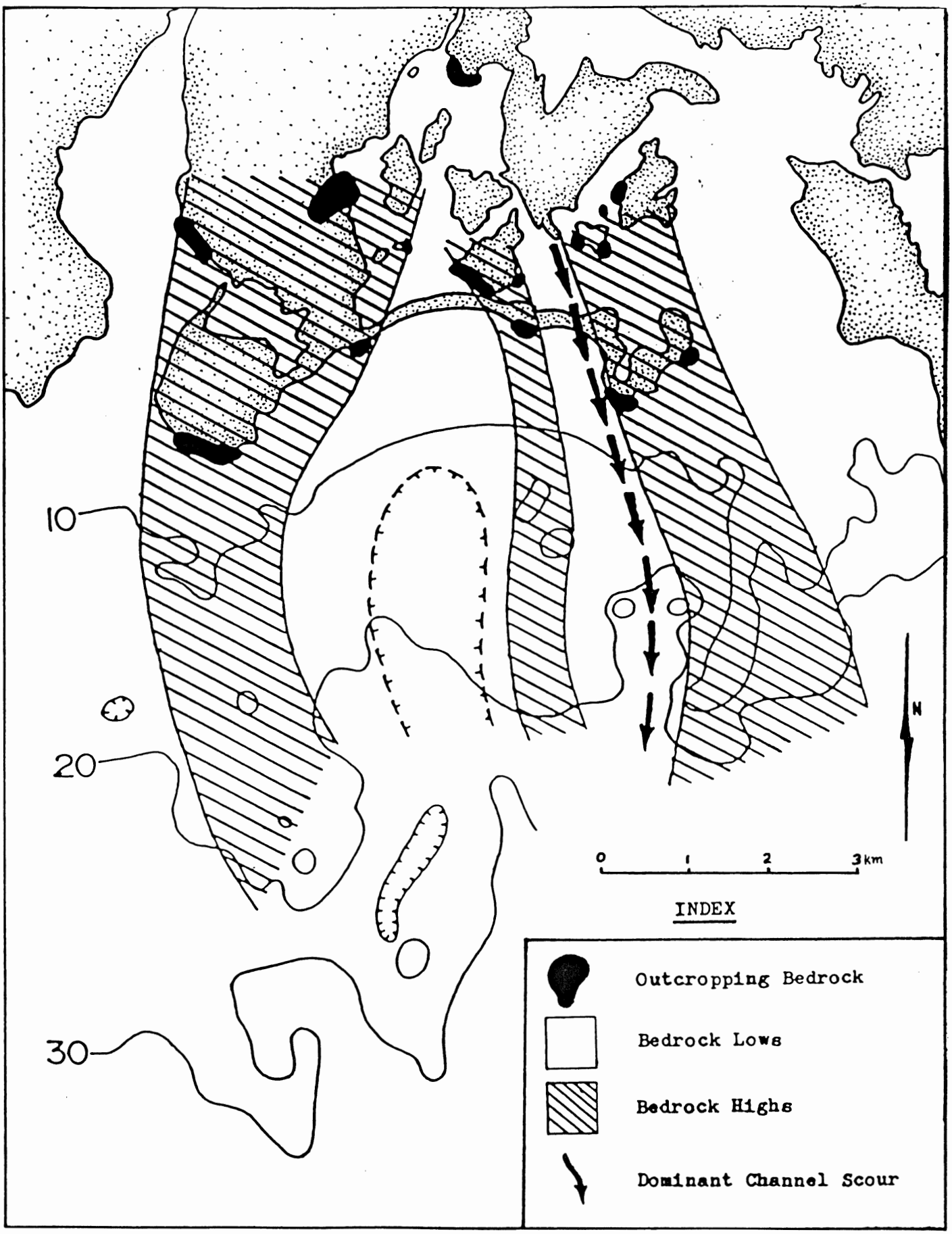

Figure 5.2 Regional bedrock topography showing bedrock 'highs' and scour channel.

'highs' can also be recognized from the bathymetry, as ridges which extend seaward from Whale Point and Flying Point. There are two bathymetric mounds seen as recognizable extensions of the mid-beach outcrop. The regional low between Whale Point and the mid-beach outcrop is a relatively uniform bedrock platform with only minimal scour features observed. Running parallel to the bedrock lineation from Flying Point, is a deeper scour feature, which cuts sharply through the beach profile and broadens as it is extended seaward.

5.3: The stability of Martinique Beach

Martinique Beach is presently in a stage of retreat placing it between Stage 4 and Stage 5 of the model. Washover features can be seen between the mid-beach outcrop and Flying Point where the dune has been breached. The position of the scour channel coincides with the position of the washover features. This thicker region of sediment may be less rigid and may partially explain the breaching of the dunes in this location.

As the RSL continues to rise the beach will be destroyed and a new beach will form further up the estuary. The formation of a new barrier beach is likely to occur within the same channels as the present beach and anchored to shoreward extensions of the same topographic 'highs' (Fig.5.3).

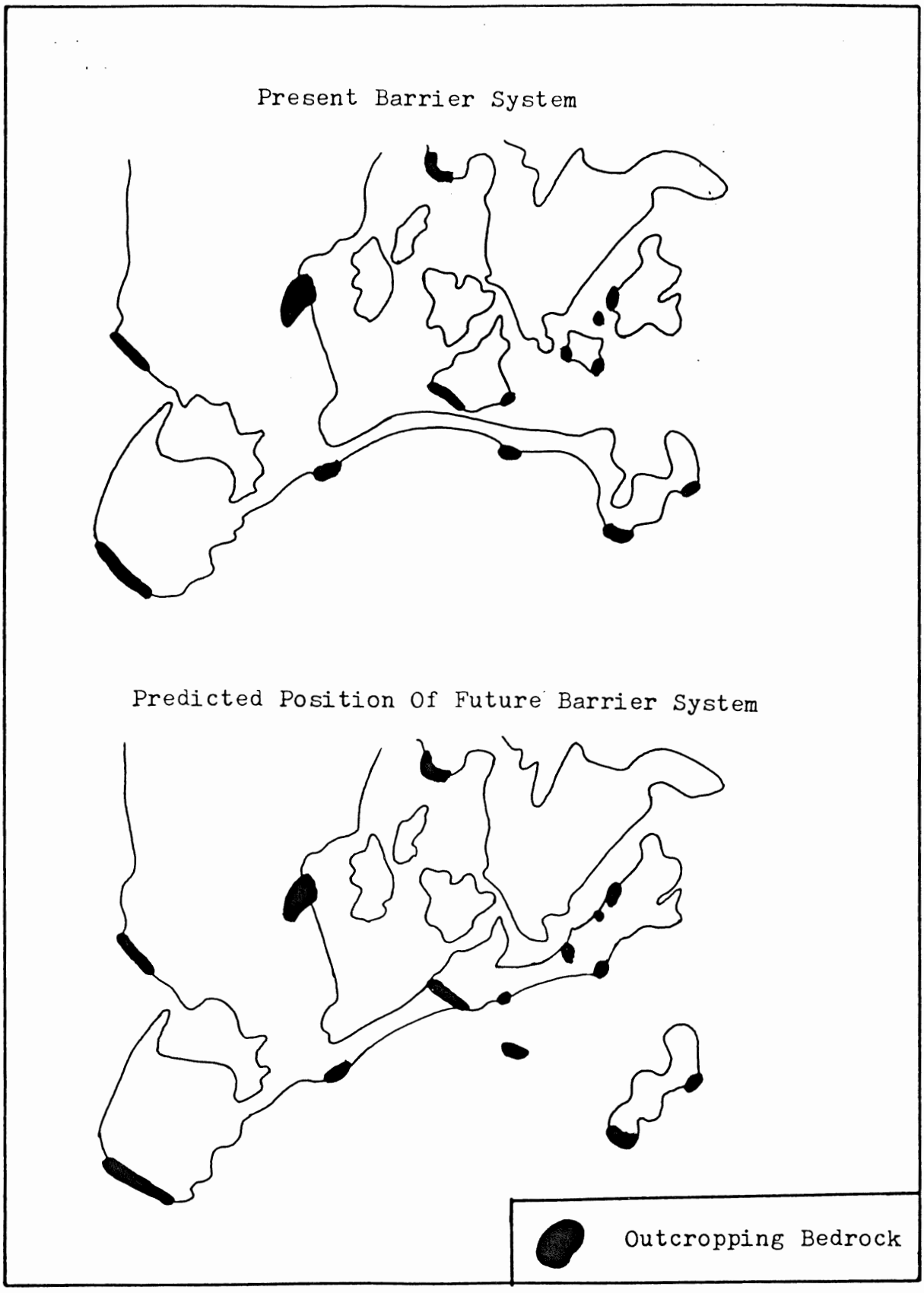

Figure 5.3 The evolution of Martinique Beach.

6: CONCLUSIONS

* This survey has produced an accurate profile of Martinique Beach using refraction seismic methods. This is the first such profile to be produced for barrier beaches found in Nova Scotia.

* The topographic bedrock 'highs' seen in the beach profile correlate well to the trends seen in the marine reflection seismic lines and positions of outcropping bedrock.

* A scour channel is seen between the mid-beach outcrop and Flying Point. This channel can be extended seaward with the aid of the marine profiles and bathymetric trends.

* The breaching of the beach system is located at the same position as the scour channel. The presence of this channel may affect the stability of overlying sediments.

* Upon destruction of the present beach, a new barrier beach is likely to be formed within the same channels anchored to shoreward extensions of the topographic 'highs'.

Boyd,R.,Bowen,A.J.,Hall,R.K.,1983
The Eastern Shore Beaches; Cow Bay,Cole Harbour, Conrads, Lawrencetown, Martinique : Final Report unpublished

Boyd,R.,Pentland,S.,1984
Shoreface Translation and the Holocene Stratigraphic Record : Examples from Nova Scotia, The Mississippi Delta and Eastern Australia.
Marine Geology, 60:391-412

Quinlan,G.,Beamont,C.,1981
A comparison of Observed and Theoretical Post-Glacial Sea Levels in Atlantic Canada.
Canadian Journal of Earth Science. 18, 1146-1163

Redpath,B.B.,1973
Seismic Refraction Exploration for Engineering Site Investigations.
National Technical Information Service, AD-768 710

Scott,D.B.,Medioli,F.S.,1982
Micropaleontological Documentation for Early Holcene Fall of Relative Sea Level on the Atlantic Coast of Nova Scotia.
Geology, 10:278-281

Sengbush,R.L.,1983
Seismic Exploration Methods
pub. International Human Resources Developement Corp. Boston

Telford,W.M.,Geldart,L.P.,Sheriff,R.E.,Keys,D.A.,1976
Applied Geophysics
pub. Cambridge University Press

Walker,R.G.,1984
Facies Models, second edition
pub. Geological Association of Canada

APPENDIX 1

Calibration Data

Format :

```
2  500.0  100.0  108.0
:     :      :      :
:     :      :      Measured Time
:     :      Control Time
:     Sweep Time
Channel
```

1	50.0	10.0	10.0
1	100.0	10.0	10.0
1	100.0	50.0	55.0
1	200.0	10.0	10.0
1	200.0	50.0	53.0
1	200.0	100.0	105.0
1	500.0	50.0	53.0
1	500.0	100.0	105.0
1	500.0	200.0	213.0
1	500.0	200.0	210.0
1	1000.0	50.0	55.0
1	1000.0	100.0	110.0
1	1000.0	200.0	220.0
1	2000.0	100.0	105.0
1	2000.0	200.0	210.0
1	2000.0	1000.0	1060.0
2	50.0	10.0	10.0
2	100.0	10.0	10.0
2	100.0	50.0	56.0
2	200.0	10.0	10.0
2	200.0	50.0	54.0
2	200.0	100.0	106.0
2	500.0	50.0	54.0
2	500.0	100.0	108.0
2	500.0	200.0	213.0
2	1000.0	50.0	50.0
2	1000.0	100.0	105.0
2	1000.0	200.0	210.0
2	2000.0	100.0	105.0
2	2000.0	200.0	210.0
2	2000.0	1000.0	1050.0
11	50.0	10.0	10.0
11	100.0	10.0	10.0
11	100.0	50.0	56.0
11	100.0	10.0	10.0
11	200.0	50.0	54.0
11	200.0	100.0	106.0
11	200.0	100.0	106.0
11	500.0	50.0	50.0
11	500.0	100.0	105.0
11	500.0	200.0	213.0
11	500.0	200.0	210.0
11	1000.0	100.0	110.0
11	1000.0	200.0	200.0
11	2000.0	200.0	210.0
11	2000.0	1000.0	1060.0
7	100.0	50.0	55.0
7	200.0	50.0	53.0
7	200.0	100.0	105.0
7	500.0	100.0	105.0
7	500.0	200.0	212.0
7	1000.0	100.0	110.0
7	1000.0	200.0	220.0
7	2000.0	200.0	210.0
7	2000.0	1000.0	1060.0

APPENDIX 2

Data Listing

standard format:

```
16      1     10.0  4.0   24.0   0.0123  2
 :      :      :     :     :      :       :
 :      :      :     :     :      :      layer
 :      :      :     :     :      :
 :      :      :     :     :     time
 :      :      :     :     :
 :      :      :     :    distance
 :      :      :     :
 :      :      :    spread
 :      :      :
 :      :     shot point distance
 :      :
 :     position (east-west)
 :
 station
```

```
1   2   5.0   5.0   15.0  .0123 3
1   2   5.0   5.0   20.0  .0142 3
1   2   5.0   5.0   25.0  .0161 3
1   2   5.0   5.0   30.0  .0170 3
1   2   5.0   5.0   35.0  .0189 3
1   2   5.0   5.0   40.0  .0199 3
1   1   5.0   5.0    5.0  .0114 2
1   1   5.0   5.0   10.0  .0142 2
1   1   5.0   5.0   10.0  .0142 3
1   1   5.0   5.0   15.0  .0151 3
1   1   5.0   5.0   20.0  .0161 3
1   1   5.0   5.0   25.0  .0180 3
1   1   5.0   5.0   30.0  .0208 3
1   1   5.0   1.0    5.0  .0076 2
1   1   5.0   1.0    6.0  .0095 2
1   1   5.0   1.0    7.0  .0114 2
1   1   5.0   1.0    8.0  .0123 2
1   1   5.0   1.0    9.0  .0132 2
1   1   5.0   1.0   10.0  .0132 3
1   1   5.0   1.0   11.0  .0142 3
1   1   5.0   1.0   12.0  .0142 3
1   1   5.0   1.0   13.0  .0151 3
1   1   5.0   1.0   14.0  .0151 3
1   1   5.0   1.0   15.0  .0151 3
1   1   5.0   1.0   16.0  .0161 3
1   1   5.0   1.0    5.0  .0095 2
1   1   5.0   1.0    6.0  .0104 2
1   1   5.0   1.0    7.0  .0104 2
1   1   5.0   1.0    8.0  .0123 2
1   1   5.0   1.0    9.0  .0132 2
1   1   5.0   1.0   10.0  .0132 3
1   1   5.0   1.0   11.0  .0142 3
1   1   5.0   1.0   12.0  .0142 3
1   1   5.0   1.0   13.0  .0142 3
1   1   5.0   1.0   14.0  .0151 3
1   1   5.0   1.0   15.0  .0151 3
1   1   5.0   1.0   16.0  .0151 3
1   2    .5   1.0     .5  .0019 1
1   2    .5   1.0    1.5  .0076 1
1   2    .5   1.0    2.5  .0085 2
1   2    .5   1.0    3.5  .0095 2
1   2    .5   1.0    4.5  .0104 2
1   2    .5   1.0    5.5  .0114 2
1   2    .5   1.0    6.5  .0123 2
1   2    .5   1.0    7.5  .0123 2
1   2    .5   1.0    8.5  .0132 2
1   2    .5   1.0    9.5  .0132 2
1   2    .5   1.0   10.5  .0132 2
1   2    .5   1.0   11.5  .0142 2
1   2   5.0   1.0    5.0  .0095 2
```

1	2	5.0	1.0	6.0	.0104	2
1	2	5.0	1.0	7.0	.0104	2
1	2	5.0	1.0	8.0	.0114	2
1	2	5.0	1.0	9.0	.0123	2
1	2	5.0	1.0	9.0	.0123	3
1	2	5.0	1.0	10.0	.0114	3
1	2	5.0	1.0	11.0	.0114	3
1	2	5.0	1.0	12.0	.0123	3
1	2	5.0	1.0	13.0	.0142	3
1	2	5.0	1.0	14.0	.0142	3
1	2	5.0	1.0	15.0	.0151	3
1	2	5.0	1.0	16.0	.0151	3
1	1	.5	1.0	.5	.0019	1
1	1	.5	1.0	1.5	.0071	1
1	1	.5	1.0	2.5	.0076	2
1	1	.5	1.0	3.5	.0085	2
1	1	.5	1.0	4.5	.0095	2
1	1	.5	1.0	5.5	.0114	2
1	1	.5	1.0	6.5	.0114	2
1	1	.5	1.0	7.5	.0114	2
1	1	.5	1.0	8.5	.0114	2
1	1	.5	1.0	9.5	.0132	2
1	1	.5	1.0	10.5	.0132	2
1	1	.5	1.0	11.5	.0142	2
5	2	5.0	5.0	5.0	.0208	2
5	2	5.0	5.0	10.0	.0237	2
5	2	5.0	5.0	15.0	.0274	2
5	2	5.0	5.0	20.0	.0293	2
5	2	5.0	5.0	25.0	.0303	3
5	2	5.0	5.0	30.0	.0322	3
5	2	5.0	5.0	35.0	.0331	3
5	2	5.0	5.0	45.0	.0350	3
5	2	5.0	5.0	50.0	.0360	3
5	2	5.0	5.0	55.0	.0369	3
5	2	5.0	5.0	60.0	.0378	3
5	2	5.0	5.0	5.0	.0180	2
5	2	5.0	5.0	10.0	.0208	2
5	2	5.0	5.0	15.0	.0246	2
5	2	5.0	5.0	20.0	.0265	2
5	2	5.0	5.0	25.0	.0293	2
5	2	5.0	5.0	25.0	.0293	3
5	2	5.0	5.0	30.0	.0307	3
5	2	5.0	5.0	35.0	.0322	3
5	2	5.0	5.0	40.0	.0336	3
5	2	5.0	5.0	45.0	.0345	3
5	2	5.0	5.0	50.0	.0360	3
5	2	5.0	5.0	55.0	.0378	3
5	2	5.0	5.0	60.0	.0383	3
5	2	10.0	5.0	10.0	.0237	2
5	2	10.0	5.0	15.0	.0274	2

5	2	10.0	5.0	20.0	.0284	3
5	2	10.0	5.0	25.0	.0303	3
5	2	10.0	5.0	30.0	.0303	3
5	2	10.0	5.0	35.0	.0303	3
5	2	10.0	5.0	40.0	.0331	3
5	2	10.0	5.0	45.0	.0331	3
5	2	10.0	5.0	50.0	.0341	3
5	2	10.0	5.0	55.0	.0350	3
5	2	10.0	5.0	60.0	.0360	3
5	2	10.0	5.0	65.0	.0360	3
5	2	20.0	5.0	20.0	.0284	3
5	2	20.0	5.0	25.0	.0303	3
5	2	20.0	5.0	30.0	.0303	3
5	2	20.0	5.0	35.0	.0322	3
5	2	20.0	5.0	40.0	.0331	3
5	2	20.0	5.0	45.0	.0341	3
5	2	20.0	5.0	50.0	.0360	3
5	2	20.0	5.0	55.0	.0360	3
5	2	20.0	5.0	60.0	.0369	3
5	2	20.0	5.0	65.0	.0378	3
5	2	20.0	5.0	70.0	.0388	3
5	2	20.0	5.0	75.0	.0397	3
5	2	20.0	5.0	20.0	.0284	3
5	2	20.0	5.0	25.0	.0293	3
5	2	20.0	5.0	30.0	.0303	3
5	2	20.0	5.0	35.0	.0312	3
5	2	20.0	5.0	40.0	.0322	3
5	2	20.0	5.0	45.0	.0341	3
5	2	20.0	5.0	50.0	.0360	3
5	2	20.0	5.0	55.0	.0369	3
5	2	20.0	5.0	60.0	.0378	3
5	2	20.0	5.0	70.0	.0407	3
5	2	20.0	5.0	75.0	.0416	3
5	1	5.0	5.0	5.0	.0219	2
5	1	5.0	5.0	10.0	.0246	2
5	1	5.0	5.0	15.0	.0265	2
5	1	5.0	5.0	20.0	.0303	2
5	1	5.0	5.0	20.0	.0303	2
5	1	5.0	5.0	25.0	.0303	3
5	1	5.0	5.0	30.0	.0312	3
5	1	5.0	5.0	35.0	.0331	3
5	1	5.0	5.0	40.0	.0350	3
5	1	5.0	5.0	45.0	.0341	3
5	1	5.0	5.0	50.0	.0350	3
5	1	5.0	5.0	55.0	.0369	3
5	1	5.0	5.0	60.0	.0369	3
5	1	10.0	5.0	10.0	.0265	2
5	1	10.0	5.0	15.0	.0293	2
5	1	10.0	5.0	20.0	.0322	2
5	1	10.0	5.0	20.0	.0322	2

5	1	10.0	5.0	25.0	.0322	3
5	1	10.0	5.0	30.0	.0331	3
5	1	10.0	5.0	35.0	.0341	3
5	1	10.0	5.0	40.0	.0350	3
5	1	10.0	5.0	45.0	.0360	3
5	1	10.0	5.0	50.0	.0369	3
5	1	10.0	5.0	55.0	.0378	3
5	1	10.0	5.0	60.0	.0388	3
5	1	10.0	5.0	65.0	.0407	3
5	1	20.0	5.0	20.0	.0312	3
5	1	20.0	5.0	25.0	.0341	3
5	1	20.0	5.0	30.0	.0322	3
5	1	20.0	5.0	35.0	.0331	3
5	1	20.0	5.0	40.0	.0341	3
5	1	20.0	5.0	45.0	.0360	3
5	1	20.0	5.0	50.0	.0369	3
5	1	20.0	5.0	55.0	.0388	3
5	1	20.0	5.0	60.0	.0397	3
5	1	20.0	5.0	65.0	.0397	3
5	1	20.0	5.0	70.0	.0407	3
5	1	20.0	5.0	75.0	.0426	3
5	1	.5	1.0	.5	.0019	1
5	1	.5	1.0	1.5	.0076	1
5	1	.5	1.0	2.5	.0114	1
5	1	.5	1.0	3.5	.0170	1
5	1	.5	1.0	4.5	.0199	1
5	1	.5	1.0	4.5	.0199	2
5	1	.5	1.0	5.5	.0208	2
5	1	.5	1.0	6.5	.0208	2
5	1	.5	1.0	7.5	.0218	2
5	1	.5	1.0	8.5	.0227	2
5	1	.5	1.0	9.5	.0227	2
5	1	.5	1.0	10.5	.0237	2
5	1	.5	1.0	11.5	.0246	2
5	2	.5	1.0	.5	.0078	1
5	2	.5	1.0	1.5	.0076	1
5	2	.5	1.0	2.5	.0123	1
5	2	.5	1.0	3.5	.0180	1
5	2	.5	1.0	4.5	.0227	1
5	2	.5	1.0	5.5	.0208	2
5	2	.5	1.0	6.5	.0208	2
5	2	.5	1.0	7.5	.0218	2
5	2	.5	1.0	8.5	.0227	2
5	2	.5	1.0	9.5	.0227	2
5	2	.5	1.0	10.5	.0237	2
5	2	.5	1.0	11.5	.0246	2
4	2	5.0	3.0	5.0	.0237	1
4	2	5.0	3.0	8.0	.0336	1
4	2	5.0	3.0	11.0	.0456	1
4	2	5.0	3.0	14.0	.0263	2

4	2	5.0	3.0	17.0	.0284	2
4	2	5.0	3.0	20.0	.0310	2
4	2	5.0	3.0	23.0	.0325	2
4	2	5.0	3.0	26.0	.0357	2
4	2	5.0	3.0	26.0	.0389	3
4	2	5.0	3.0	29.0	.0401	3
4	2	5.0	3.0	32.0	.0412	3
4	2	5.0	3.0	35.0	.0416	3
4	2	5.0	3.0	38.0	.0428	3
4	1	5.0	3.0	5.0	.0239	1
4	1	5.0	3.0	8.0	.0323	1
4	1	5.0	3.0	8.0	.0225	2
4	1	5.0	3.0	11.0	.0237	2
4	1	5.0	3.0	17.0	.0268	2
4	1	5.0	3.0	20.0	.0312	2
4	1	5.0	3.0	23.0	.0322	2
4	1	5.0	3.0	26.0	.0356	2
4	1	5.0	3.0	20.0	.0382	3
4	1	5.0	3.0	23.0	.0394	3
4	1	5.0	3.0	26.0	.0397	3
4	1	5.0	3.0	29.0	.0408	3
4	1	5.0	3.0	32.0	.0411	3
4	1	5.0	3.0	35.0	.0424	3
4	1	5.0	3.0	38.0	.0426	3
4	1	1.5	3.0	1.5	.0076	1
4	1	1.5	3.0	4.5	.0216	1
4	1	1.5	3.0	4.5	.0216	2
4	1	1.5	3.0	7.5	.0230	2
4	1	1.5	3.0	10.5	.0242	2
4	1	1.5	3.0	13.5	.0265	2
4	1	1.5	3.0	16.5	.0279	2
4	2	1.5	3.0	1.5	.0077	1
4	2	1.5	3.0	4.5	.0218	1
4	2	1.5	3.0	4.5	.0218	2
4	2	1.5	3.0	7.5	.0235	2
4	2	1.5	3.0	10.5	.0237	2
4	2	1.5	3.0	13.5	.0258	2
4	2	1.5	3.0	16.5	.0270	2
6	2	5.0	3.0	5.0	.0140	2
6	2	5.0	3.0	8.0	.0167	2
6	2	5.0	3.0	11.0	.0188	2
6	2	5.0	3.0	14.0	.0200	2
6	2	5.0	3.0	17.0	.0209	2
6	2	5.0	3.0	20.0	.0241	2
6	2	5.0	3.0	23.0	.0255	2
6	2	5.0	3.0	17.0	.0277	3
6	2	5.0	3.0	20.0	.0291	3
6	2	5.0	3.0	20.0	.0302	3
6	2	5.0	3.0	26.0	.0307	3
6	2	5.0	3.0	29.0	.0303	3

6	2	5.0	3.0	32.0	.0319	3
6	2	5.0	3.0	35.0	.0330	3
6	2	5.0	3.0	38.0	.0325	3
6	1	5.0	3.0	5.0	.0161	2
6	1	5.0	3.0	8.0	.0174	2
6	1	5.0	3.0	11.0	.0192	2
6	1	5.0	3.0	14.0	.0205	2
6	1	5.0	3.0	17.0	.0223	2
6	1	5.0	3.0	20.0	.0243	2
6	1	5.0	3.0	23.0	.0265	2
6	1	5.0	3.0	26.0	.0291	2
6	1	5.0	3.0	29.0	.0306	2
6	1	5.0	3.0	29.0	.0322	3
6	1	5.0	3.0	32.0	.0322	3
6	1	5.0	3.0	35.0	.0332	3
6	1	5.0	3.0	38.0	.0338	3
6	1	1.5	3.0	1.5	.0056	1
6	1	1.5	3.0	4.5	.0144	1
6	1	1.5	3.0	4.5	.0144	2
6	1	1.5	3.0	7.5	.0150	2
6	1	1.5	3.0	10.5	.0161	2
6	1	1.5	3.0	13.5	.0189	2
6	1	1.5	3.0	16.5	.0204	2
6	2	1.5	3.0	1.5	.0056	1
6	2	1.5	3.0	4.5	.0142	1
6	2	1.5	3.0	4.5	.0142	2
6	2	1.5	3.0	7.5	.0150	2
6	2	1.5	3.0	10.5	.0178	2
6	2	1.5	3.0	13.5	.0199	2
6	2	1.5	3.0	16.5	.0216	2
6	1	1.5	3.0	1.5	.0057	1
6	1	1.5	3.0	4.5	.0199	1
6	1	1.5	3.0	7.5	.0303	1
6	1	1.5	3.0	10.5	.0464	1
6	1	1.5	3.0	13.5	.0568	1
6	1	1.5	3.0	16.5	.0662	1
6	2	1.5	3.0	1.5	.0076	1
6	2	1.5	3.0	4.5	.0208	1
6	2	1.5	3.0	7.5	.0303	1
6	2	1.5	3.0	10.5	.0378	1
6	2	1.5	3.0	13.5	.0558	1
6	2	1.5	3.0	16.5	.0662	1
7	2	5.0	5.0	5.0	.0162	2
7	2	5.0	5.0	10.0	.0199	2
7	2	5.0	5.0	15.0	.0233	2
7	2	5.0	5.0	20.0	.0259	2
7	2	5.0	5.0	25.0	.0295	2
7	2	5.0	5.0	30.0	.0334	2
7	2	5.0	5.0	35.0	.0360	2
7	2	5.0	5.0	40.0	.0383	2

7	2	5.0	5.0	35.0	.0407	3
7	2	5.0	5.0	40.0	.0408	3
7	2	5.0	5.0	45.0	.0416	3
7	2	5.0	5.0	50.0	.0435	3
7	2	5.0	5.0	55.0	.0459	3
7	2	5.0	5.0	60.0	.0473	3
7	1	2.5	5.0	2.5	.0132	1
7	1	2.5	5.0	7.5	.0197	2
7	1	2.5	5.0	12.5	.0218	2
7	1	2.5	5.0	17.5	.0246	2
7	1	2.5	5.0	22.5	.0272	2
7	1	2.5	5.0	27.5	.0302	2
7	2	2.5	5.0	2.5	.0132	1
7	2	2.5	5.0	7.5	.0180	2
7	2	2.5	5.0	12.5	.0210	2
7	2	2.5	5.0	17.5	.0237	2
7	2	2.5	5.0	22.5	.0284	2
7	2	2.5	5.0	27.5	.0302	2
7	1	5.0	5.0	5.0	.0161	2
7	1	5.0	5.0	10.0	.0191	2
7	1	5.0	5.0	15.0	.0222	2
7	1	5.0	5.0	20.0	.0251	2
7	1	5.0	5.0	30.0	.0331	3
7	1	5.0	5.0	35.0	.0360	3
7	1	5.0	5.0	40.0	.0369	3
7	1	5.0	5.0	45.0	.0388	3
14	2	10.0	4.0	10.0	.0148	2
14	2	10.0	4.0	14.0	.0186	2
14	2	10.0	4.0	18.0	.0194	2
14	2	10.0	4.0	22.0	.0230	2
14	2	10.0	4.0	26.0	.0254	2
14	2	10.0	4.0	30.0	.0282	2
14	2	10.0	4.0	38.0	.0311	2
14	2	10.0	4.0	42.0	.0337	2
14	2	10.0	4.0	46.0	.0354	2
14	2	10.0	4.0	50.0	.0378	2
14	2	10.0	4.0	54.0	.0391	2
14	1	10.0	4.0	10.0	.0139	2
14	1	10.0	4.0	14.0	.0164	2
14	1	10.0	4.0	18.0	.0181	2
14	1	10.0	4.0	22.0	.0209	2
14	1	10.0	4.0	26.0	.0236	2
14	1	10.0	4.0	30.0	.0256	2
14	1	10.0	4.0	38.0	.0275	3
14	1	10.0	4.0	42.0	.0281	3
14	1	10.0	4.0	50.0	.0295	3
14	1	10.0	4.0	54.0	.0311	3
14	1	2.0	4.0	2.0	.0101	2
14	1	2.0	4.0	6.0	.0125	2
14	1	2.0	4.0	10.0	.0146	2

14	1	2.0	4.0	14.0	.0169	2
14	1	2.0	4.0	18.0	.0199	2
14	1	2.0	4.0	22.0	.0217	2
14	2	2.0	4.0	2.0	.0105	2
14	2	2.0	4.0	6.0	.0132	2
14	2	2.0	4.0	10.0	.0145	2
14	2	2.0	4.0	14.0	.0162	2
14	2	2.0	4.0	18.0	.0196	2
14	2	2.0	4.0	22.0	.0214	2
13	1	10.0	4.0	10.0	.0117	2
13	1	10.0	4.0	14.0	.0154	2
13	1	10.0	4.0	18.0	.0170	2
13	1	10.0	4.0	22.0	.0191	2
13	1	10.0	4.0	26.0	.0217	2
13	1	10.0	4.0	30.0	.0242	2
13	1	10.0	4.0	34.0	.0272	2
13	1	10.0	4.0	38.0	.0292	2
13	1	10.0	4.0	42.0	.0301	3
13	1	10.0	4.0	46.0	.0309	3
13	1	10.0	4.0	50.0	.0311	3
13	1	10.0	4.0	54.0	.0322	3
13	1	2.0	4.0	2.0	.0065	2
13	1	2.0	4.0	6.0	.0087	2
13	1	2.0	4.0	10.0	.0112	2
13	1	2.0	4.0	14.0	.0141	2
13	1	2.0	4.0	18.0	.0165	2
13	1	2.0	4.0	22.0	.0176	2
13	2	2.0	4.0	2.0	.0077	2
13	2	2.0	4.0	6.0	.0086	2
13	2	2.0	4.0	10.0	.0116	2
13	2	2.0	4.0	14.0	.0139	2
13	2	2.0	4.0	18.0	.0168	2
13	2	2.0	4.0	22.0	.0200	2
13	2	10.0	4.0	10.0	.0116	2
13	2	10.0	4.0	14.0	.0144	2
13	2	10.0	4.0	18.0	.0164	2
13	2	10.0	4.0	22.0	.0196	2
13	2	10.0	4.0	26.0	.0218	2
13	2	10.0	4.0	30.0	.0255	3
13	2	10.0	4.0	34.0	.0272	3
13	2	10.0	4.0	38.0	.0284	3
13	2	10.0	4.0	42.0	.0292	3
13	2	10.0	4.0	46.0	.0302	3
13	2	10.0	4.0	50.0	.0313	3
13	2	10.0	4.0	54.0	.0321	2
12	4	5.0	3.0	5.0	.0095	2
12	4	5.0	3.0	8.0	.0111	2
12	4	5.0	3.0	11.0	.0125	2
12	4	5.0	3.0	14.0	.0136	2
12	4	5.0	3.0	17.0	.0146	2

12	4	5.0	3.0	20.0	.0161	2
12	4	5.0	3.0	23.0	.0172	2
12	4	5.0	3.0	26.0	.0185	2
12	4	5.0	3.0	29.0	.0194	2
12	4	5.0	3.0	32.0	.0206	3
12	4	5.0	3.0	35.0	.0214	3
12	4	5.0	3.0	38.0	.0217	3
12	3	5.0	3.0	5.0	.0026	2
12	3	5.0	3.0	8.0	.0041	2
12	3	5.0	3.0	11.0	.0061	2
12	3	5.0	3.0	14.0	.0079	2
12	3	5.0	3.0	17.0	.0095	2
12	3	5.0	3.0	20.0	.0114	2
12	3	5.0	3.0	23.0	.0124	3
12	3	5.0	3.0	26.0	.0132	3
12	3	5.0	3.0	29.0	.0139	3
12	3	5.0	3.0	32.0	.0159	3
12	3	5.0	3.0	35.0	.0152	3
12	3	5.0	3.0	38.0	.0170	3
12	3	1.5	3.0	1.5	.0016	2
12	3	1.5	3.0	4.5	.0034	2
12	3	1.5	3.0	7.5	.0061	2
12	3	1.5	3.0	10.5	.0091	2
12	3	1.5	3.0	13.5	.0114	2
12	3	1.5	3.0	16.5	.0132	2
12	4	1.5	3.0	1.5	.0016	2
12	4	1.5	3.0	4.5	.0027	2
12	4	1.5	3.0	7.5	.0044	2
12	4	1.5	3.0	10.5	.0058	2
12	4	1.5	3.0	13.5	.0076	2
12	4	1.5	3.0	16.5	.0093	2
12	4	1.5	3.0	10.5	.0058	3
12	4	1.5	3.0	13.5	.0059	3
12	4	1.5	3.0	16.5	.0066	3
11	2	5.0	3.0	5.0	.0076	2
11	2	5.0	3.0	8.0	.0100	2
11	2	5.0	3.0	11.0	.0115	2
11	2	5.0	3.0	14.0	.0136	2
11	2	5.0	3.0	17.0	.0161	2
11	2	5.0	3.0	23.0	.0198	2
11	2	5.0	3.0	23.0	.0198	3
11	2	5.0	3.0	26.0	.0218	3
11	2	5.0	3.0	29.0	.0221	3
11	2	5.0	3.0	32.0	.0226	3
11	2	5.0	3.0	35.0	.0230	3
11	2	5.0	3.0	5.0	.0073	2
11	2	5.0	3.0	8.0	.0095	2
11	2	5.0	3.0	11.0	.0111	2
11	2	5.0	3.0	14.0	.0131	2
11	2	5.0	3.0	17.0	.0147	2

11	2	5.0	3.0	20.0	.0161	2
11	2	5.0	3.0	23.0	.0183	2
11	2	5.0	3.0	26.0	.0214	2
11	2	5.0	3.0	29.0	.0214	3
11	2	5.0	3.0	32.0	.0222	3
11	2	5.0	3.0	35.0	.0225	3
11	2	5.0	3.0	38.0	.0227	3
11	1	1.5	3.0	1.5	.0059	2
11	1	1.5	3.0	4.5	.0079	2
11	1	1.5	3.0	7.5	.0096	2
11	1	1.5	3.0	10.5	.0114	2
11	1	1.5	3.0	13.5	.0135	2
11	1	1.5	3.0	16.5	.0149	2
11	2	1.5	3.0	1.5	.0057	2
11	2	1.5	3.0	4.5	.0081	2
11	2	1.5	3.0	7.5	.0098	2
11	2	1.5	3.0	10.5	.0114	2
11	2	1.5	3.0	13.5	.0132	2
11	2	1.5	3.0	16.5	.0139	2
11	1	5.0	3.0	5.0	.0066	2
11	1	5.0	3.0	8.0	.0086	2
11	1	5.0	3.0	11.0	.0106	2
11	1	5.0	3.0	14.0	.0126	2
11	1	5.0	3.0	17.0	.0144	2
11	1	5.0	3.0	20.0	.0157	2
11	1	5.0	3.0	23.0	.0172	2
11	1	5.0	3.0	26.0	.0187	3
11	1	5.0	3.0	29.0	.0195	3
11	1	5.0	3.0	32.0	.0207	3
11	1	5.0	3.0	35.0	.0215	3
11	1	5.0	3.0	38.0	.0225	3
10	1	10.0	4.0	10.0	.0145	2
10	1	10.0	4.0	14.0	.0173	2
10	1	10.0	4.0	18.0	.0206	2
10	1	10.0	4.0	22.0	.0230	3
10	1	10.0	4.0	26.0	.0246	3
10	1	10.0	4.0	30.0	.0255	3
10	1	10.0	4.0	34.0	.0265	3
10	1	10.0	4.0	38.0	.0265	3
10	1	10.0	4.0	42.0	.0273	3
10	1	10.0	4.0	50.0	.0301	3
10	1	10.0	4.0	54.0	.0296	3
10	1	10.0	4.0	10.0	.0142	2
10	1	10.0	4.0	14.0	.0172	2
10	1	10.0	4.0	18.0	.0211	2
10	1	10.0	4.0	22.0	.0231	2
10	1	10.0	4.0	26.0	.0251	3
10	1	10.0	4.0	30.0	.0254	3
10	1	10.0	4.0	34.0	.0261	3
10	1	10.0	4.0	38.0	.0271	3

10	1	10.0	4.0	42.0	.0274	3
10	1	10.0	4.0	46.0	.0284	3
10	1	10.0	4.0	50.0	.0291	3
10	1	10.0	4.0	54.0	.0296	3
10	1	2.0	4.0	2.0	.0079	1
10	1	2.0	4.0	6.0	.0132	2
10	1	2.0	4.0	10.0	.0149	2
10	1	2.0	4.0	14.0	.0175	2
10	1	2.0	4.0	18.0	.0207	2
10	1	2.0	4.0	14.0	.0210	3
10	1	2.0	4.0	18.0	.0221	3
10	1	2.0	4.0	22.0	.0229	3
10	2	2.0	4.0	2.0	.0079	1
10	2	2.0	4.0	6.0	.0121	2
10	2	2.0	4.0	10.0	.0149	2
10	2	2.0	4.0	14.0	.0170	2
10	2	2.0	4.0	18.0	.0219	2
10	2	2.0	4.0	14.0	.0204	3
10	2	2.0	4.0	18.0	.0219	3
10	2	2.0	4.0	22.0	.0234	3
10	2	10.0	4.0	10.0	.0154	2
10	2	10.0	4.0	14.0	.0178	2
10	2	10.0	4.0	18.0	.0202	2
10	2	10.0	4.0	22.0	.0227	2
10	2	10.0	4.0	26.0	.0236	3
10	2	10.0	4.0	30.0	.0249	3
10	2	10.0	4.0	34.0	.0249	3
10	2	10.0	4.0	38.0	.0265	3
10	2	10.0	4.0	42.0	.0271	3
10	2	10.0	4.0	46.0	.0279	3
10	2	10.0	4.0	50.0	.0292	3
10	2	10.0	4.0	54.0	.0296	3
10	2	10.0	4.0	10.0	.0153	2
10	2	10.0	4.0	14.0	.0181	2
10	2	10.0	4.0	18.0	.0199	2
10	2	10.0	4.0	22.0	.0226	2
10	2	10.0	4.0	26.0	.0236	3
10	2	10.0	4.0	30.0	.0244	3
10	2	10.0	4.0	34.0	.0245	3
10	2	10.0	4.0	38.0	.0254	3
10	2	10.0	4.0	42.0	.0271	3
10	2	10.0	4.0	46.0	.0274	3
10	2	10.0	4.0	50.0	.0291	3
10	2	10.0	4.0	54.0	.0293	3
9	1	10.0	4.0	10.0	.0189	2
9	1	10.0	4.0	14.0	.0218	2
9	1	10.0	4.0	22.0	.0286	2
9	1	10.0	4.0	26.0	.0293	2
9	1	10.0	4.0	30.0	.0311	3
9	1	10.0	4.0	34.0	.0315	3

9	1	10.0	4.0	38.0	.0327	3
9	1	10.0	4.0	42.0	.0325	3
9	1	10.0	4.0	46.0	.0332	3
9	1	10.0	4.0	50.0	.0337	3
9	1	10.0	4.0	54.0	.0341	3
9	1	2.0	4.0	2.0	.0104	1
9	1	2.0	4.0	6.0	.0132	2
9	1	2.0	4.0	10.0	.0153	2
9	1	2.0	4.0	14.0	.0182	2
9	1	2.0	4.0	18.0	.0200	2
9	1	2.0	4.0	14.0	.0215	3
9	1	2.0	4.0	18.0	.0226	3
9	1	2.0	4.0	22.0	.0222	3
9	2	2.0	4.0	2.0	.0104	1
9	2	2.0	4.0	6.0	.0141	2
9	2	2.0	4.0	10.0	.0168	2
9	2	2.0	4.0	14.0	.0194	2
9	2	2.0	4.0	18.0	.0219	2
9	2	2.0	4.0	22.0	.0237	2
9	2	2.0	4.0	6.0	.0226	3
9	2	2.0	4.0	10.0	.0236	3
9	2	2.0	4.0	14.0	.0246	3
9	2	2.0	4.0	18.0	.0261	3
9	2	2.0	4.0	22.0	.0274	3
9	2	10.0	4.0	10.0	.0142	2
9	2	10.0	4.0	14.0	.0163	2
9	2	10.0	4.0	18.0	.0189	2
9	2	10.0	4.0	22.0	.0206	2
9	2	10.0	4.0	26.0	.0237	2
9	2	10.0	4.0	30.0	.0269	3
9	2	10.0	4.0	34.0	.0270	3
9	2	10.0	4.0	38.0	.0286	3
9	2	10.0	4.0	42.0	.0299	3
9	2	10.0	4.0	46.0	.0312	3
9	2	10.0	4.0	50.0	.0325	3
9	2	10.0	4.0	54.0	.0323	3
8	1	10.0	4.0	10.0	.0151	2
8	1	10.0	4.0	14.0	.0183	2
8	1	10.0	4.0	18.0	.0193	2
8	1	10.0	4.0	22.0	.0218	2
8	1	10.0	4.0	26.0	.0237	2
8	1	10.0	4.0	30.0	.0277	3
8	1	10.0	4.0	34.0	.0286	3
8	1	10.0	4.0	38.0	.0298	3
8	1	10.0	4.0	42.0	.0309	3
8	1	10.0	4.0	46.0	.0315	3
8	1	10.0	4.0	50.0	.0322	3
8	1	10.0	4.0	54.0	.0332	3
8	1	2.0	4.0	2.0	.0102	2
8	1	2.0	4.0	6.0	.0124	2

8	1	2.0	4.0	10.0	.0150	2
8	1	2.0	4.0	14.0	.0173	2
8	1	2.0	4.0	18.0	.0199	2
8	1	2.0	4.0	22.0	.0223	2
8	2	2.0	4.0	2.0	.0098	2
8	2	2.0	4.0	6.0	.0123	2
8	2	2.0	4.0	10.0	.0144	2
8	2	2.0	4.0	14.0	.0173	2
8	2	2.0	4.0	18.0	.0199	2
8	2	2.0	4.0	22.0	.0218	2
8	2	10.0	4.0	10.0	.0154	2
8	2	10.0	4.0	14.0	.0180	2
8	2	10.0	4.0	18.0	.0199	2
8	2	10.0	4.0	22.0	.0227	2
8	2	10.0	4.0	26.0	.0246	2
8	2	10.0	4.0	30.0	.0274	2
8	2	10.0	4.0	34.0	.0292	2
8	2	10.0	4.0	26.0	.0292	3
8	2	10.0	4.0	30.0	.0301	3
8	2	10.0	4.0	34.0	.0303	3
8	2	10.0	4.0	38.0	.0306	3
8	2	10.0	4.0	42.0	.0312	3
8	2	10.0	4.0	46.0	.0322	3
8	2	10.0	4.0	50.0	.0329	3
8	2	10.0	4.0	54.0	.0333	3
2	2	5.0	3.0	5.0	.0120	2
2	2	5.0	3.0	8.0	.0137	2
2	2	5.0	3.0	11.0	.0151	2
2	2	5.0	3.0	14.0	.0168	2
2	2	5.0	3.0	17.0	.0192	2
2	2	5.0	3.0	20.0	.0208	2
2	2	5.0	3.0	23.0	.0227	2
2	2	5.0	3.0	26.0	.0246	2
2	2	5.0	3.0	29.0	.0265	2
2	2	5.0	3.0	14.0	.0284	3
2	2	5.0	3.0	17.0	.0291	3
2	2	5.0	3.0	20.0	.0297	3
2	2	5.0	3.0	23.0	.0305	3
2	2	5.0	3.0	26.0	.0218	2
2	2	5.0	3.0	29.0	.0237	2
2	2	5.0	3.0	32.0	.0251	2
2	2	5.0	3.0	35.0	.0265	2
2	2	5.0	3.0	38.0	.0284	2
2	1	5.0	3.0	5.0	.0126	2
2	1	5.0	3.0	8.0	.0151	2
2	1	5.0	3.0	11.0	.0161	2
2	1	5.0	3.0	14.0	.0180	2
2	1	5.0	3.0	17.0	.0202	2
2	1	5.0	3.0	20.0	.0214	2
2	1	5.0	3.0	23.0	.0238	2

2	1	5.0	3.0	17.0	.0161	3
2	1	5.0	3.0	20.0	.0161	3
2	1	5.0	3.0	26.0	.0170	3
2	1	5.0	3.0	35.0	.0208	3
2	1	1.5	3.0	1.5	.0078	2
2	1	1.5	3.0	4.5	.0118	2
2	1	1.5	3.0	7.5	.0137	2
2	1	1.5	3.0	10.5	.0154	2
2	1	1.5	3.0	13.5	.0178	2
2	1	1.5	3.0	16.5	.0189	2
2	2	1.5	3.0	1.5	.0078	2
2	2	1.5	3.0	4.5	.0118	2
2	2	1.5	3.0	7.5	.0142	2
2	2	1.5	3.0	10.5	.0152	2
2	2	1.5	3.0	13.5	.0172	2
2	2	1.5	3.0	16.5	.0199	2
16	2	5.0	4.0	5.0	.0095	2
16	2	5.0	4.0	9.0	.0134	2
16	2	5.0	4.0	13.0	.0189	2
16	2	5.0	4.0	17.0	.0206	2
16	2	5.0	4.0	21.0	.0222	2
16	2	5.0	4.0	25.0	.0246	2
16	2	5.0	4.0	37.0	.0246	2
16	2	5.0	4.0	41.0	.0374	2
16	2	5.0	4.0	45.0	.0397	2
16	2	5.0	4.0	49.0	.0416	2
16	2	5.0	4.0	5.0	.0095	2
16	2	5.0	4.0	9.0	.0151	2
16	2	5.0	4.0	13.0	.0199	2
16	2	5.0	4.0	17.0	.0213	2
16	2	5.0	4.0	21.0	.0232	2
16	2	5.0	4.0	25.0	.0265	2
16	2	5.0	4.0	37.0	.0360	2
16	2	5.0	4.0	41.0	.0378	2
16	2	5.0	4.0	45.0	.0397	2
16	2	5.0	4.0	49.0	.0426	2
16	2	5.0	4.0	37.0	.0324	3
16	2	5.0	4.0	41.0	.0331	3
16	2	5.0	4.0	45.0	.0339	3
16	2	5.0	4.0	49.0	.0364	3
16	1	5.0	4.0	5.0	.0114	2
16	1	5.0	4.0	9.0	.0154	2
16	1	5.0	4.0	13.0	.0189	2
16	1	5.0	4.0	17.0	.0218	2
16	1	5.0	4.0	21.0	.0237	2
16	1	5.0	4.0	25.0	.0255	2
16	1	5.0	4.0	29.0	.0274	2
16	1	5.0	4.0	33.0	.0295	2
16	1	5.0	4.0	37.0	.0350	2
16	1	5.0	4.0	37.0	.0397	3

16	1	5.0	4.0	41.0	.0407	3
16	1	5.0	4.0	45.0	.0410	3
16	1	5.0	4.0	49.0	.0419	3
16	1	5.0	4.0	5.0	.0118	2
16	1	5.0	4.0	9.0	.0161	2
16	1	5.0	4.0	13.0	.0192	2
16	1	5.0	4.0	17.0	.0218	2
16	1	5.0	4.0	21.0	.0232	2
16	1	5.0	4.0	25.0	.0255	2
16	1	5.0	4.0	29.0	.0274	2
16	1	5.0	4.0	33.0	.0299	2
16	1	5.0	4.0	37.0	.0345	2
16	1	5.0	4.0	41.0	.0369	2
16	1	5.0	4.0	45.0	.0388	2
16	1	5.0	4.0	49.0	.0395	2
16	1	5.0	4.0	37.0	.0388	3
16	1	5.0	4.0	41.0	.0400	3
16	1	5.0	4.0	45.0	.0409	3
16	1	5.0	4.0	49.0	.0419	3
16	2	2.0	4.0	2.0	.0061	2
16	2	2.0	4.0	6.0	.0114	2
16	2	2.0	4.0	10.0	.0153	2
16	2	2.0	4.0	14.0	.0183	2
16	2	2.0	4.0	18.0	.0197	2
16	2	2.0	4.0	22.0	.0222	2
16	1	2.0	4.0	2.0	.0061	2
16	1	2.0	4.0	6.0	.0112	2
16	1	2.0	4.0	10.0	.0151	2
16	1	2.0	4.0	14.0	.0180	2
16	1	2.0	4.0	18.0	.0218	2
16	1	2.0	4.0	22.0	.0237	2
15	2	5.0	5.0	5.0	.0132	2
15	2	5.0	5.0	10.0	.0164	2
15	2	5.0	5.0	15.0	.0208	2
15	2	5.0	5.0	20.0	.0227	2
15	2	5.0	5.0	25.0	.0252	2
15	2	5.0	5.0	40.0	.0341	2
15	2	5.0	5.0	30.0	.0341	3
15	2	5.0	5.0	35.0	.0353	3
15	2	5.0	5.0	45.0	.0369	3
15	2	5.0	5.0	50.0	.0377	3
15	2	5.0	5.0	55.0	.0387	3
15	1	5.0	5.0	5.0	.0114	2
15	1	5.0	5.0	10.0	.0142	2
15	1	5.0	5.0	15.0	.0168	2
15	1	5.0	5.0	20.0	.0189	2
15	1	5.0	5.0	25.0	.0214	2
15	1	5.0	5.0	30.0	.0246	2
15	1	5.0	5.0	40.0	.0331	3
15	1	5.0	5.0	45.0	.0341	3

15	1	5.0	5.0	50.0	.0350	3
15	1	5.0	5.0	55.0	.0360	3
15	1	5.0	5.0	60.0	.0369	3
15	1	2.5	5.0	2.5	.0095	2
15	1	2.5	5.0	7.5	.0132	2
15	1	2.5	5.0	12.5	.0178	2
15	1	2.5	5.0	17.5	.0203	2
15	1	2.5	5.0	22.5	.0227	2
15	1	2.5	5.0	27.5	.0255	2
15	2	2.5	5.0	5.5	.0095	2
15	2	2.5	5.0	7.5	.0123	2
15	2	2.5	5.0	12.5	.0151	2
15	2	2.5	5.0	17.5	.0189	2
15	2	2.5	5.0	22.5	.0218	2
15	2	2.5	5.0	27.5	.0237	2

APPENDIX 3

Time-Distance Plots of Data

Title Reference:

3L 06 E
: : :
: : Position(East)
: Station
Layer

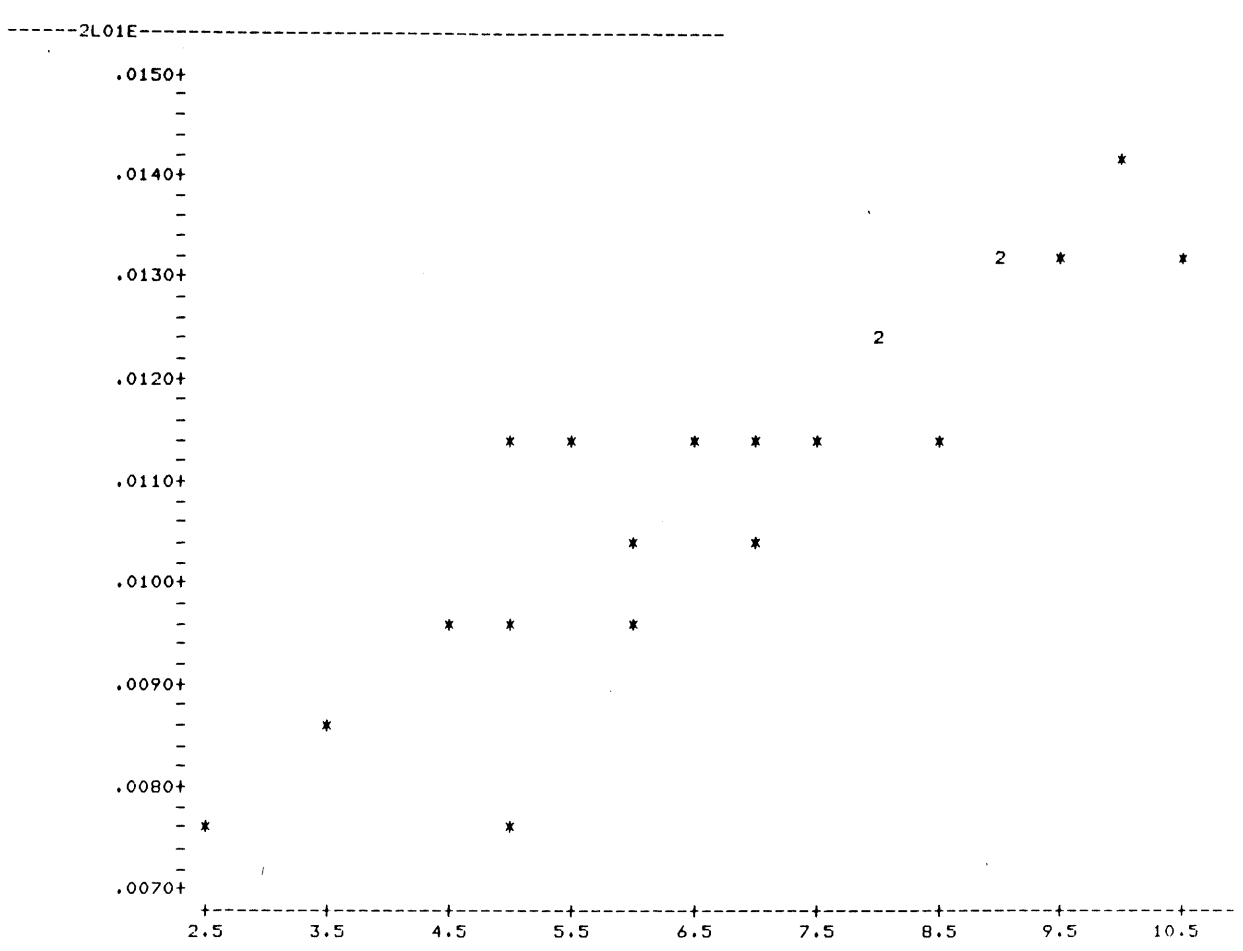
------2L01E----------
.0150+
.0140+
.0130+
.0120+
.0110+
.0100+
.0090+
.0080+
.0070+
2.5
3.5
4.5
5.5
6.5
7.5
8.5
9.5
10.5

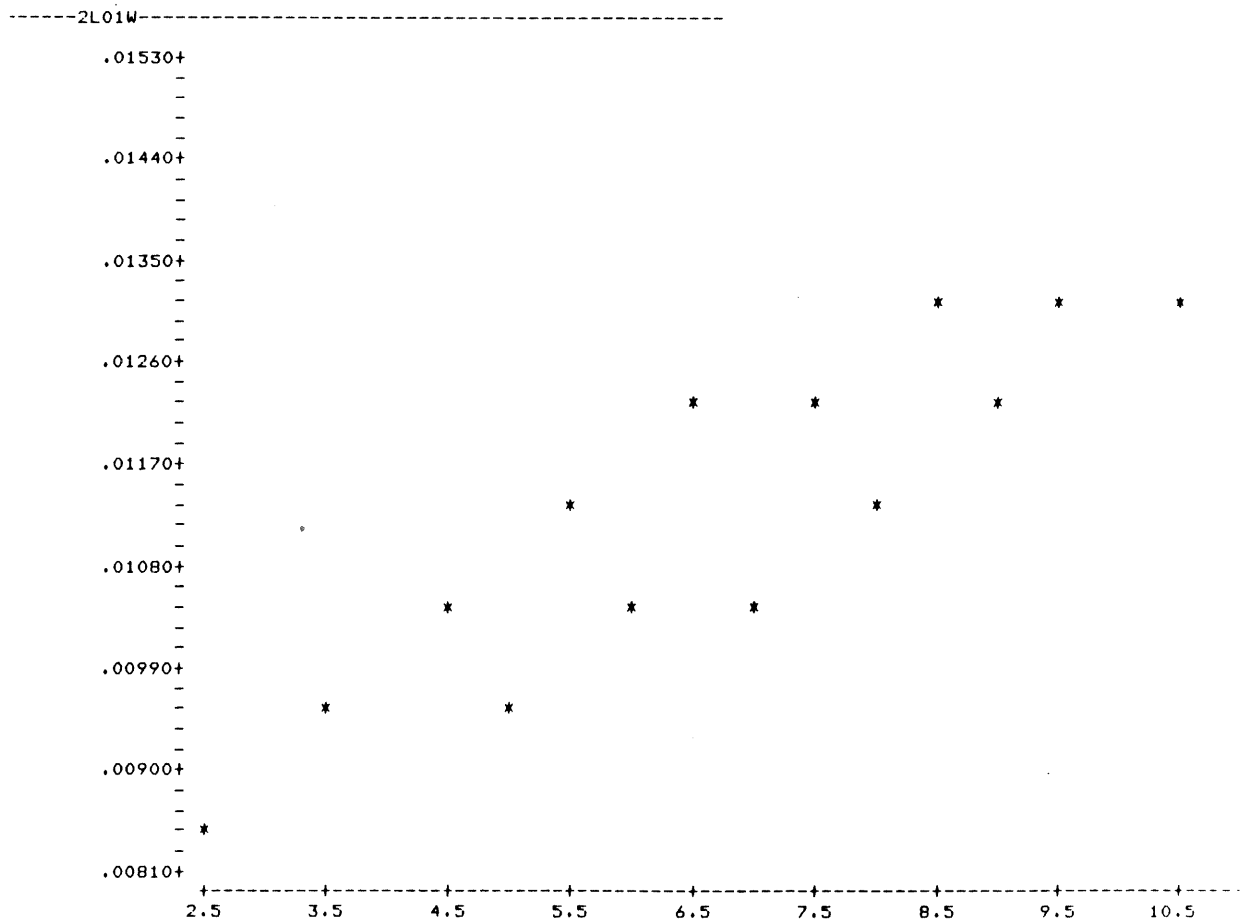
------2L01W----------
.01530+
.01440+
.01350+
.01260+
.01170+
.01080+
.00990+
.00900+
.00810+
2.5
3.5
4.5
5.5
6.5
7.5
8.5
9.5
10.5

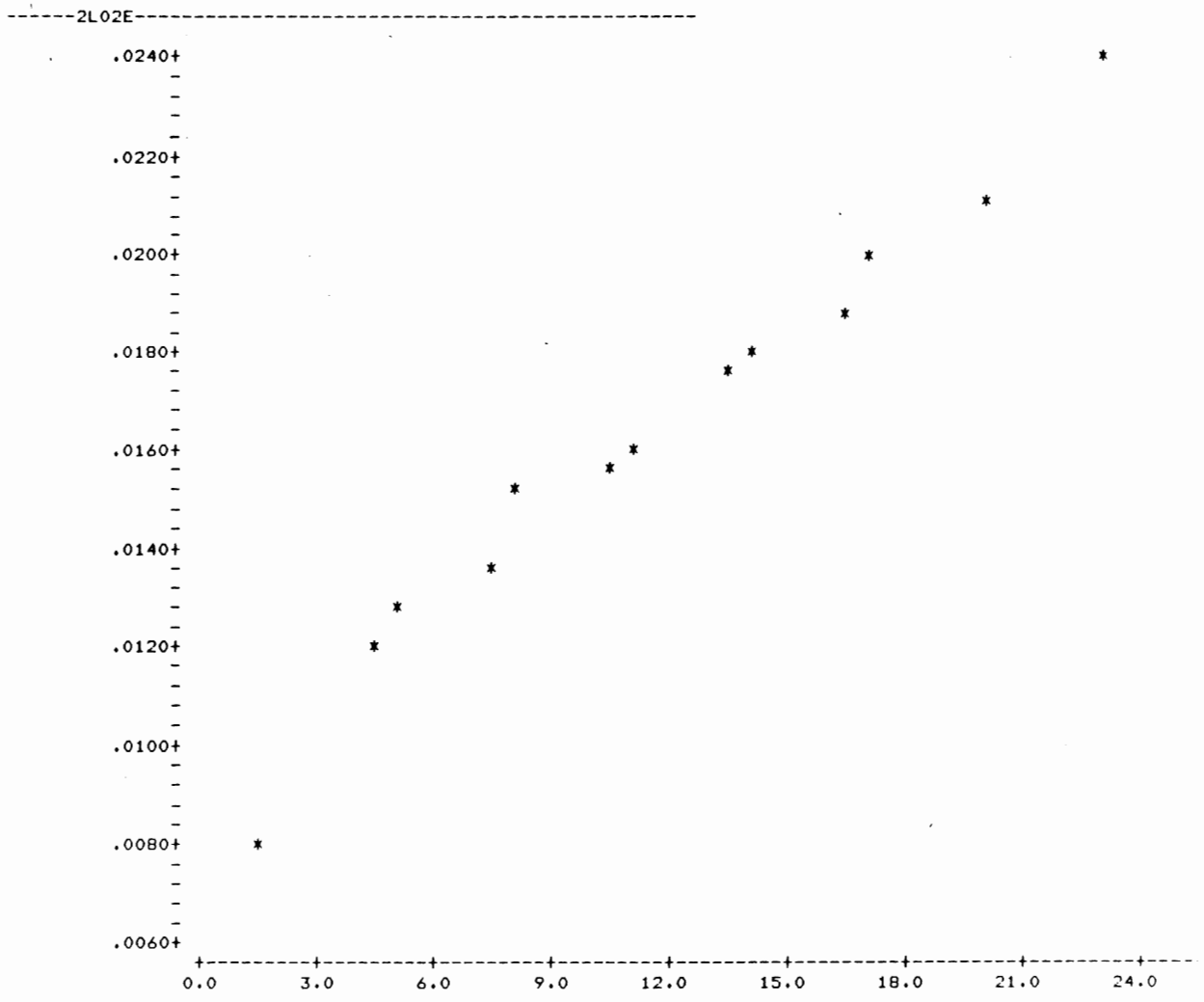
------2L02E----------
.0240+
.0220+
.0200+
.0180+
.0160+
.0140+
.0120+
.0100+
.0080+
.0060+
0.0
3.0
6.0
9.0
12.0
15.0
18.0
21.0
24.0

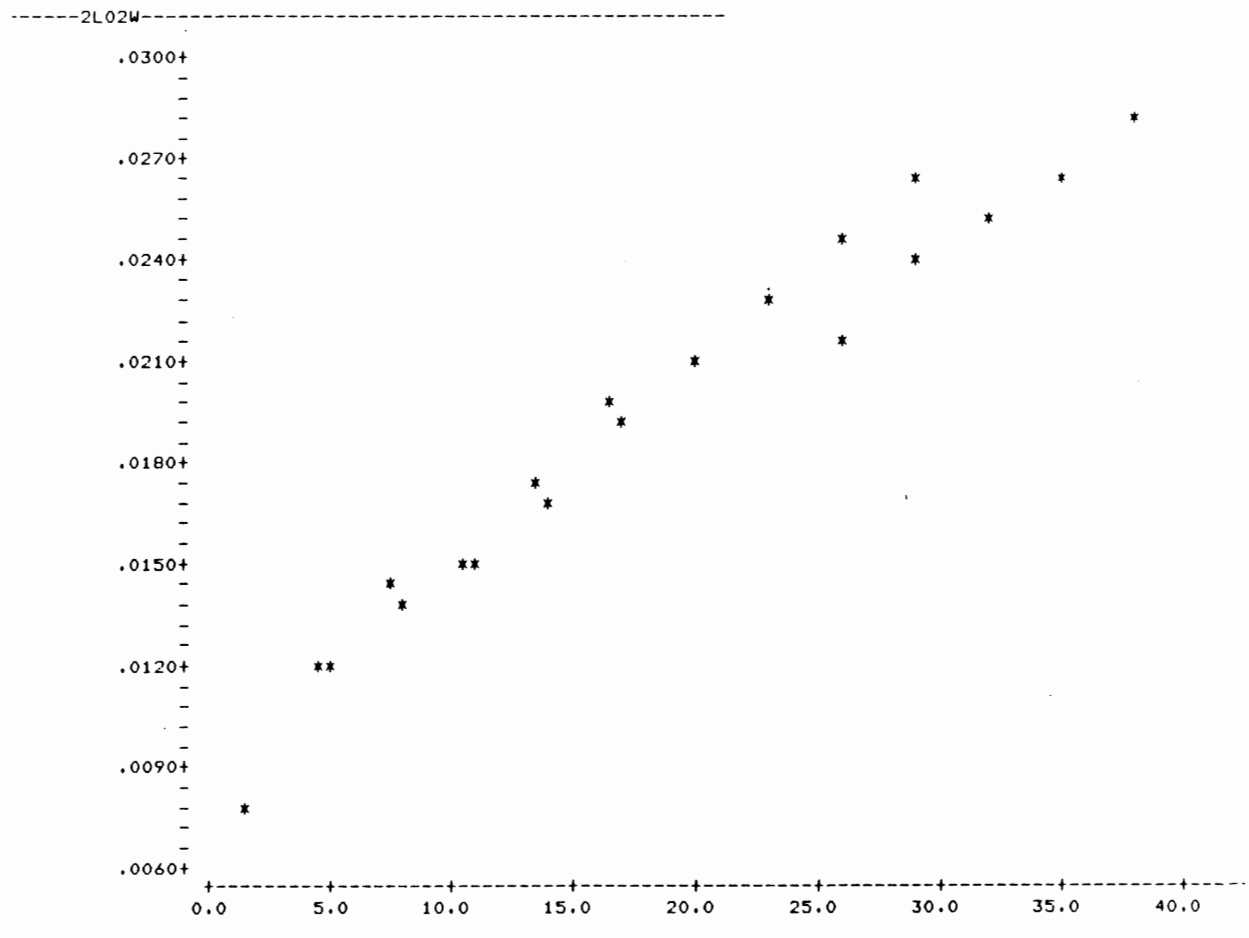
------2L02W----------
.0300+
.0270+
.0240+
.0210+
.0180+
.0150+
.0120+
.0090+
.0060+
0.0
5.0
10.0
15.0
20.0
25.0
30.0
35.0
40.0

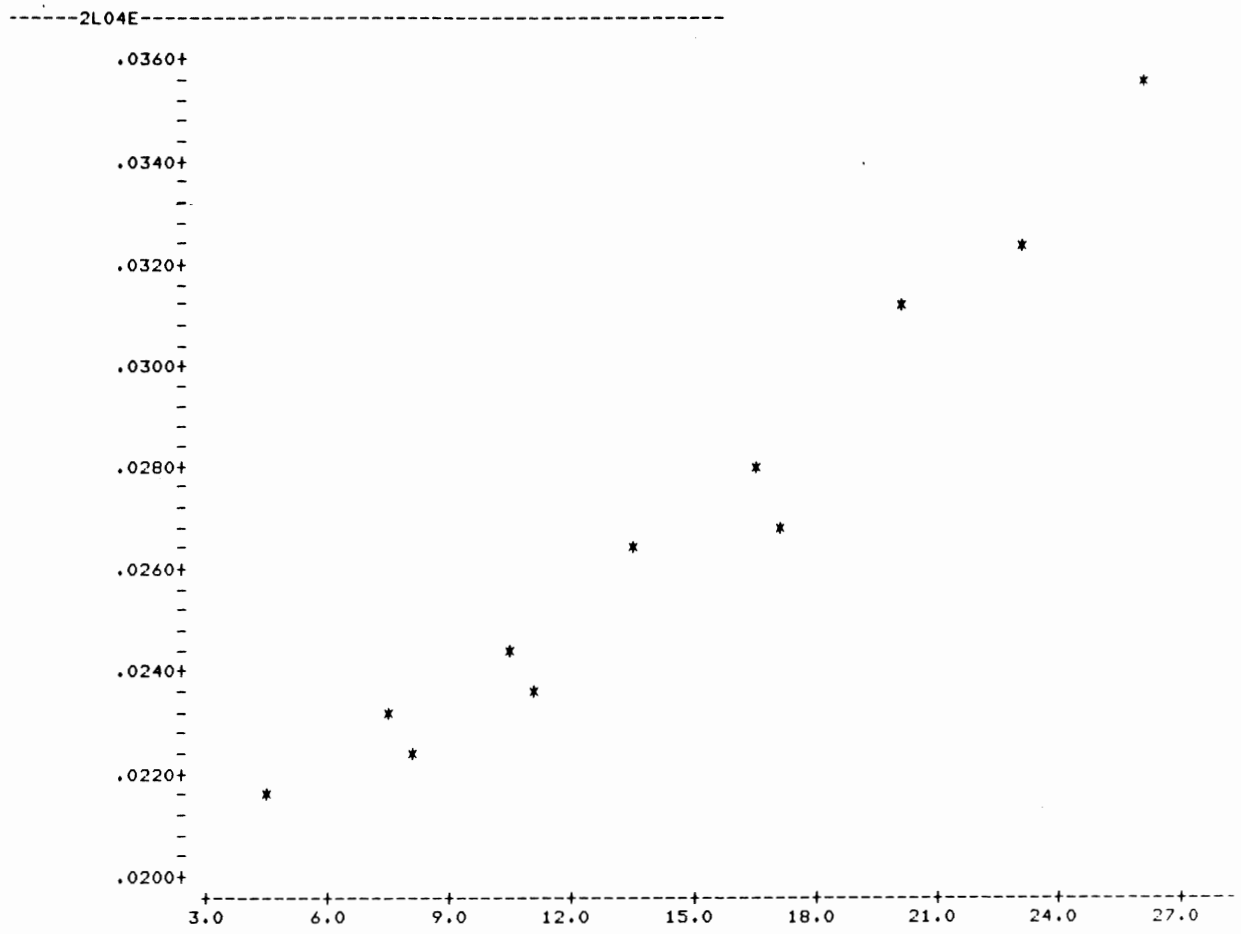
------2L04E----------
.0360+
.0340+
.0320+
.0300+
.0280+
.0260+
.0240+
.0220+
.0200+
3.0
6.0
9.0
12.0
15.0
18.0
21.0
24.0
27.0

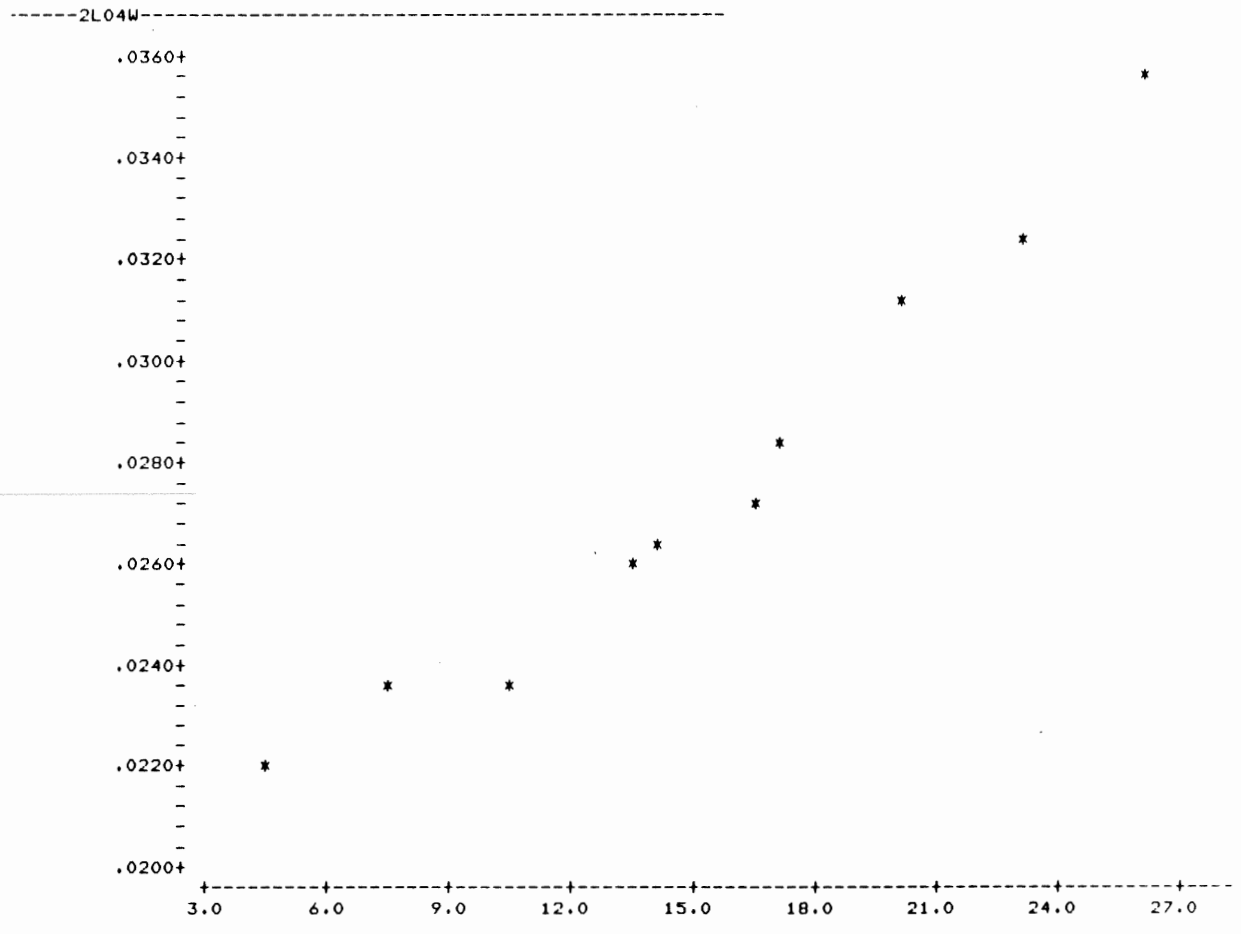
------2L04W----------
.0360+
.0340+
.0320+
.0300+
.0280+
.0260+
.0240+
.0220+
.0200+
3.0
6.0
9.0
12.0
15.0
18.0
21.0
24.0
27.0

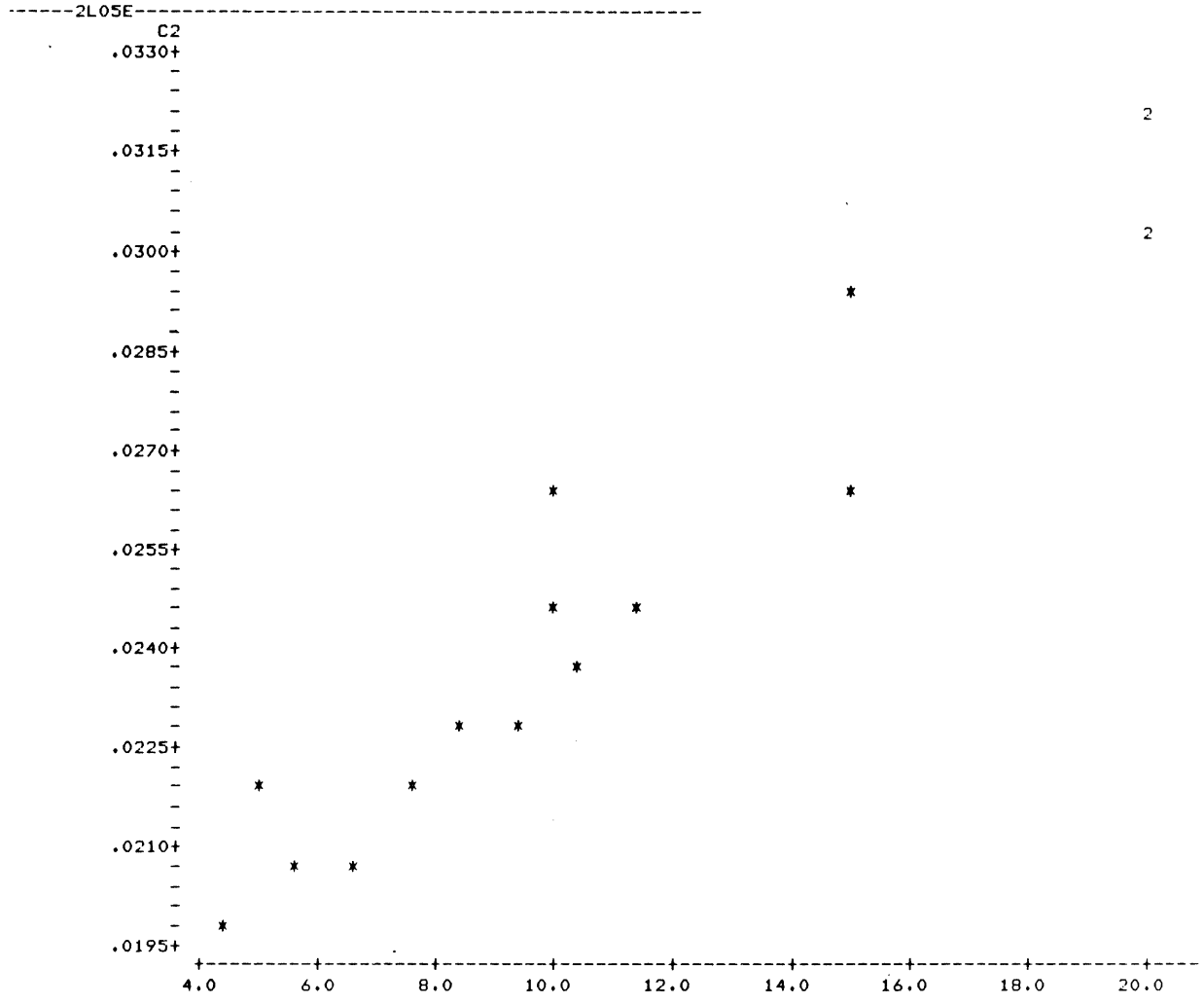
------2L05E----------
C2
.0330+
.0315+
.0300+
.0285+
.0270+
.0255+
.0240+
.0225+
.0210+
.0195+
4.0
6.0
8.0
10.0
12.0
14.0
16.0
18.0
20.0

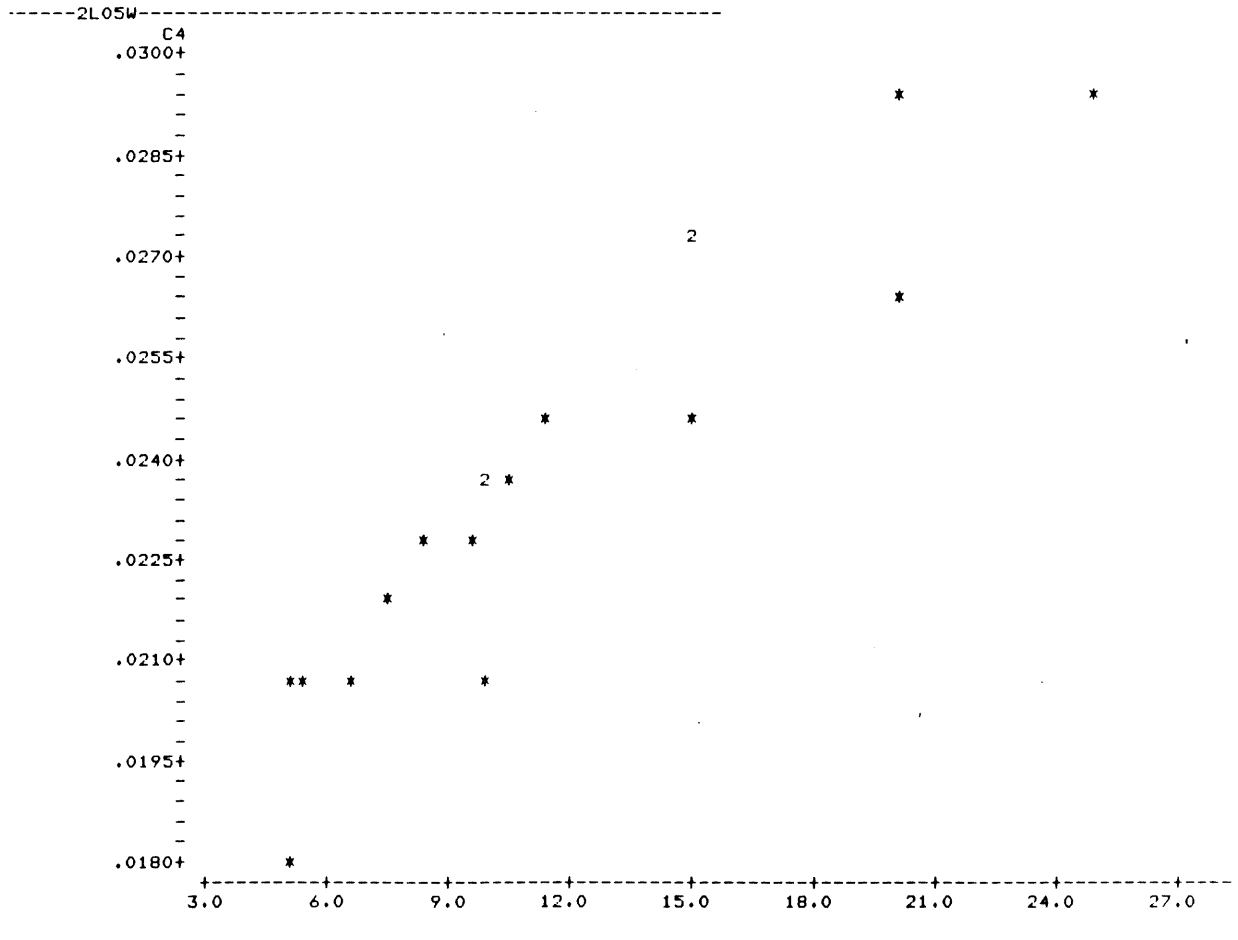
------2L05W----------
C4
.0300+
.0285+
.0270+
.0255+
.0240+
.0225+
.0210+
.0195+
.0180+
3.0
6.0
9.0
12.0
15.0
18.0
21.0
24.0
27.0

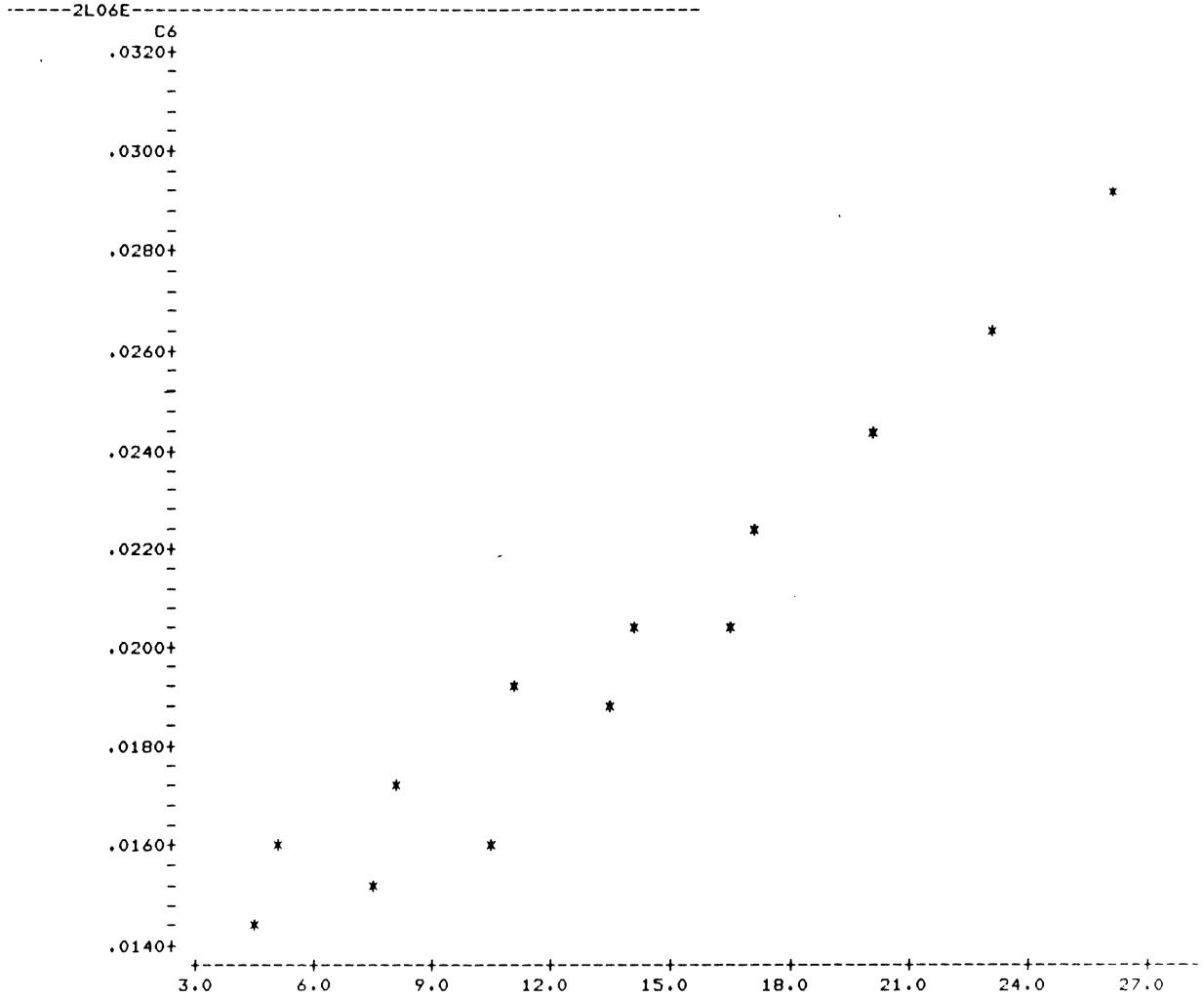
------2L06E----------
C6
.0320+
.0300+
.0280+
.0260+
.0240+
.0220+
.0200+
.0180+
.0160+
.0140+
3.0
6.0
9.0
12.0
15.0
18.0
21.0
24.0
27.0

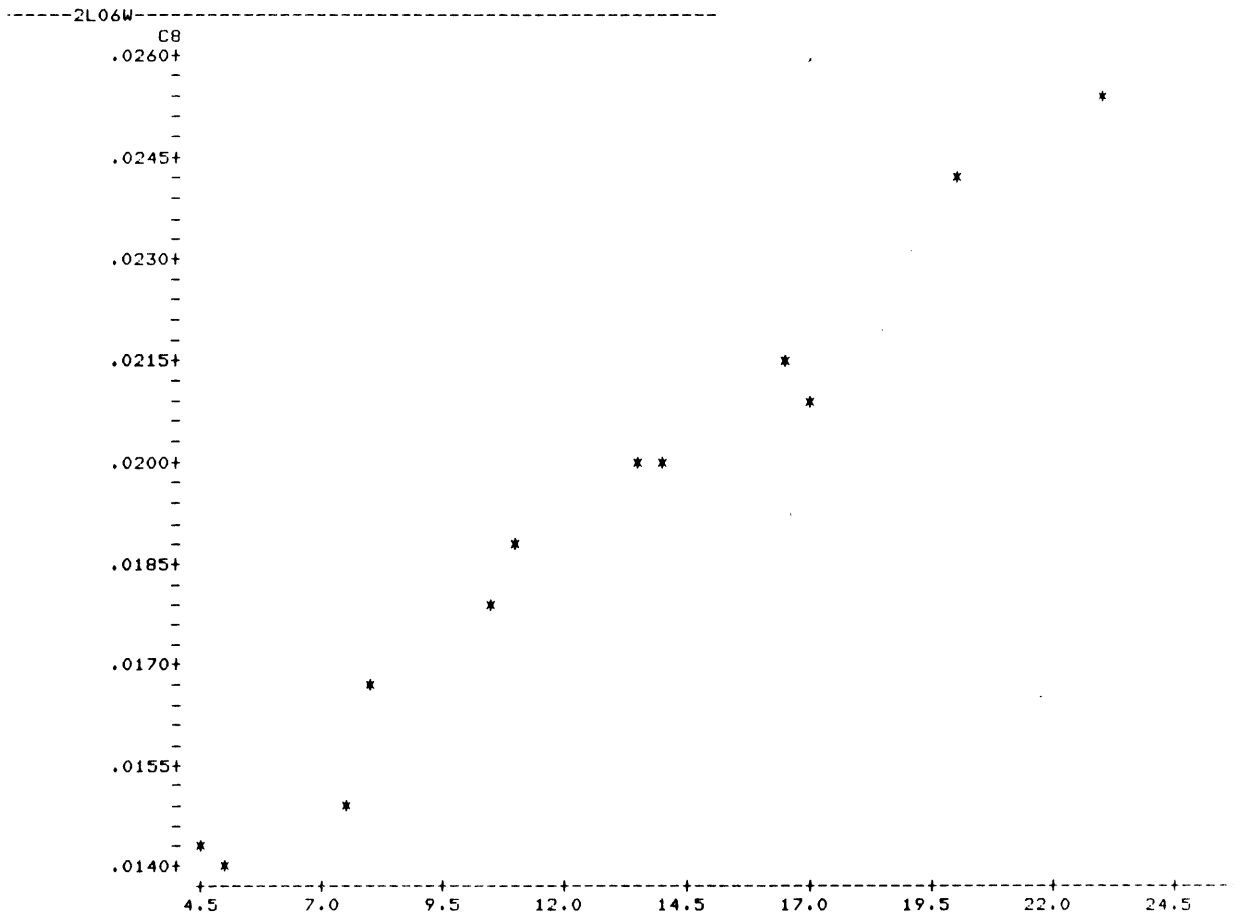
------2L06W----------
C8
.0260+
.0245+
.0230+
.0215+
.0200+
.0185+
.0170+
.0155+
.0140+
4.5
7.0
9.5
12.0
14.5
17.0
19.5
22.0
24.5

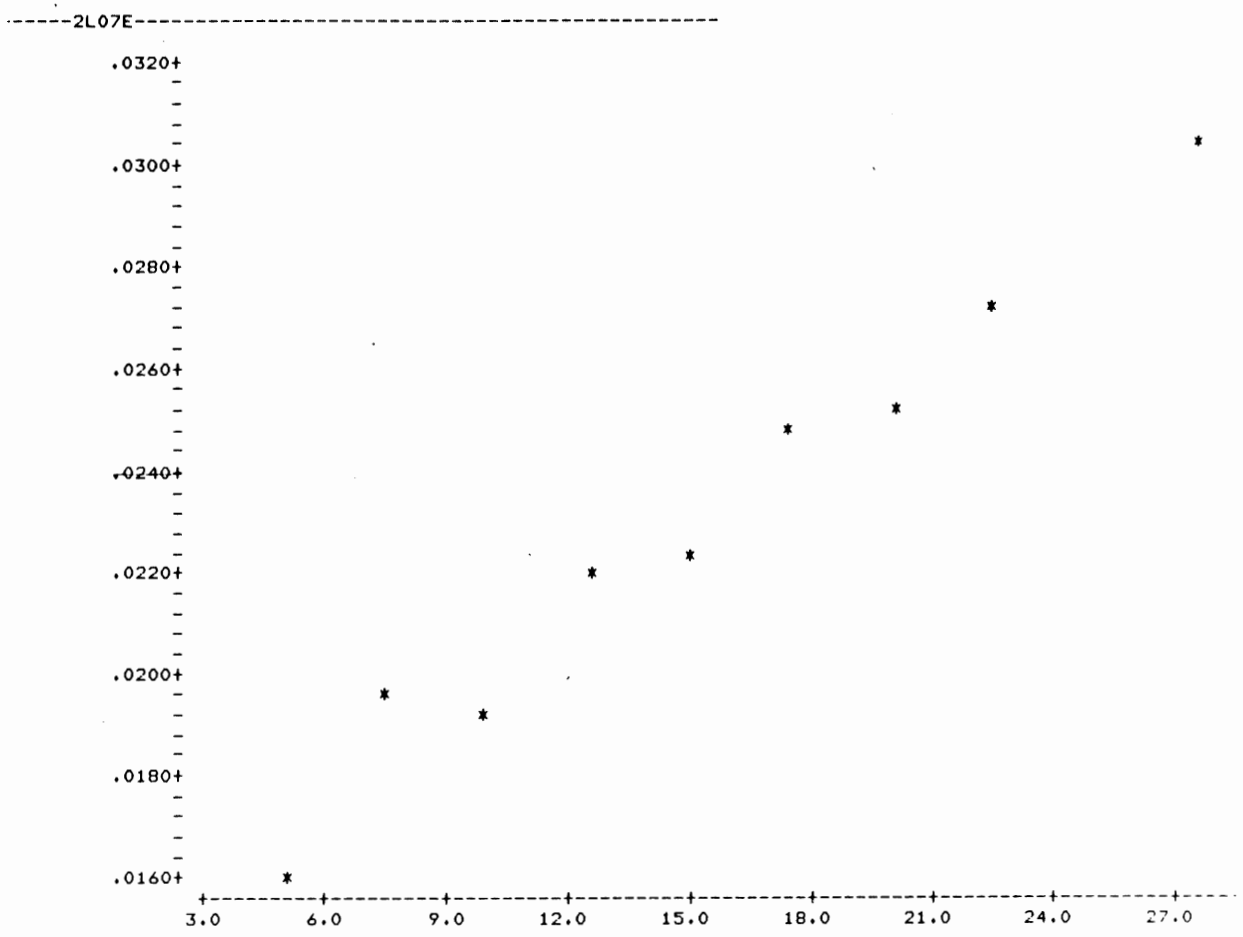
-----2L07E----------
.0320+
.0300+
.0280+
.0260+
.0240+
.0220+
.0200+
.0180+
.0160+
3.0
6.0
9.0
12.0
15.0
18.0
21.0
24.0
27.0

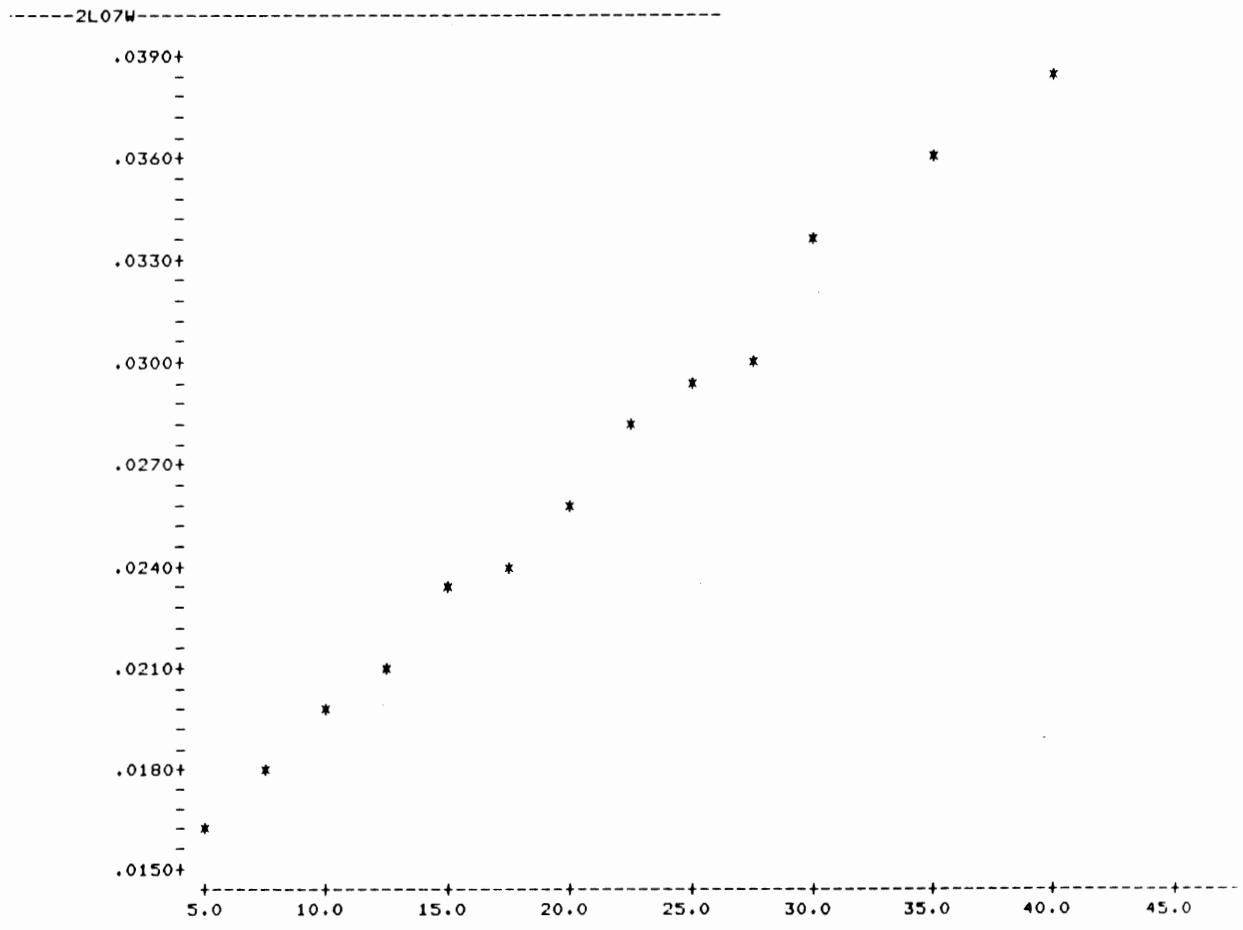
-----2L07W----------
.0390+
.0360+
.0330+
.0300+
.0270+
.0240+
.0210+
.0180+
.0150+
5.0
10.0
15.0
20.0
25.0
30.0
35.0
40.0
45.0

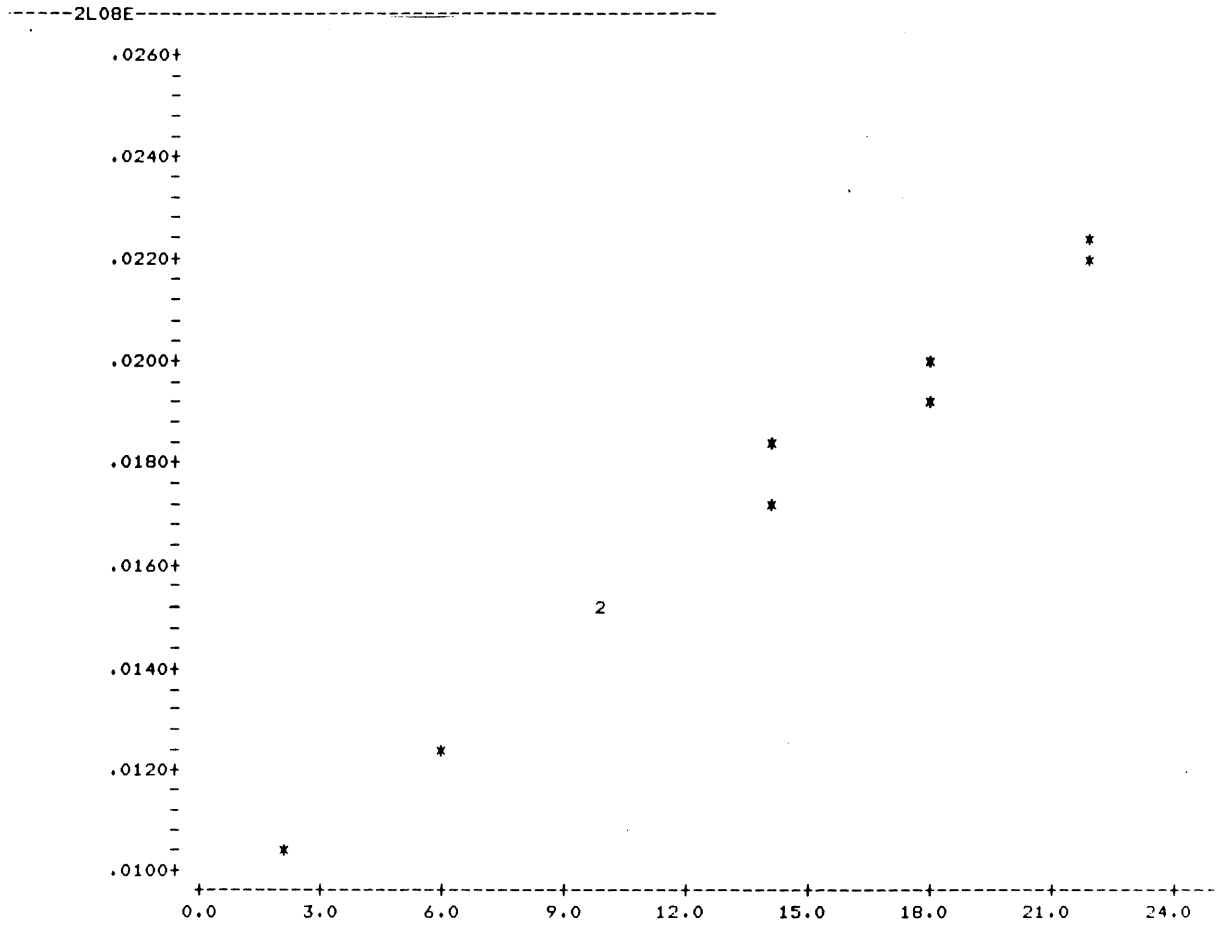
-----2L08E----------
.0260+
.0240+
.0220+
.0200+
.0180+
.0160+
.0140+
.0120+
.0100+
2
0.0
3.0
6.0
9.0
12.0
15.0
18.0
21.0
24.0

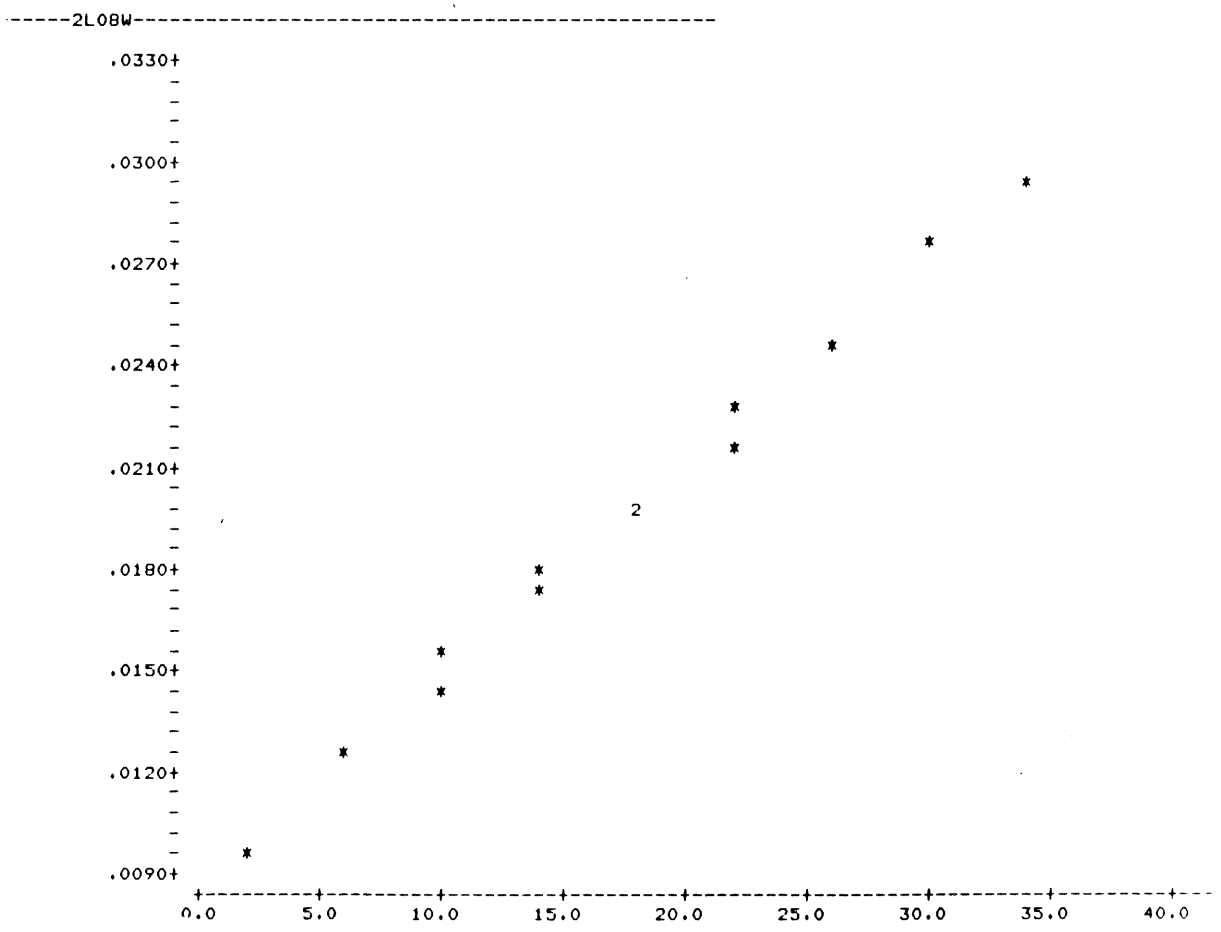
-----2L08W----------
.0330+
.0300+
.0270+
.0240+
.0210+
.0180+
.0150+
.0120+
.0090+
2
0.0
5.0
10.0
15.0
20.0
25.0
30.0
35.0
40.0

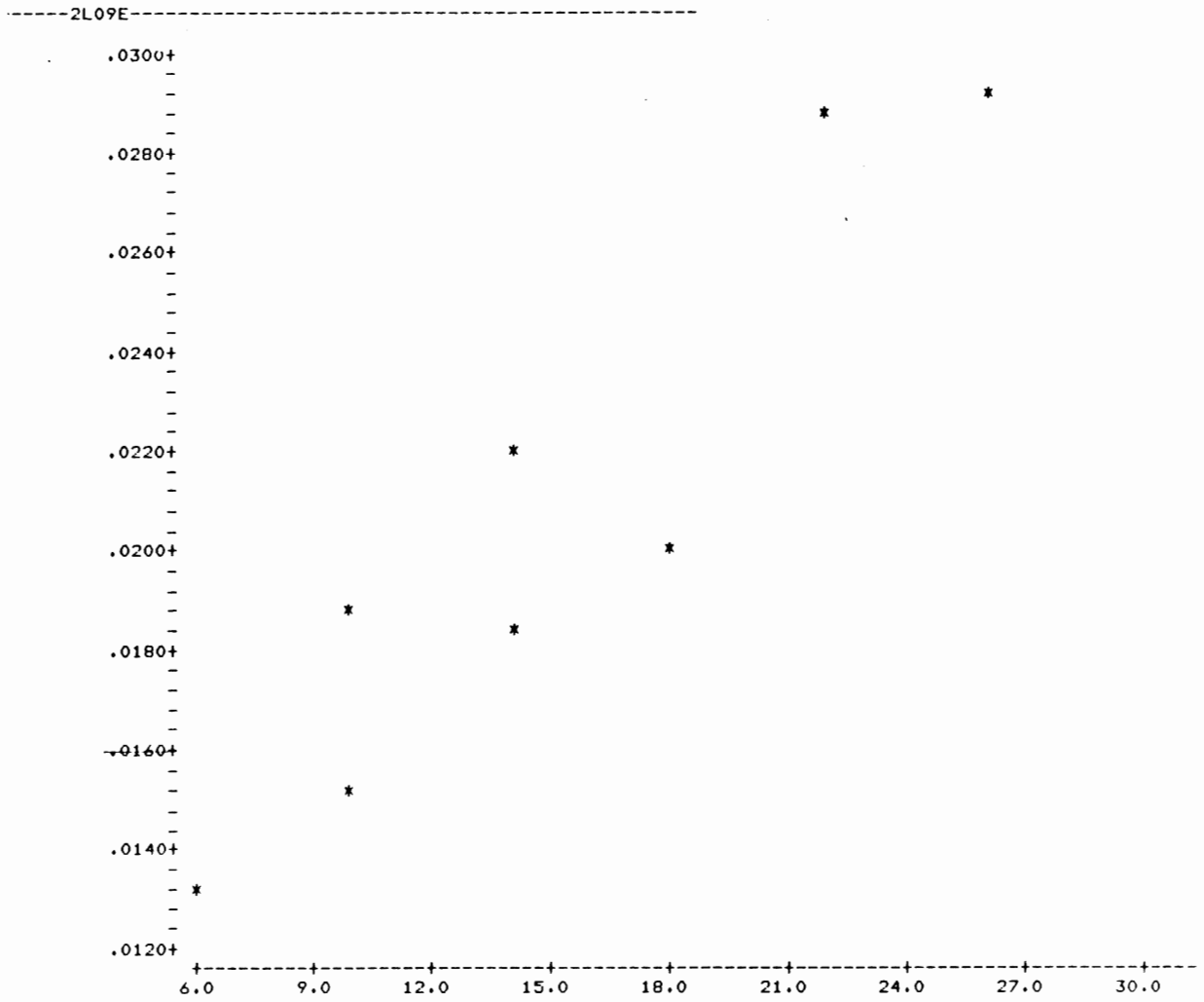
-----2L09E----------
.0300+
.0280+
.0260+
.0240+
.0220+
.0200+
.0180+
.0160+
.0140+
.0120+
6.0
9.0
12.0
15.0
18.0
21.0
24.0
27.0
30.0

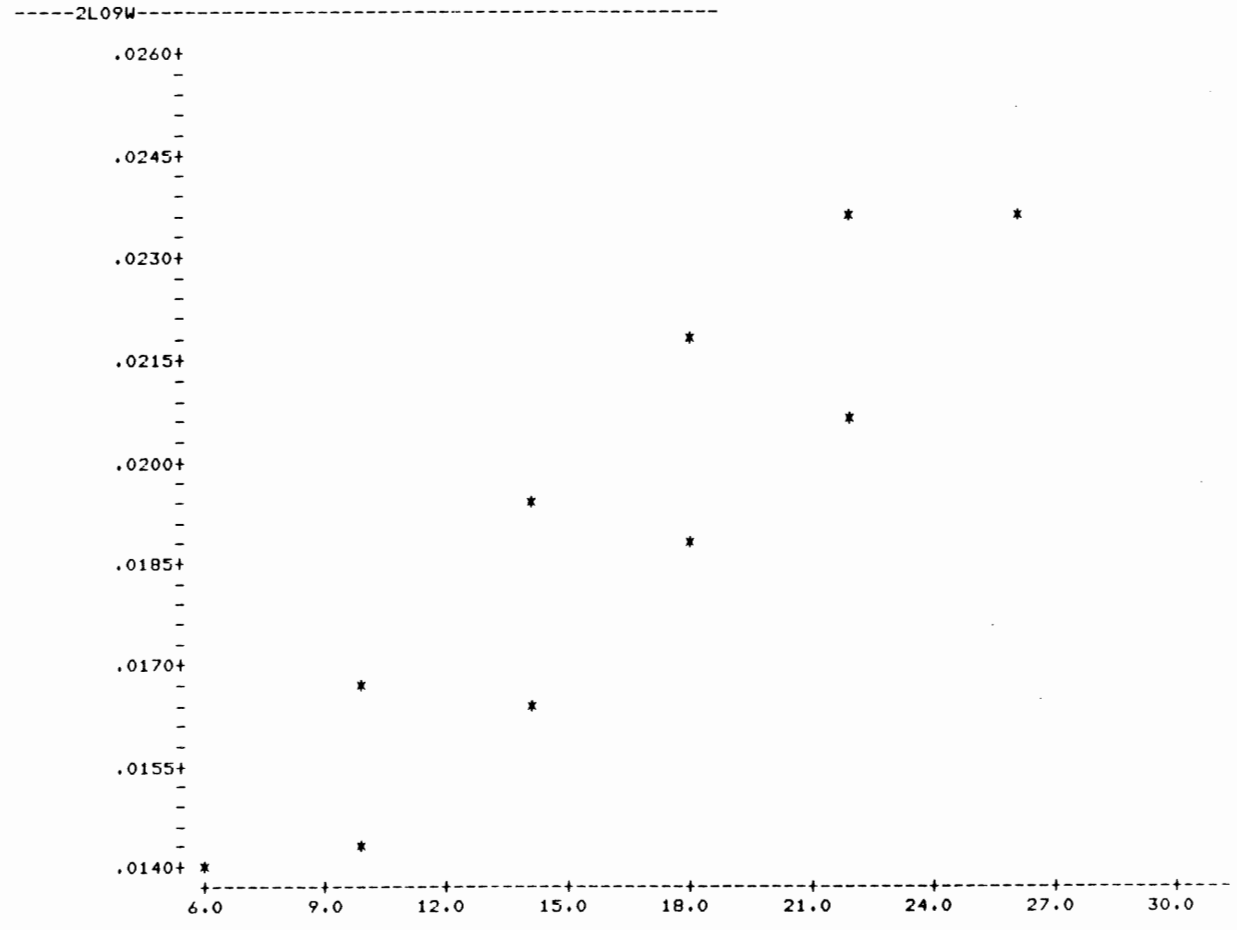
-----2L09W----------
.0260+
.0245+
.0230+
.0215+
.0200+
.0185+
.0170+
.0155+
.0140+
6.0
9.0
12.0
15.0
18.0
21.0
24.0
27.0
30.0

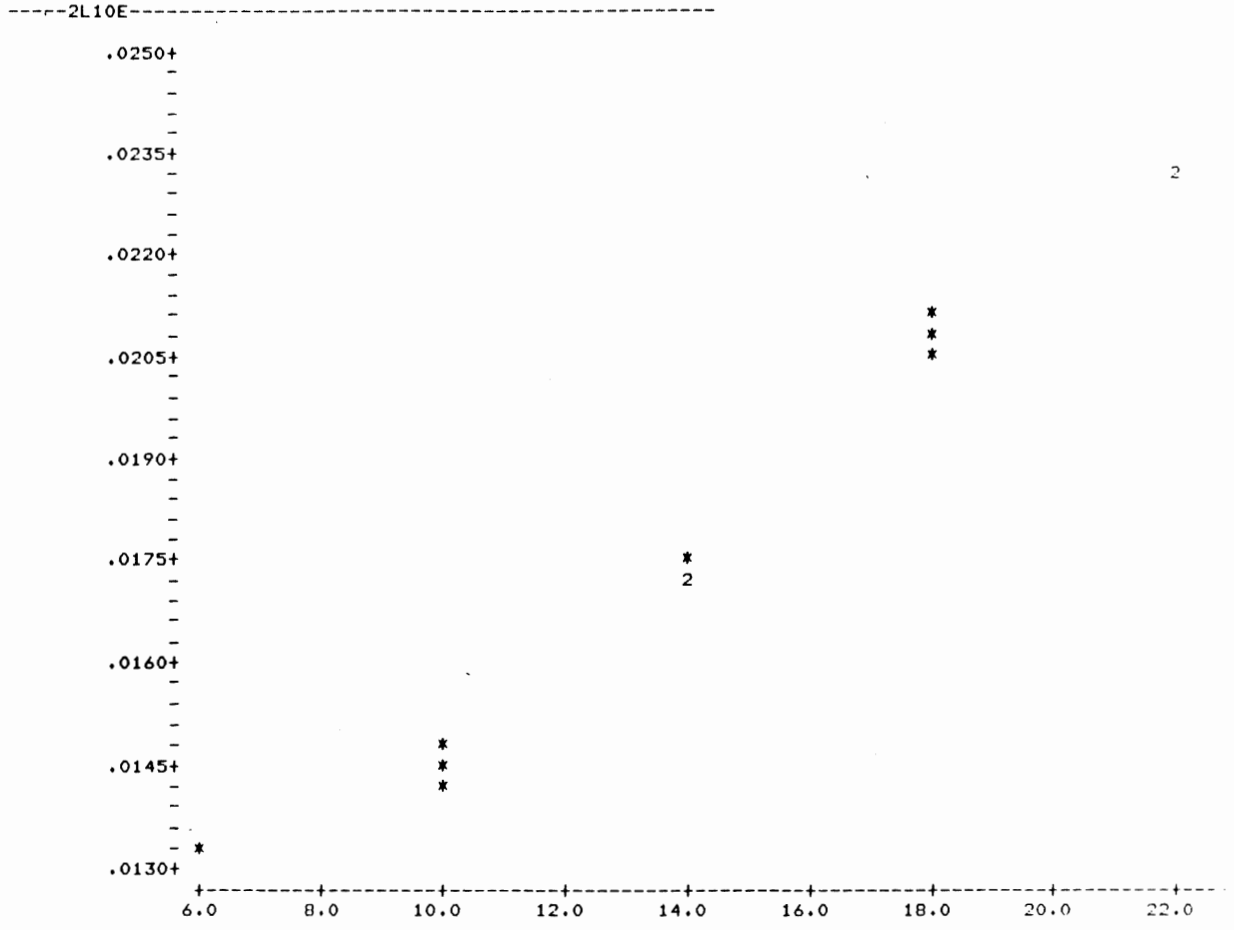
-----2L10E----------
.0250+
.0235+
.0220+
.0205+
.0190+
.0175+
.0160+
.0145+
.0130+
6.0
8.0
10.0
12.0
14.0
16.0
18.0
20.0
22.0

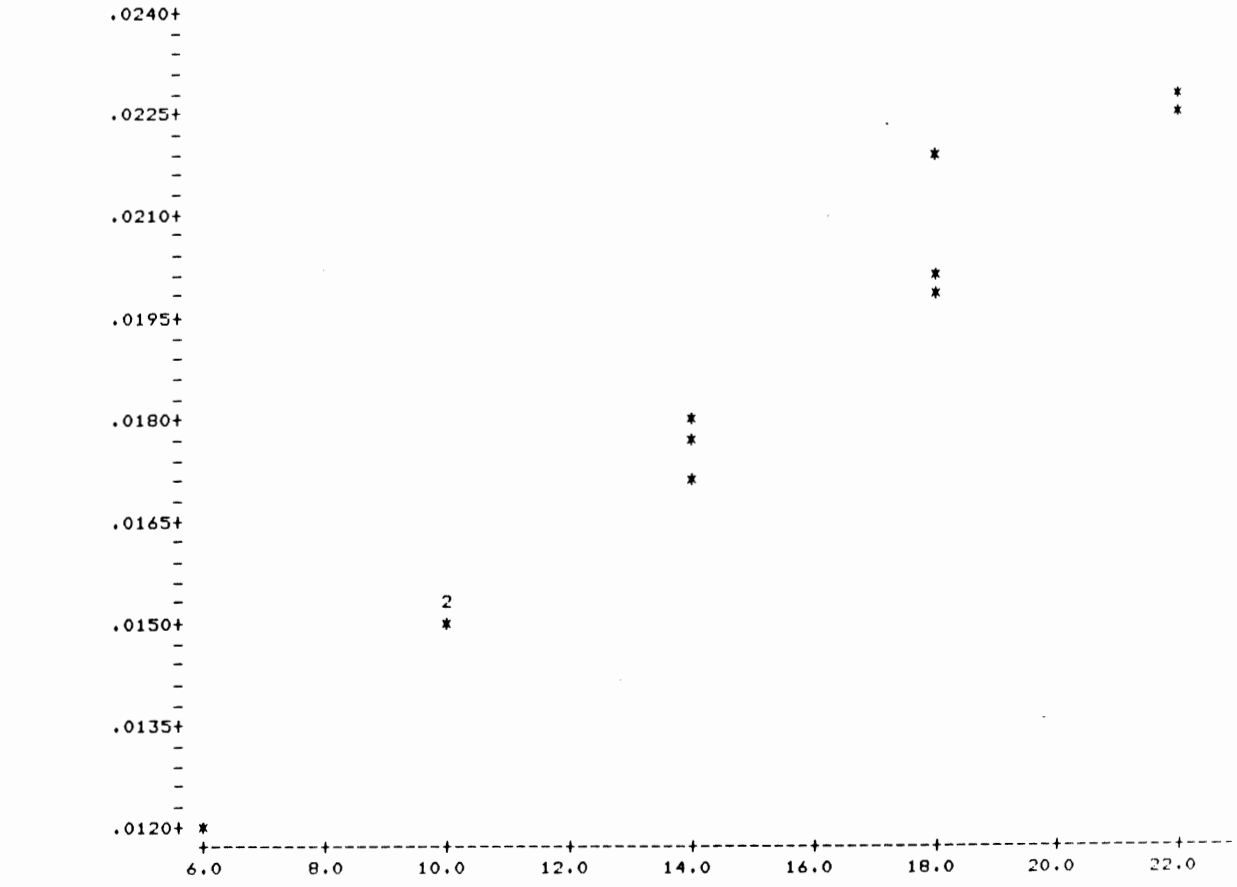
-----2L10W----------
.0240+
.0225+
.0210+
.0195+
.0180+
.0165+
.0150+
.0135+
.0120+
6.0
8.0
10.0
12.0
14.0
16.0
18.0
20.0
22.0

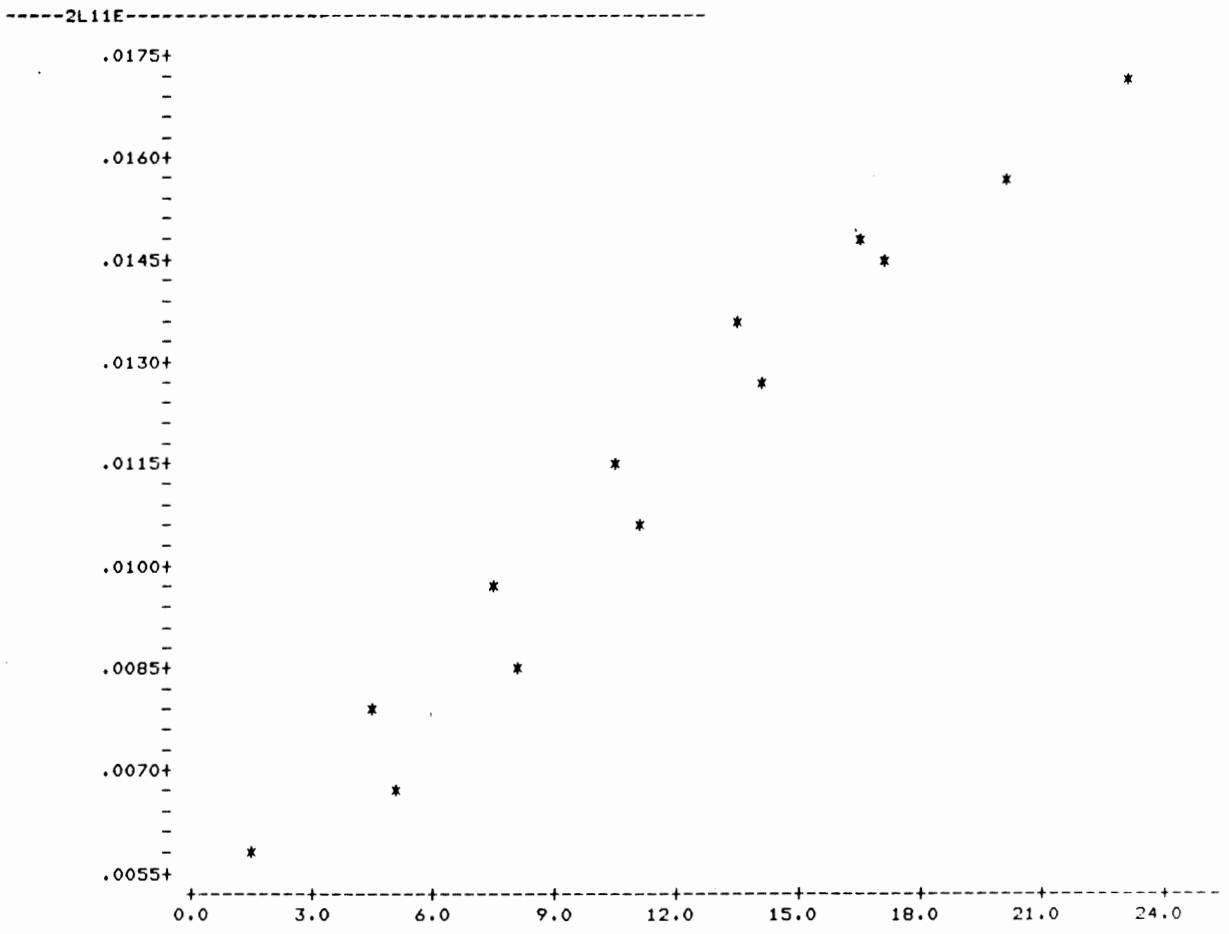
-----2L11E----------
.0175+
.0160+
.0145+
.0130+
.0115+
.0100+
.0085+
.0070+
.0055+
0.0
3.0
6.0
9.0
12.0
15.0
18.0
21.0
24.0

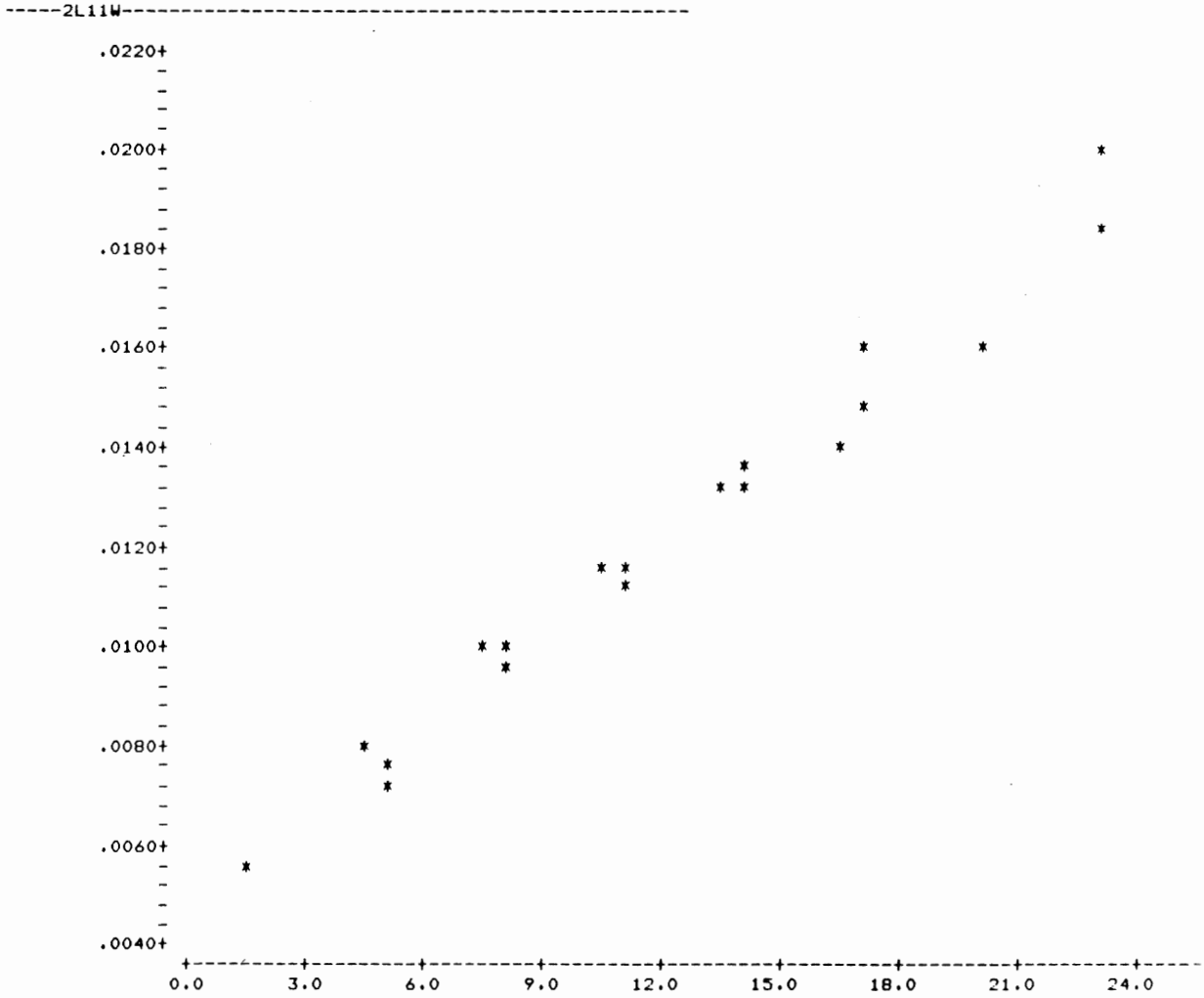
-----2L11W----------
.0220+
.0200+
.0180+
.0160+
.0140+
.0120+
.0100+
.0080+
.0060+
.0040+
0.0
3.0
6.0
9.0
12.0
15.0
18.0
21.0
24.0

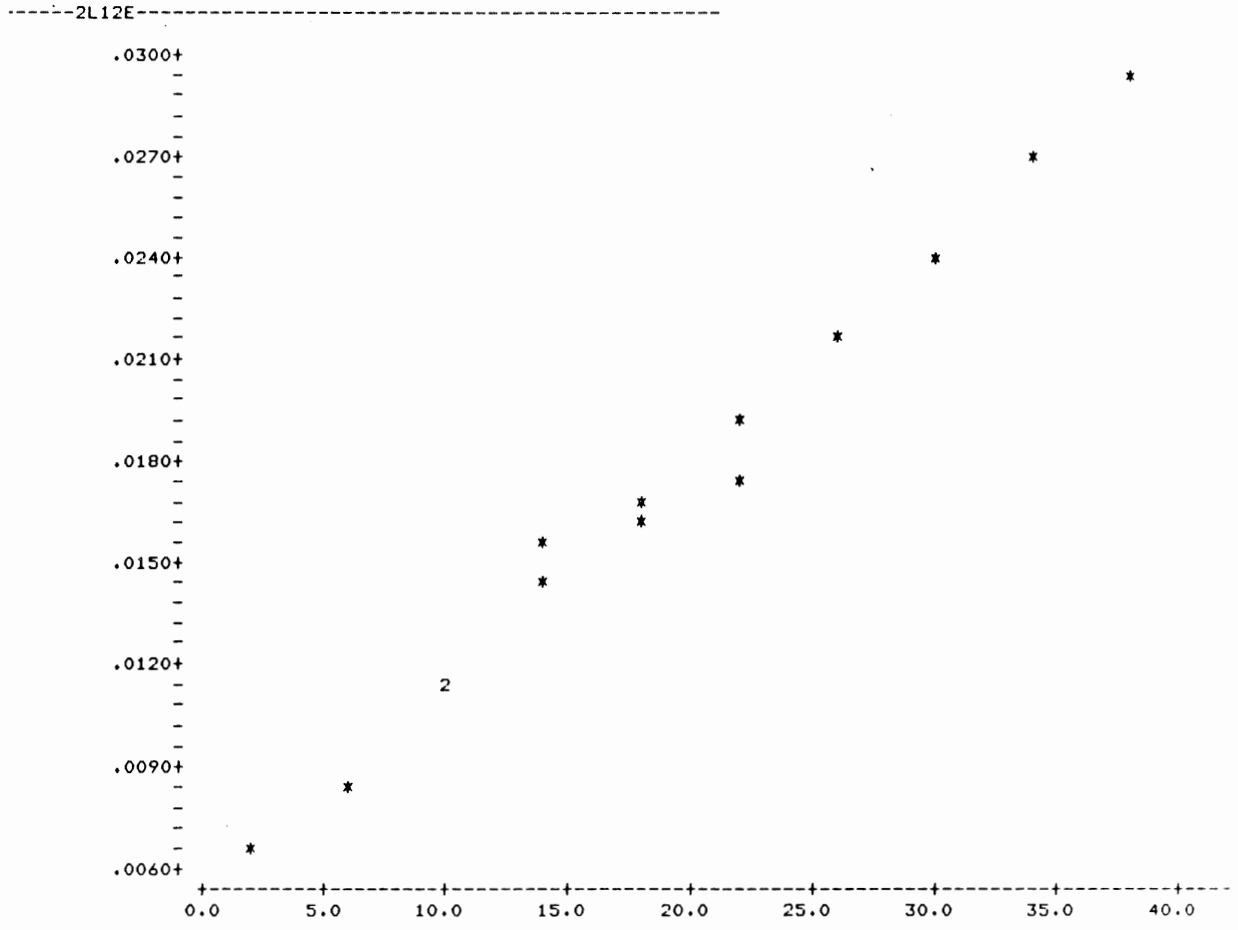
-----2L12E----------
.0300+
.0270+
.0240+
.0210+
.0180+
.0150+
.0120+
.0090+
.0060+
2
0.0
5.0
10.0
15.0
20.0
25.0
30.0
35.0
40.0

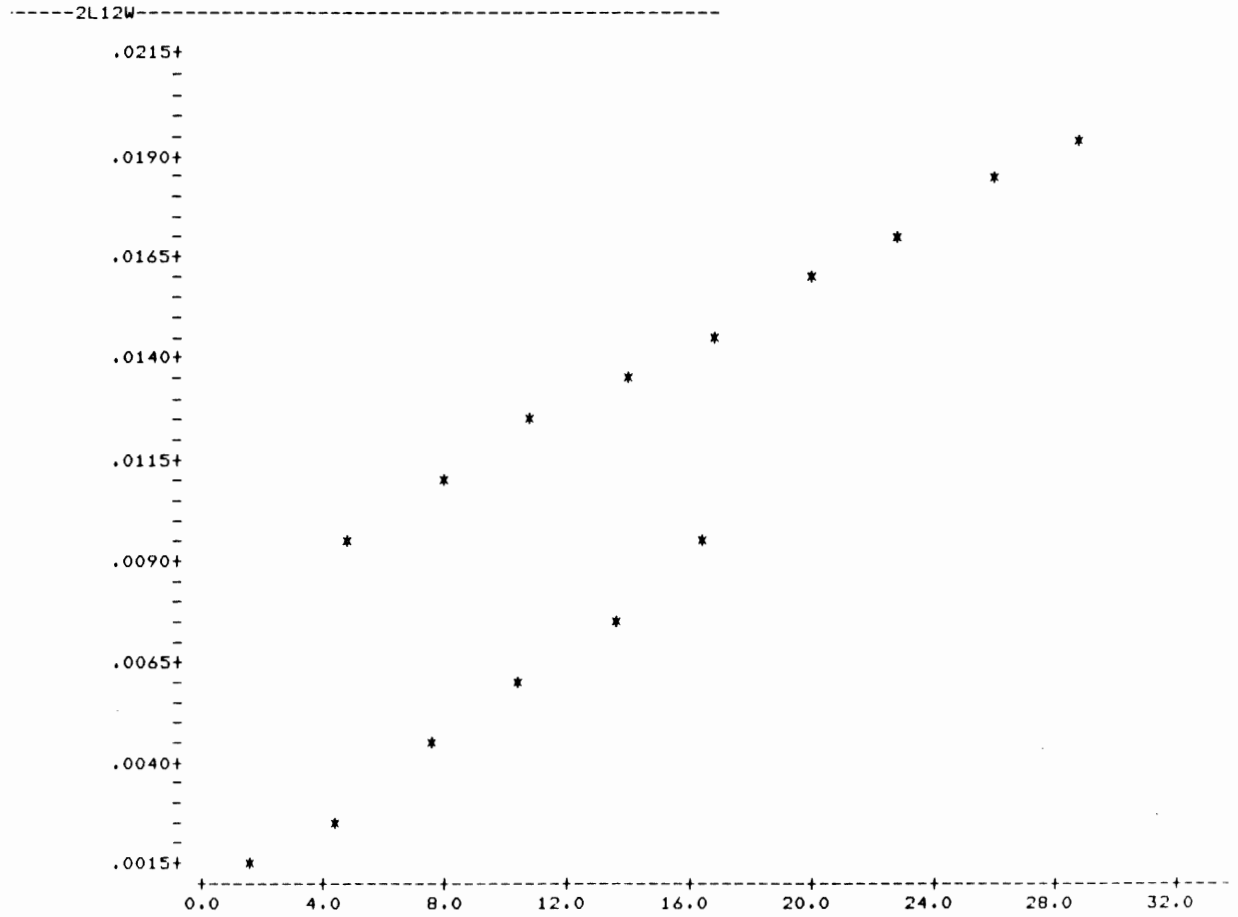
-----2L12W----------
.0215+
.0190+
.0165+
.0140+
.0115+
.0090+
.0065+
.0040+
.0015+
0.0
4.0
8.0
12.0
16.0
20.0
24.0
28.0
32.0

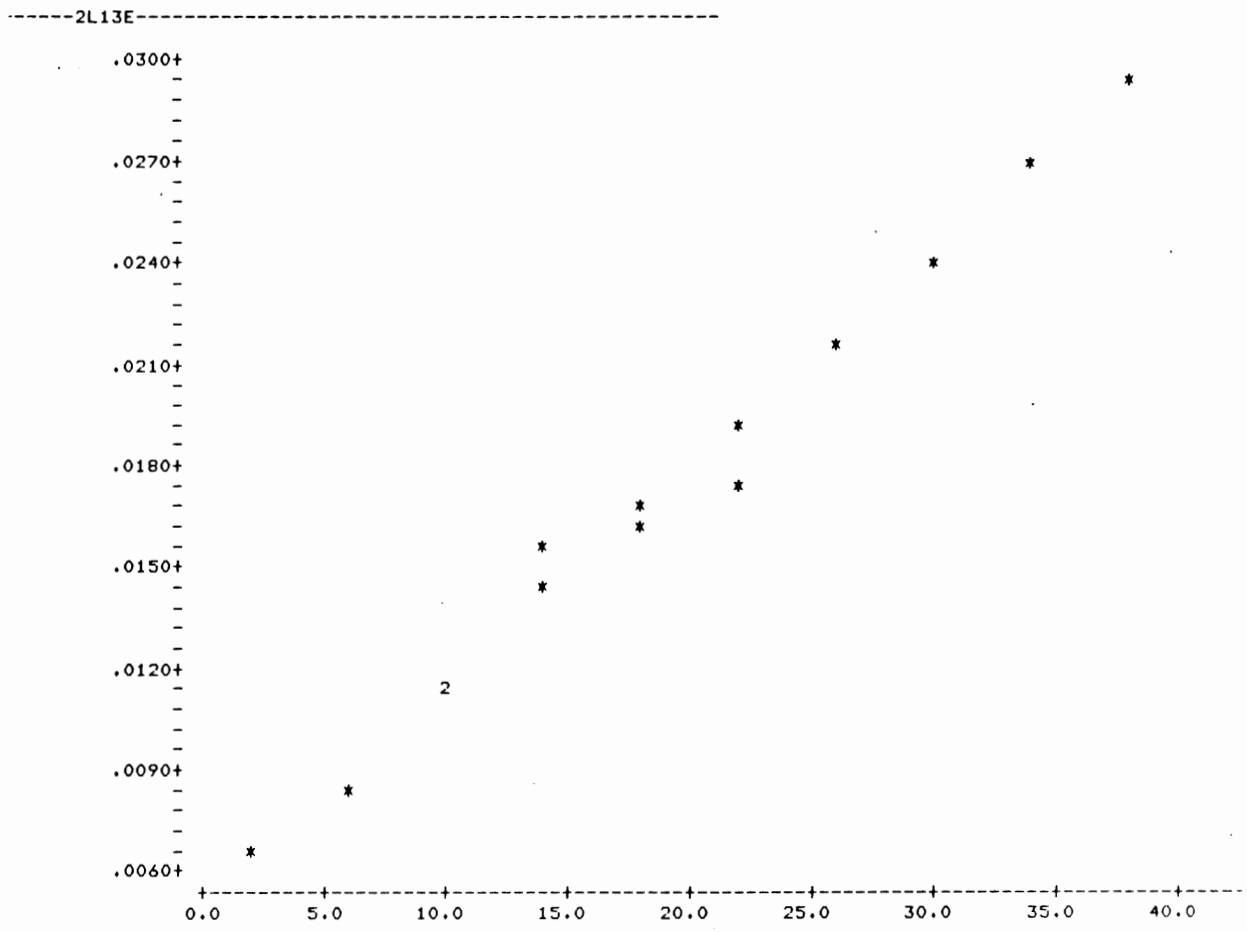
------2L13E----------
.0300+
.0270+
.0240+
.0210+
.0180+
.0150+
.0120+
.0090+
.0060+
2
0.0
5.0
10.0
15.0
20.0
25.0
30.0
35.0
40.0

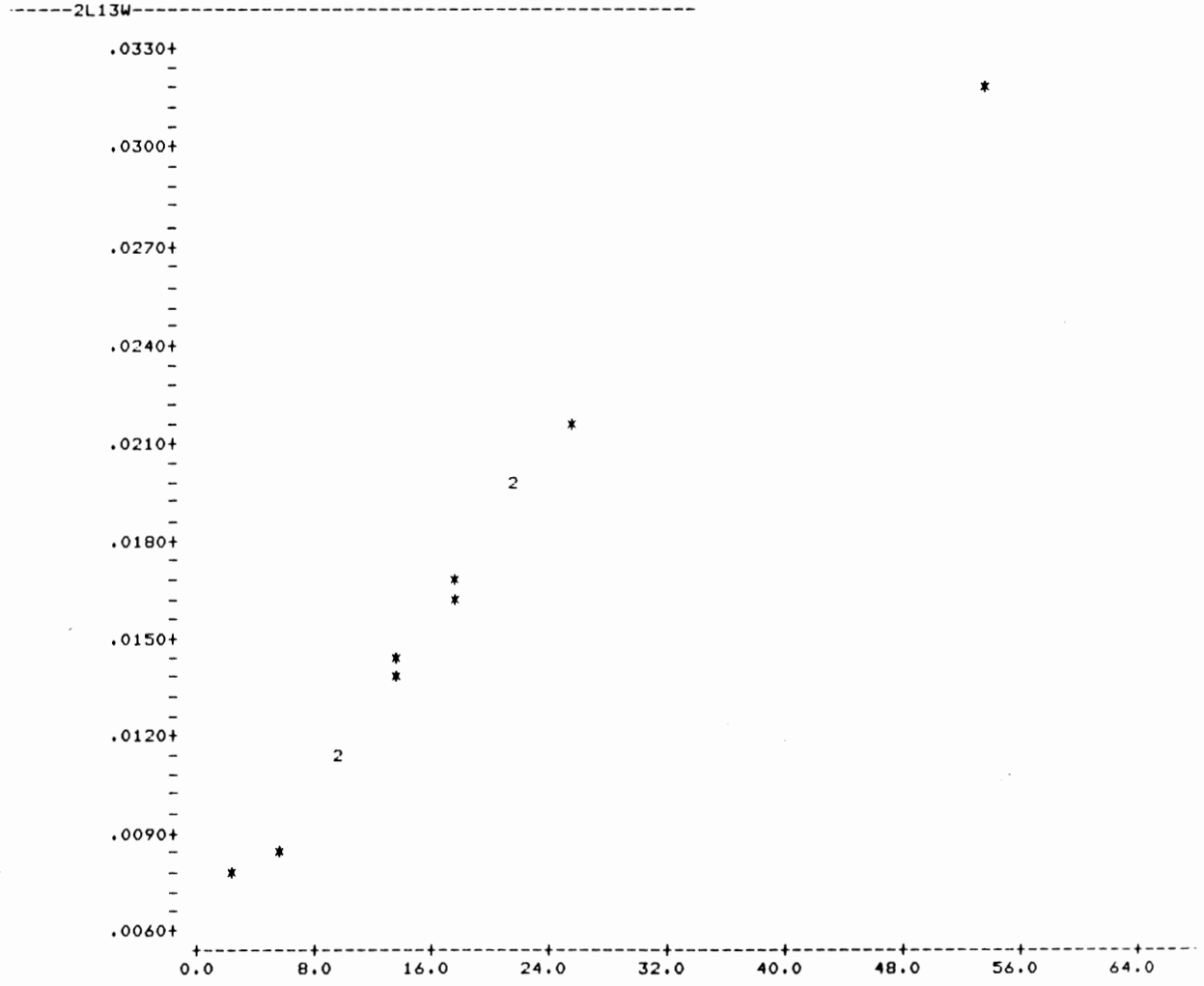
------2L13W----------
.0330+
.0300+
.0270+
.0240+
.0210+
.0180+
.0150+
.0120+
.0090+
.0060+
2
2
0.0
8.0
16.0
24.0
32.0
40.0
48.0
56.0
64.0

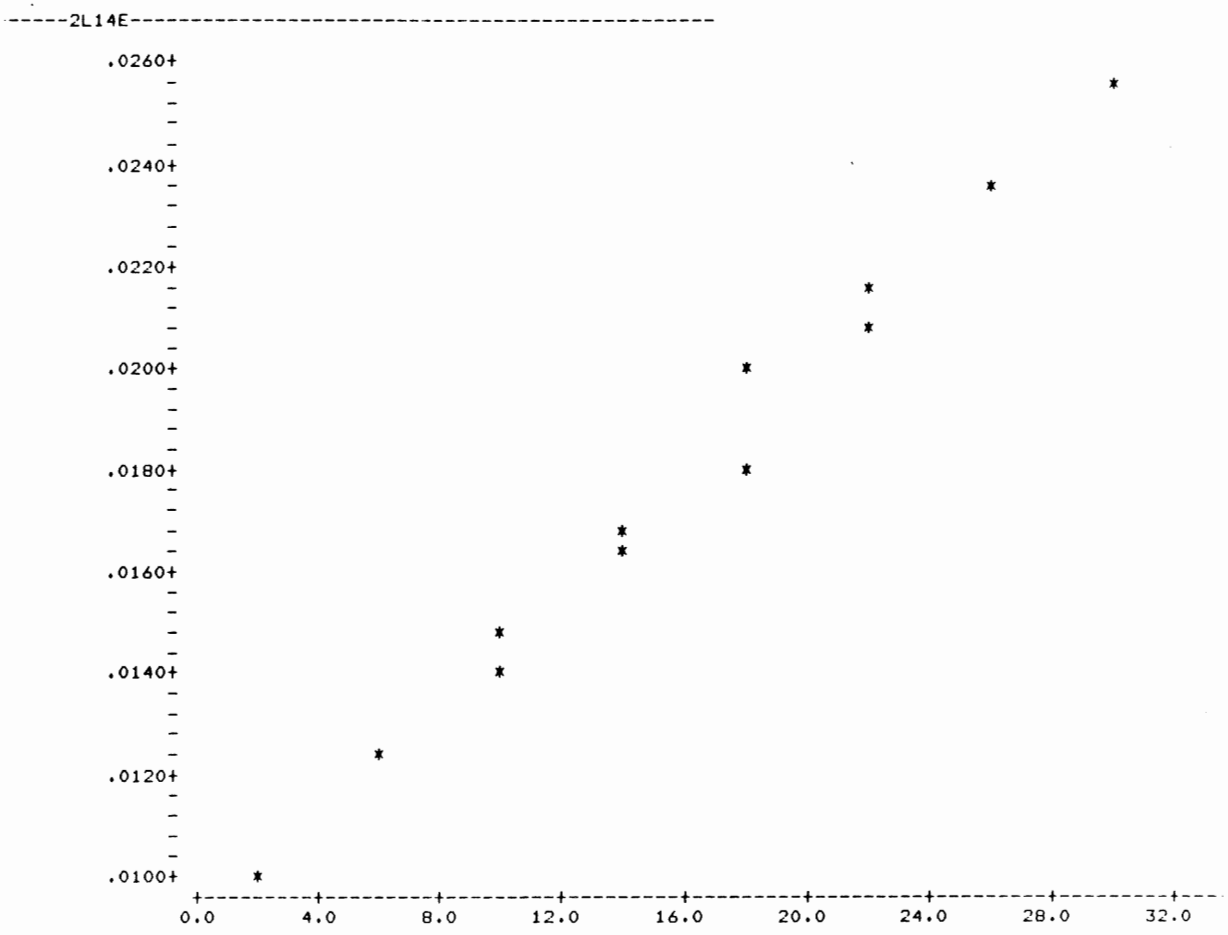
-----2L14E----------
.0260+
.0240+
.0220+
.0200+
.0180+
.0160+
.0140+
.0120+
.0100+
0.0
4.0
8.0
12.0
16.0
20.0
24.0
28.0
32.0

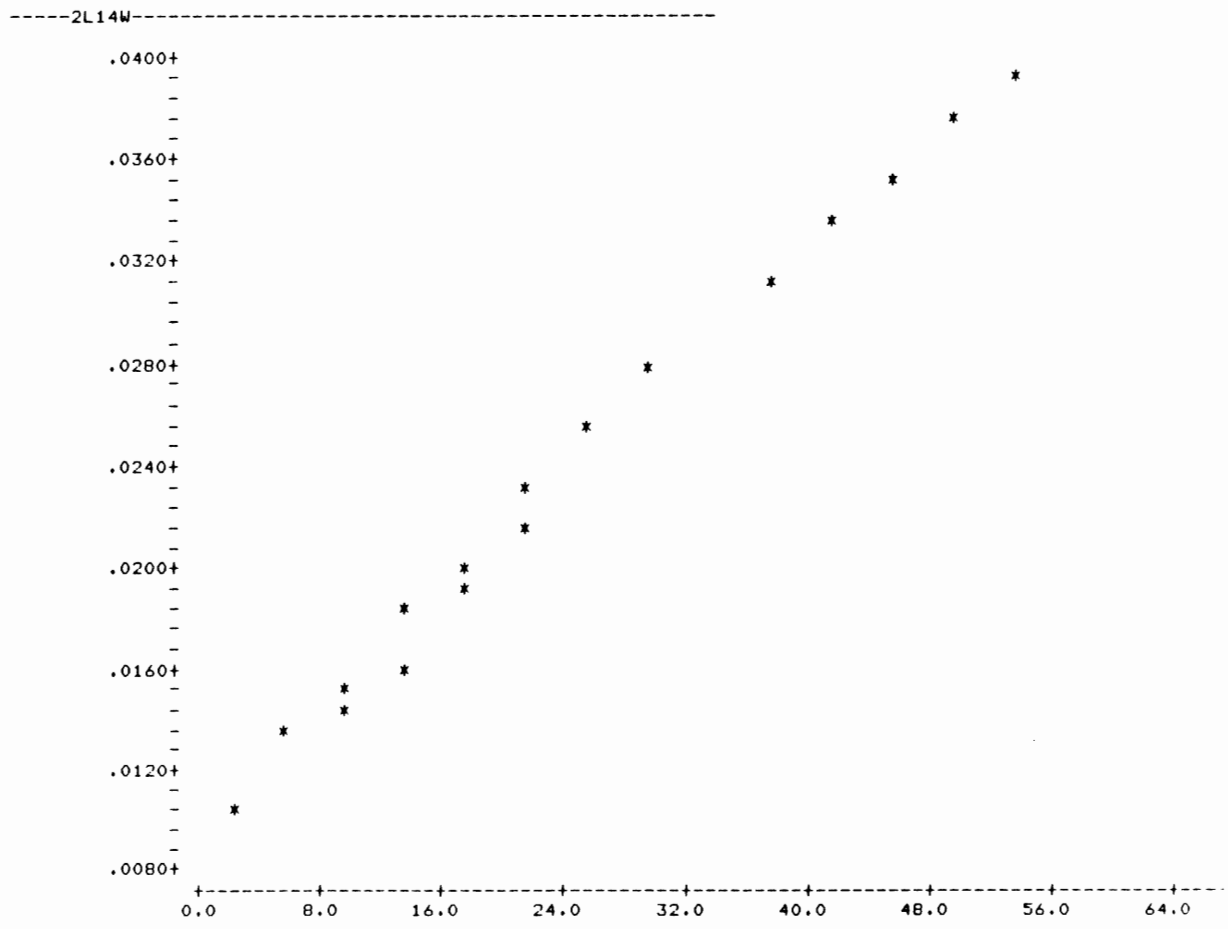
-----2L14W----------
.0400+
.0360+
.0320+
.0280+
.0240+
.0200+
.0160+
.0120+
.0080+
0.0
8.0
16.0
24.0
32.0
40.0
48.0
56.0
64.0

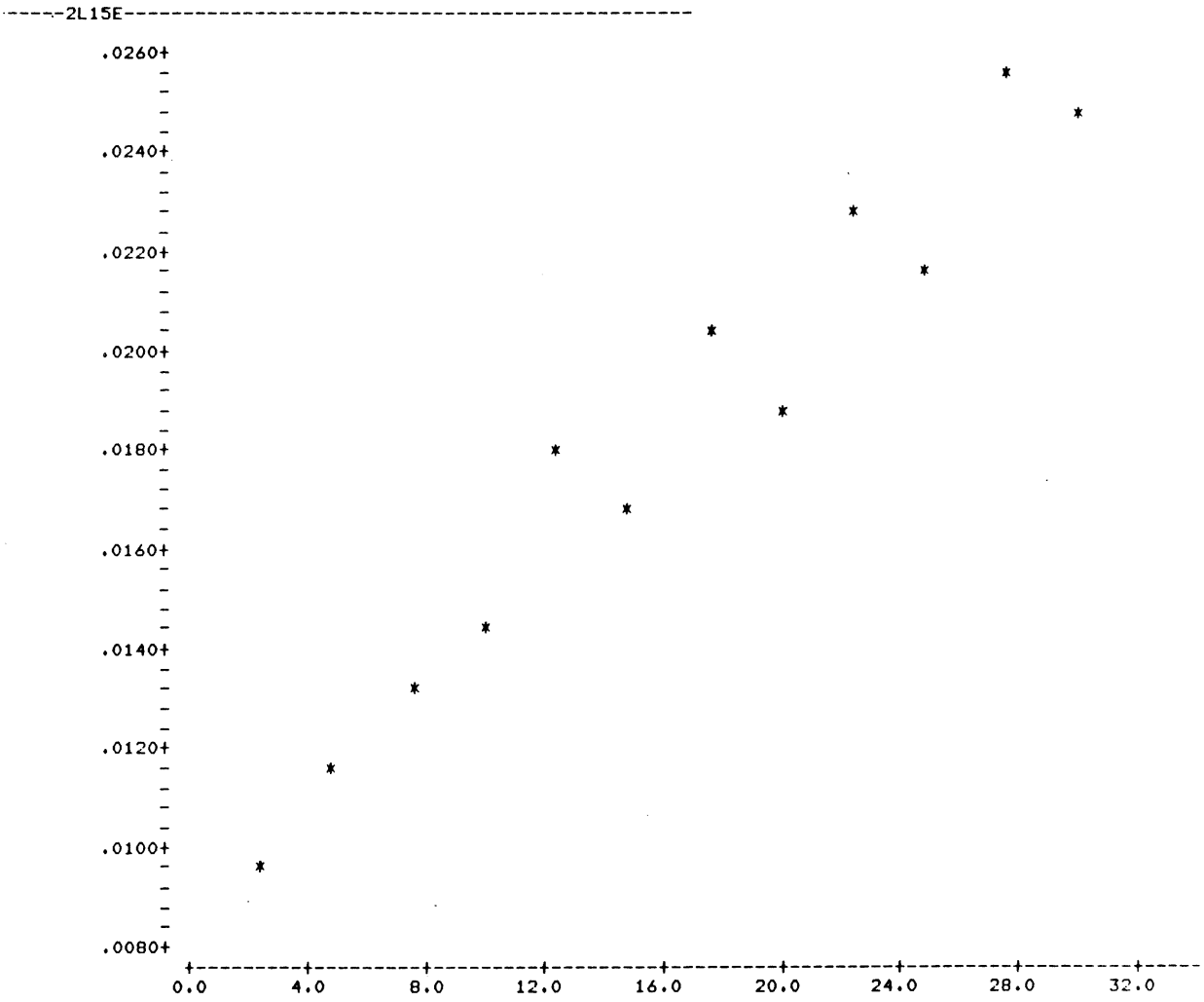
-----2L15E----------
.0260+
.0240+
.0220+
.0200+
.0180+
.0160+
.0140+
.0120+
.0100+
.0080+
0.0
4.0
8.0
12.0
16.0
20.0
24.0
28.0
32.0

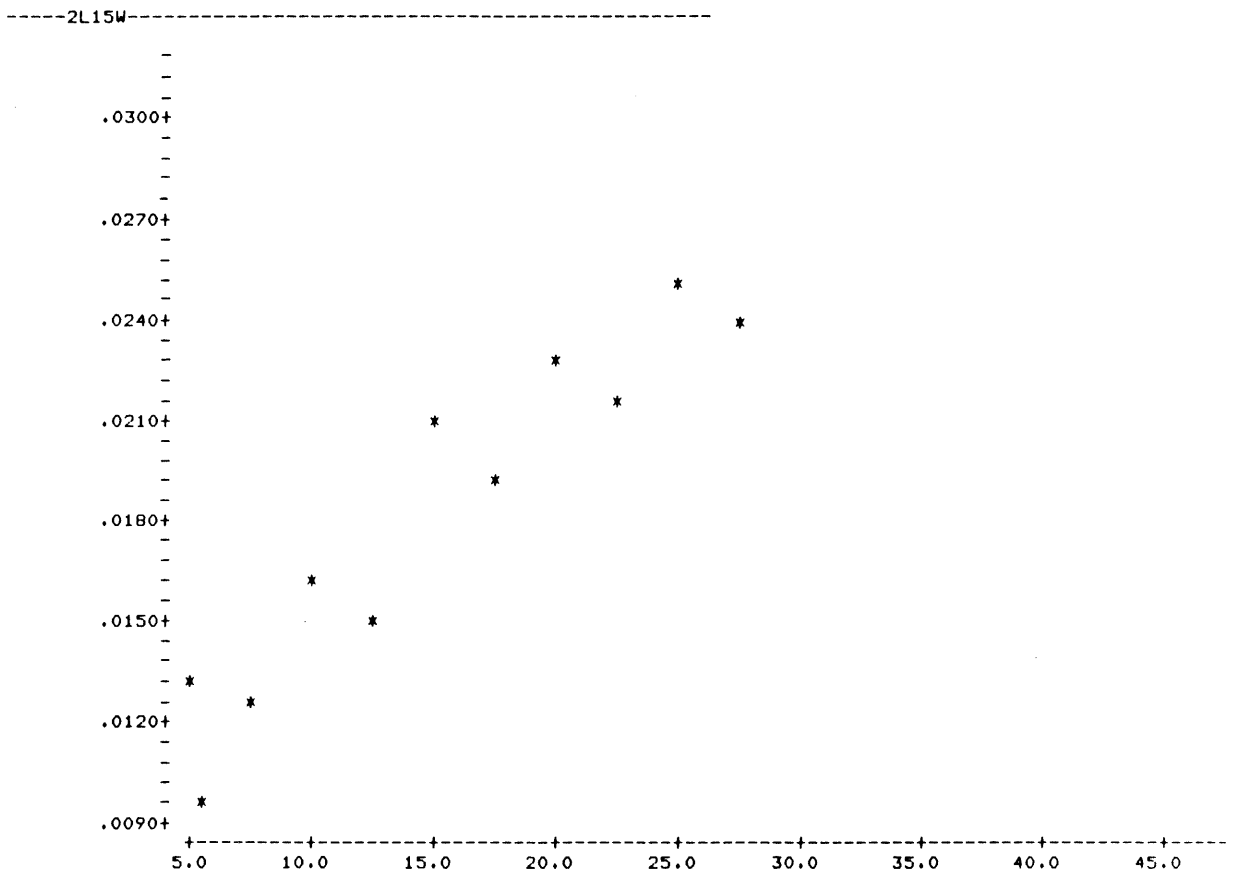
-----2L15W----------
.0300+
.0270+
.0240+
.0210+
.0180+
.0150+
.0120+
.0090+
5.0
10.0
15.0
20.0
25.0
30.0
35.0
40.0
45.0

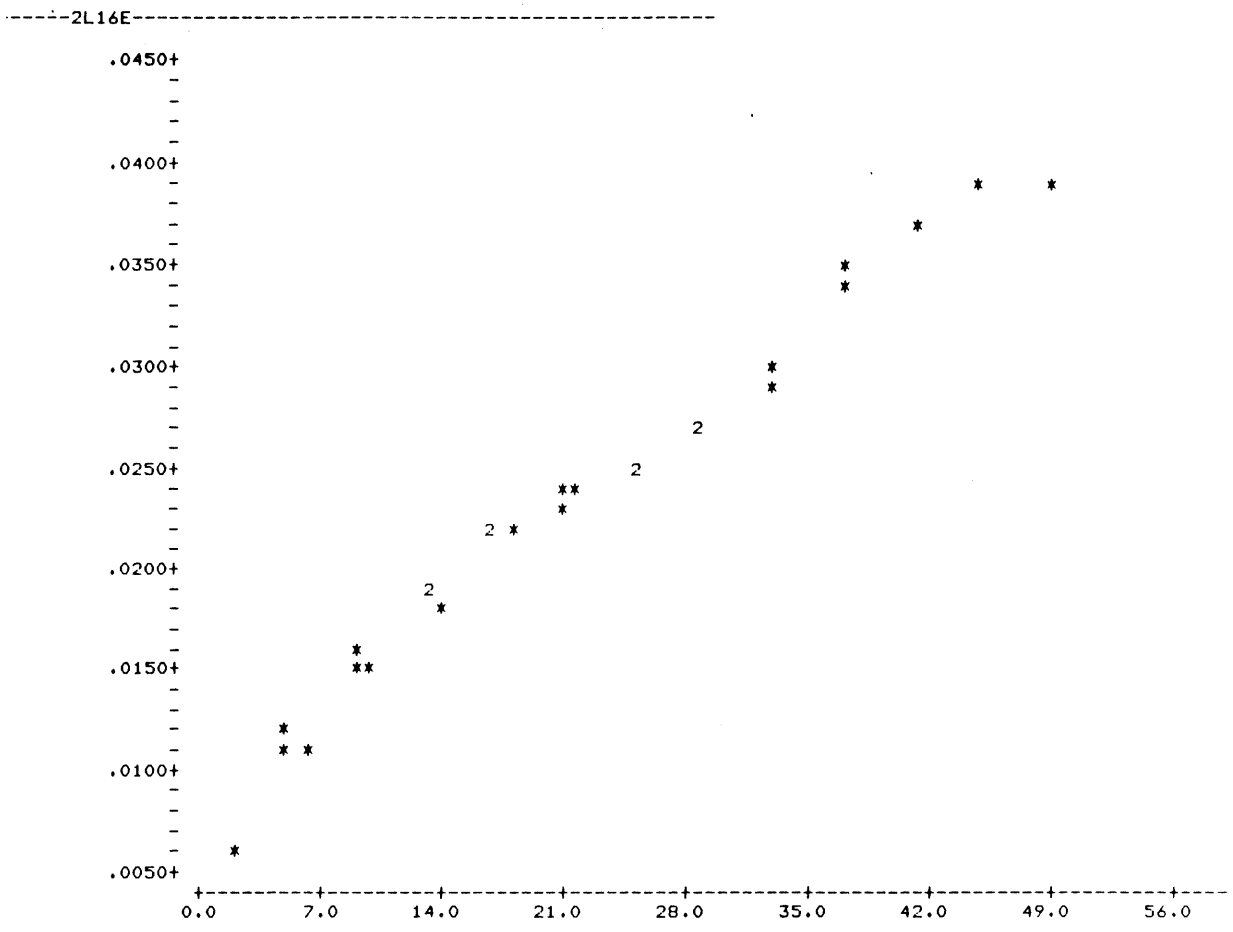
-----2L16E----------
.0450+
.0400+
.0350+
.0300+
.0250+
.0200+
.0150+
.0100+
.0050+
0.0
7.0
14.0
21.0
28.0
35.0
42.0
49.0
56.0

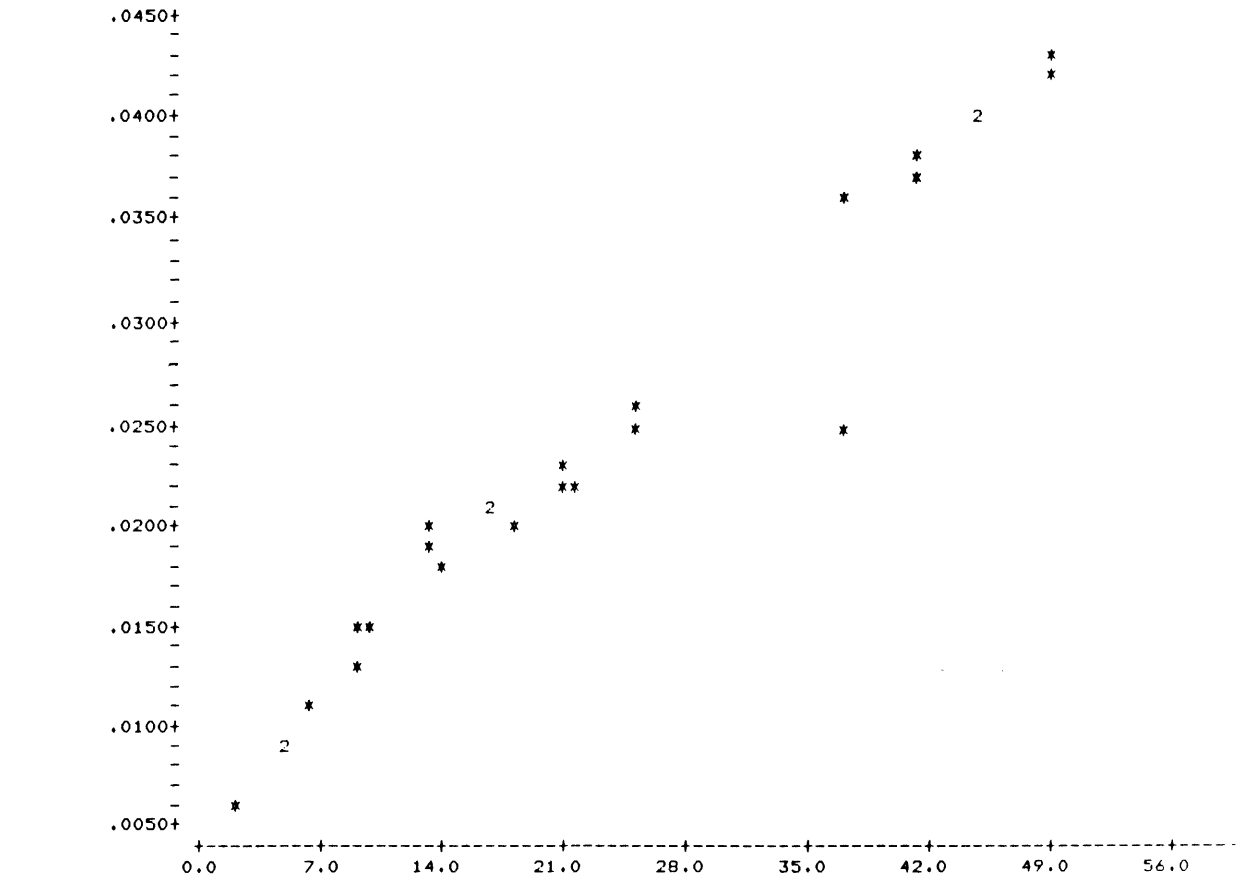
-----2L16W----------
.0450+
.0400+
.0350+
.0300+
.0250+
.0200+
.0150+
.0100+
.0050+
0.0
7.0
14.0
21.0
28.0
35.0
42.0
49.0
56.0

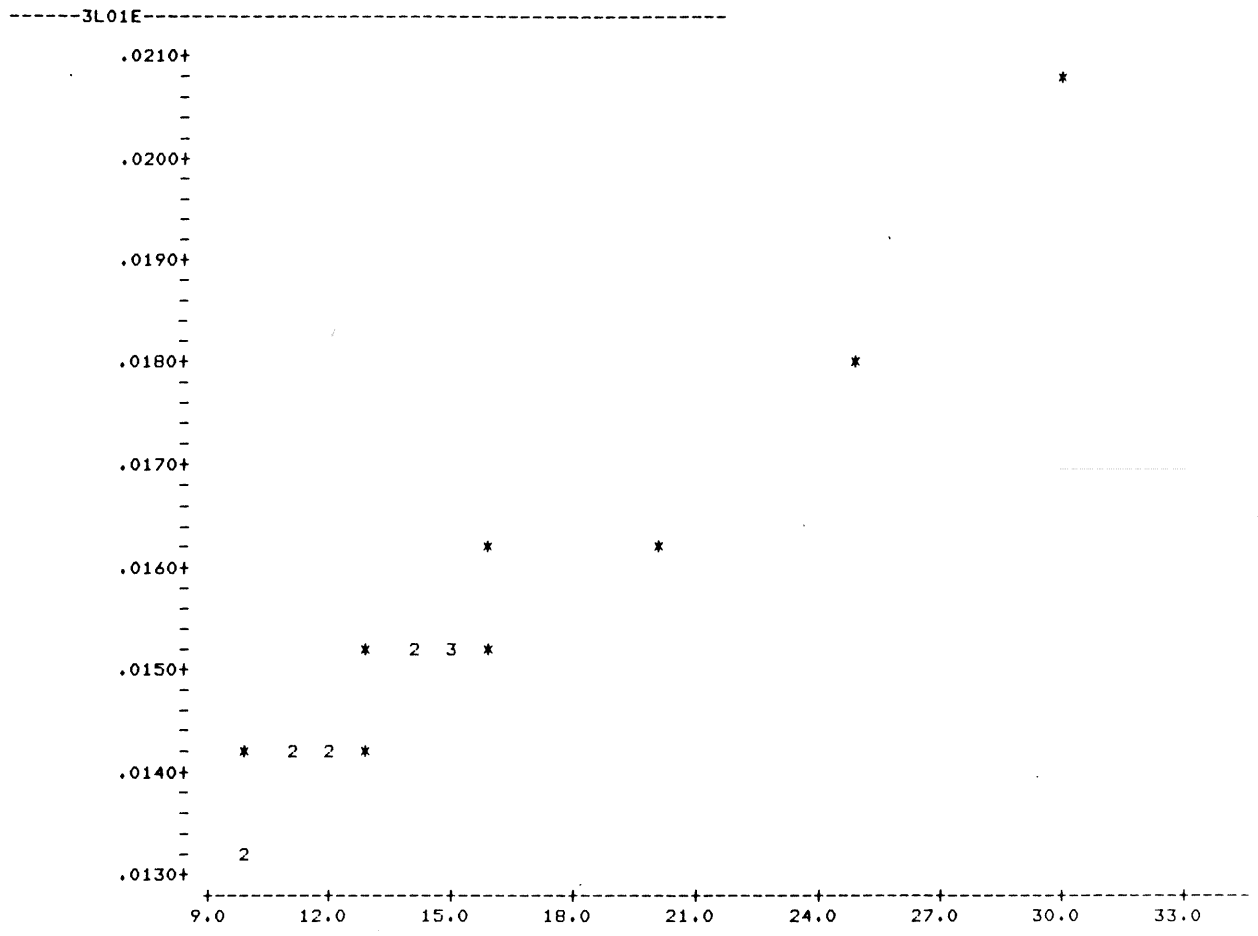
------3L01E----------
.0210+
.0200+
.0190+
.0180+
.0170+
.0160+
.0150+
.0140+
.0130+
2 2 2
2
9.0
12.0
15.0
18.0
21.0
24.0
27.0
30.0
33.0

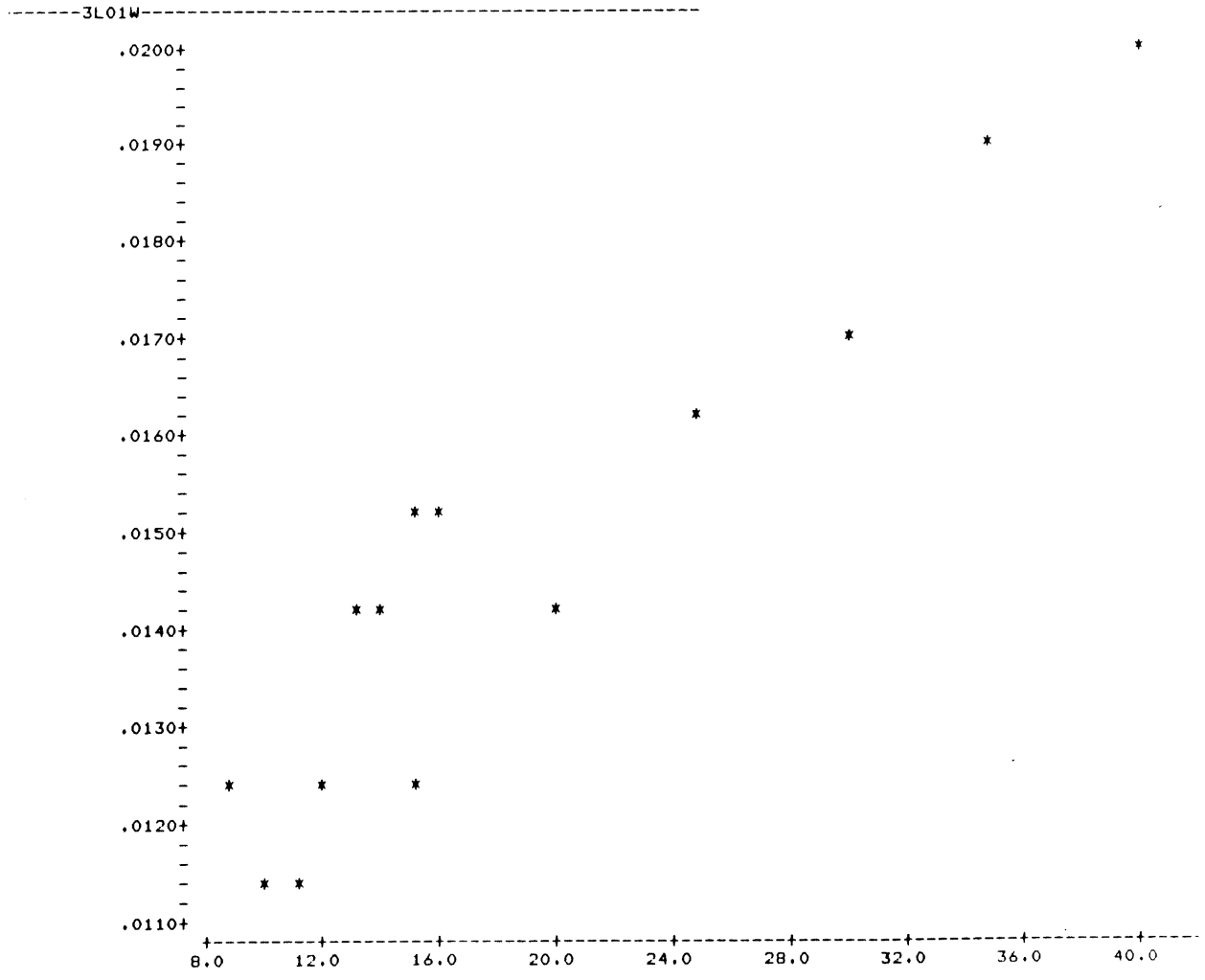
------3L01W----------
.0200+
.0190+
.0180+
.0170+
.0160+
.0150+
.0140+
.0130+
.0120+
.0110+
8.0
12.0
16.0
20.0
24.0
28.0
32.0
36.0
40.0

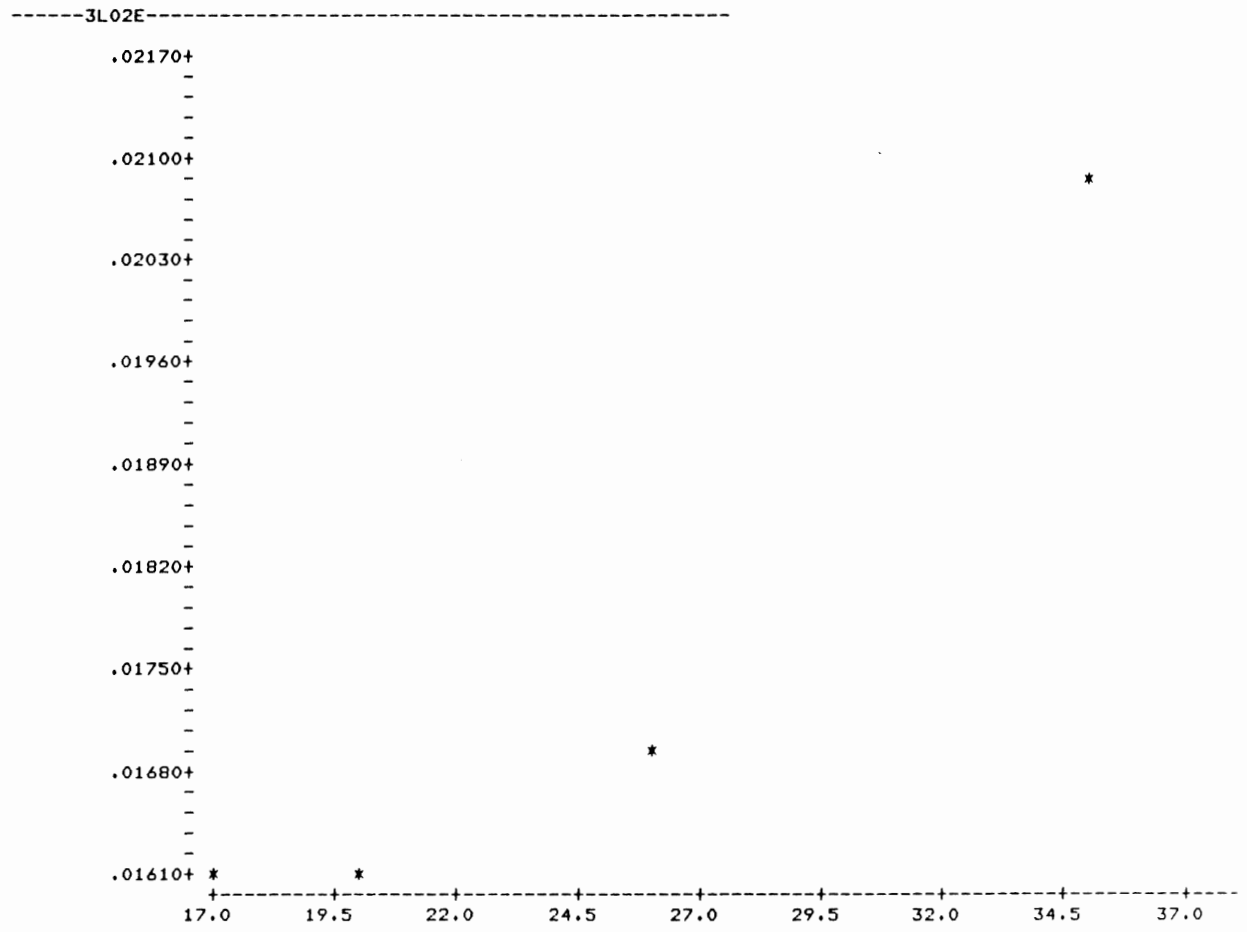
------3L02E----------
.02170+
.02100+
.02030+
.01960+
.01890+
.01820+
.01750+
.01680+
.01610+
17.0
19.5
22.0
24.5
27.0
29.5
32.0
34.5
37.0

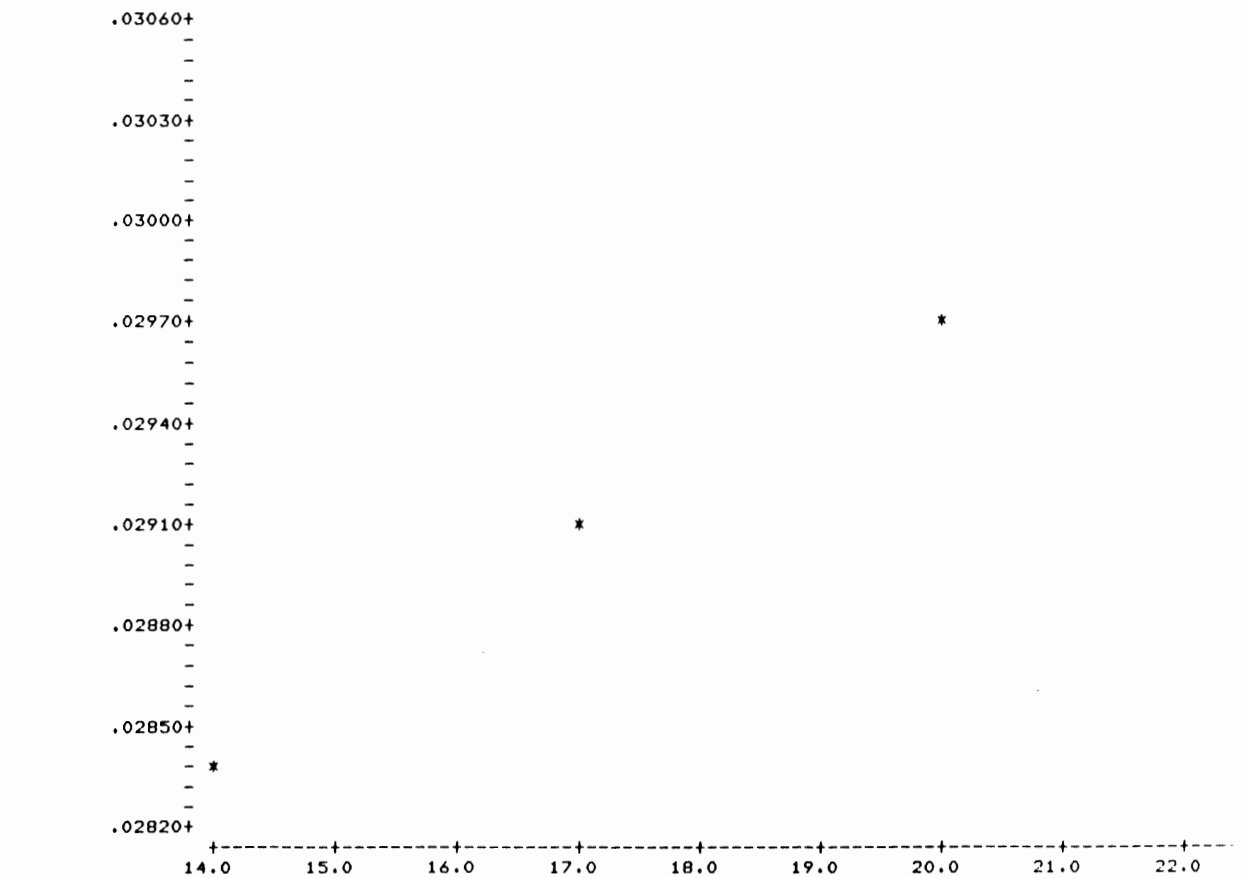
-------3L02W----------
.03060+
.03030+
.03000+
.02970+
.02940+
.02910+
.02880+
.02850+
.02820+
14.0
15.0
16.0
17.0
18.0
19.0
20.0
21.0
22.0

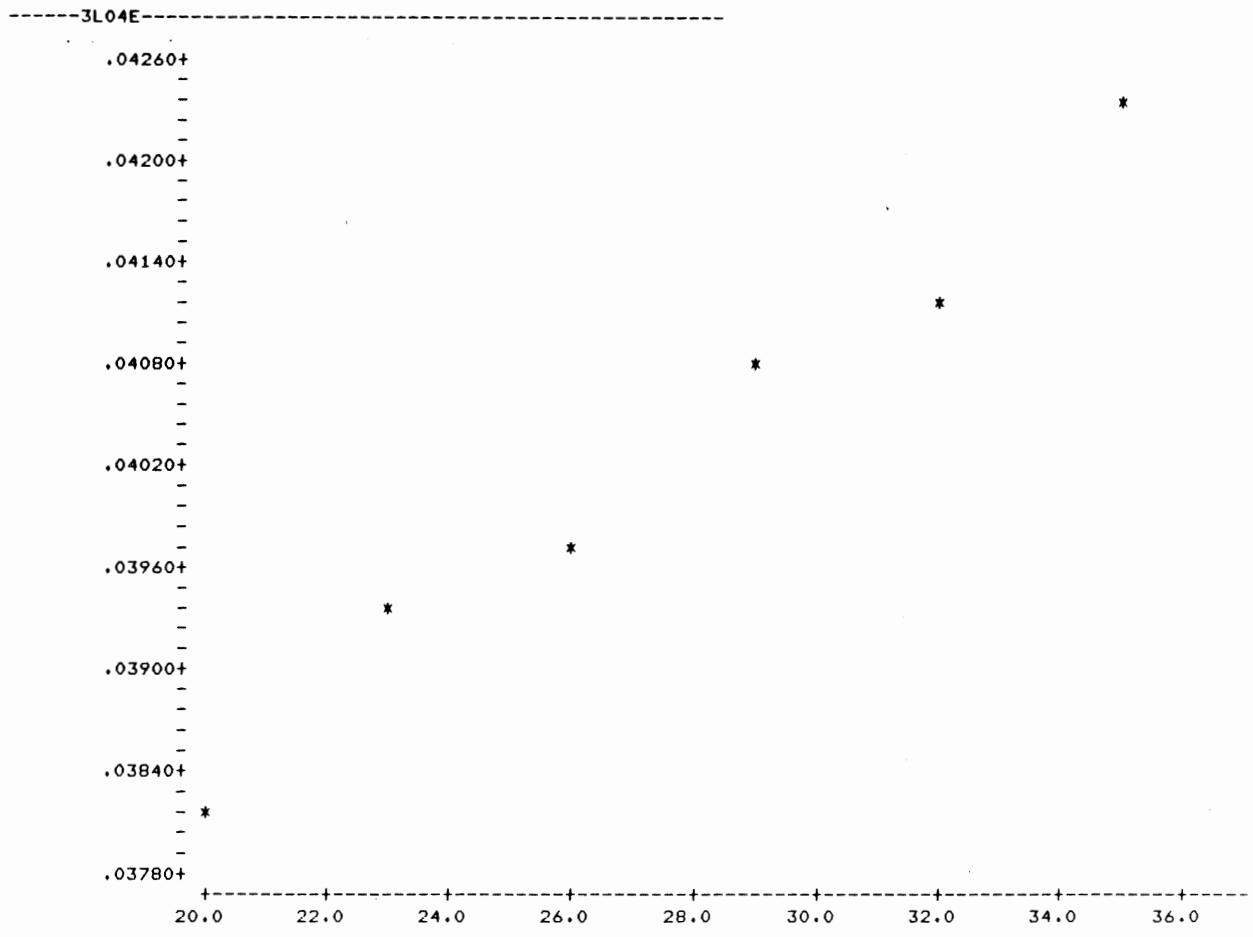
------3L04E----------
.04260+
.04200+
.04140+
.04080+
.04020+
.03960+
.03900+
.03840+
.03780+
20.0
22.0
24.0
26.0
28.0
30.0
32.0
34.0
36.0

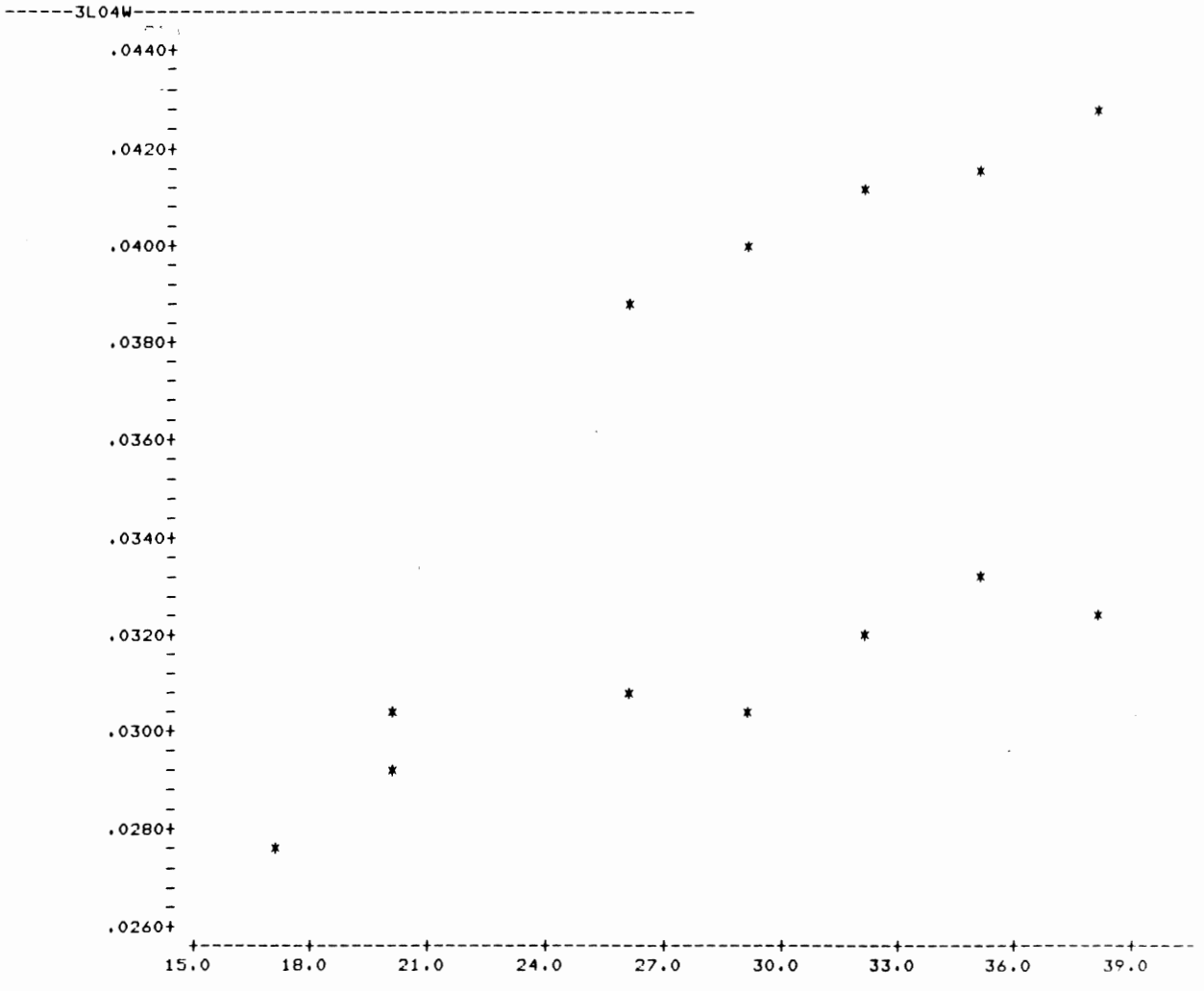
------3L04W----------
.0440+
.0420+
.0400+
.0380+
.0360+
.0340+
.0320+
.0300+
.0280+
.0260+
15.0
18.0
21.0
24.0
27.0
30.0
33.0
36.0
39.0

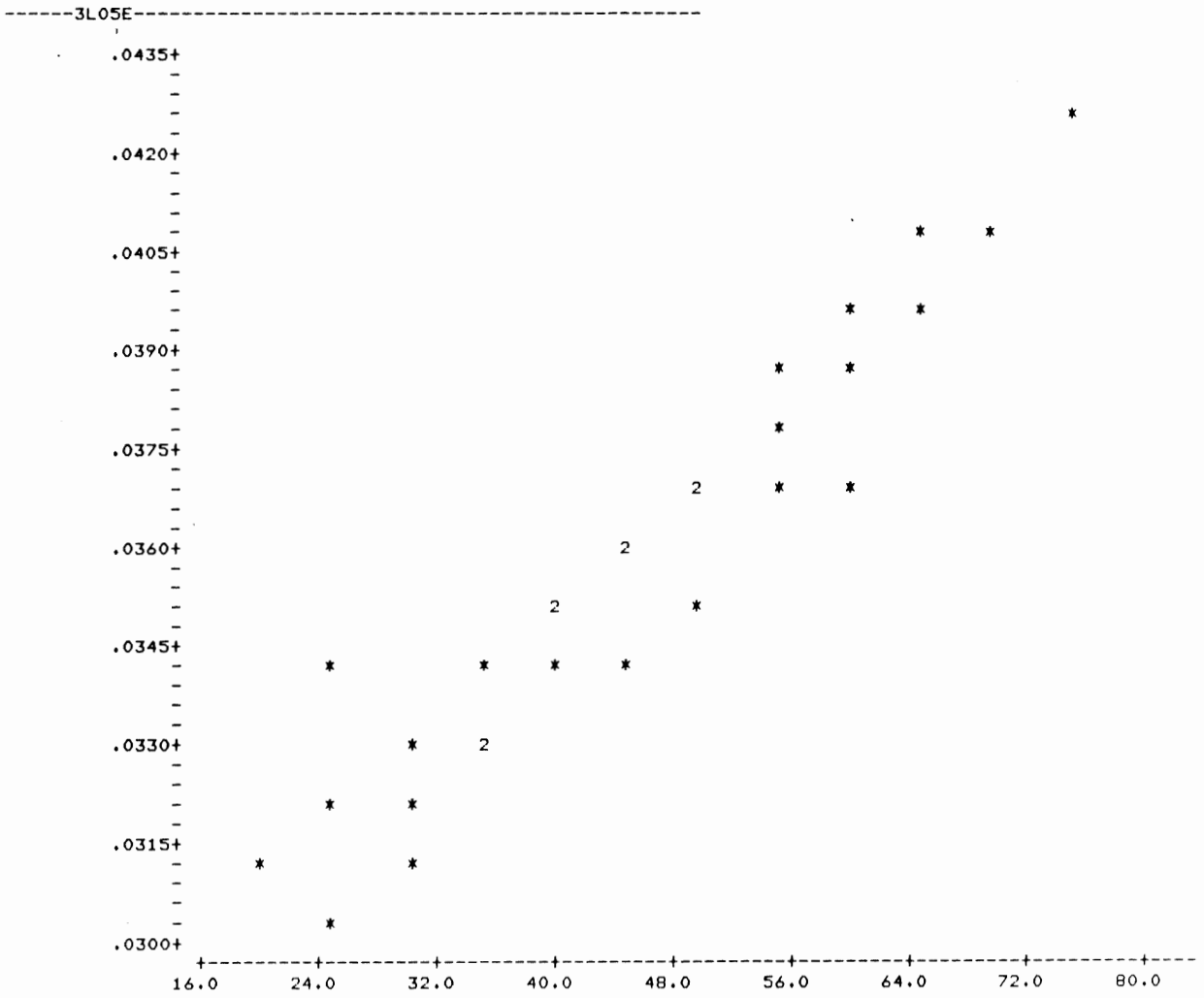
------3L05E----------
.0435+
.0420+
.0405+
.0390+
.0375+
.0360+
.0345+
.0330+
.0315+
.0300+
16.0
24.0
32.0
40.0
48.0
56.0
64.0
72.0
80.0

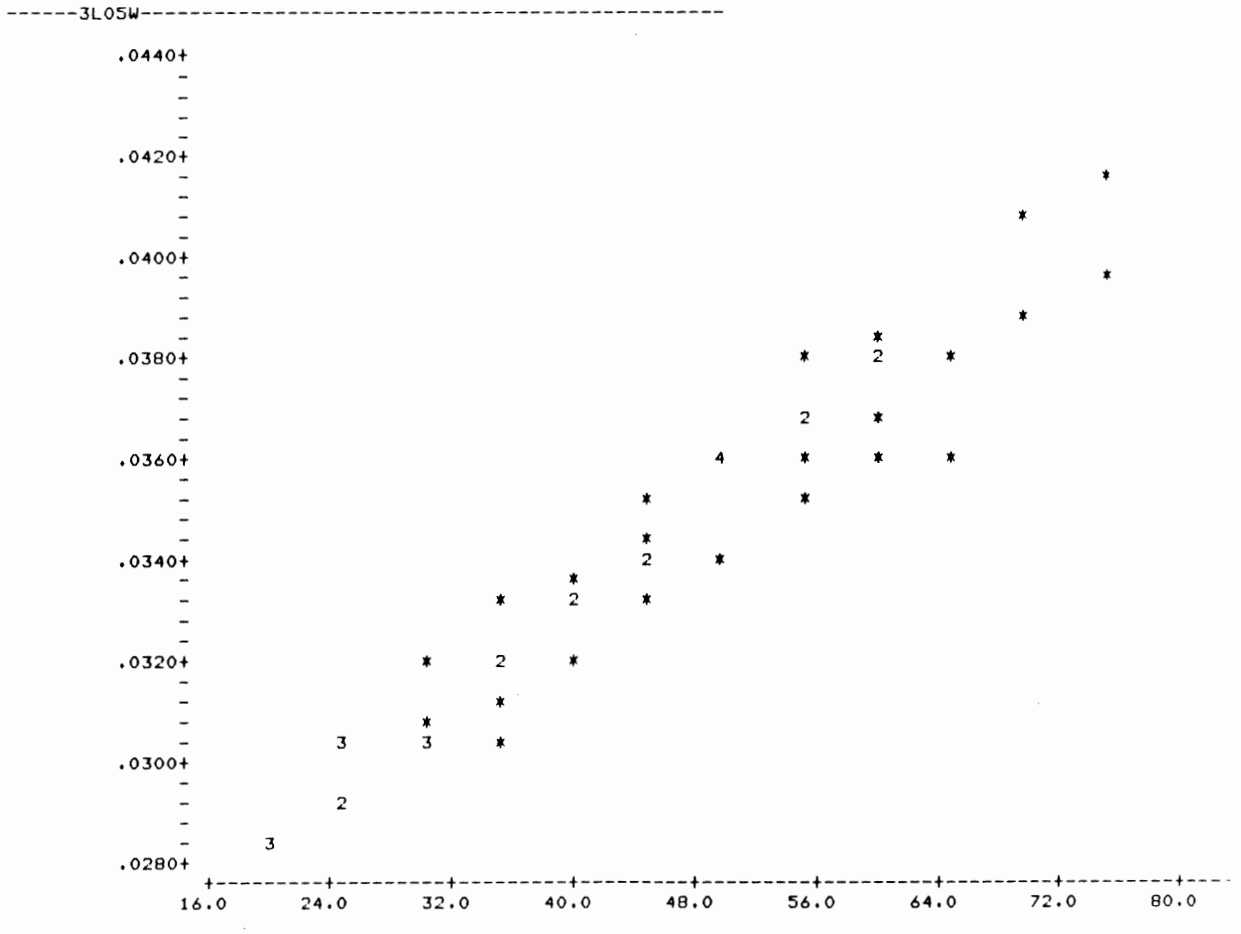
------3L05W----------
.0440+
.0420+
.0400+
.0380+
.0360+
.0340+
.0320+
.0300+
.0280+
16.0
24.0
32.0
40.0
48.0
56.0
64.0
72.0
80.0

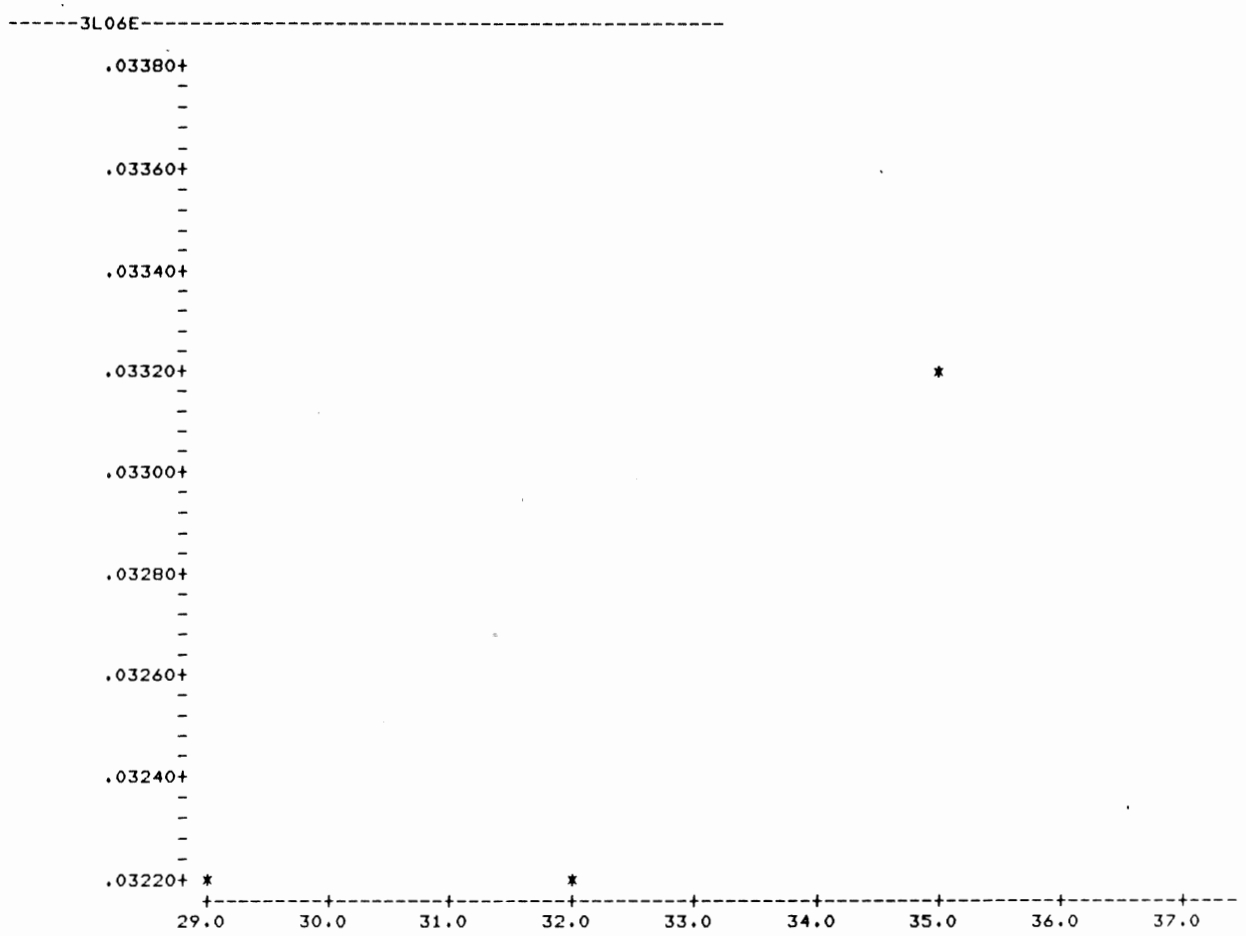
------3L06E----------
.03380+
.03360+
.03340+
.03320+
.03300+
.03280+
.03260+
.03240+
.03220+
29.0
30.0
31.0
32.0
33.0
34.0
35.0
36.0
37.0

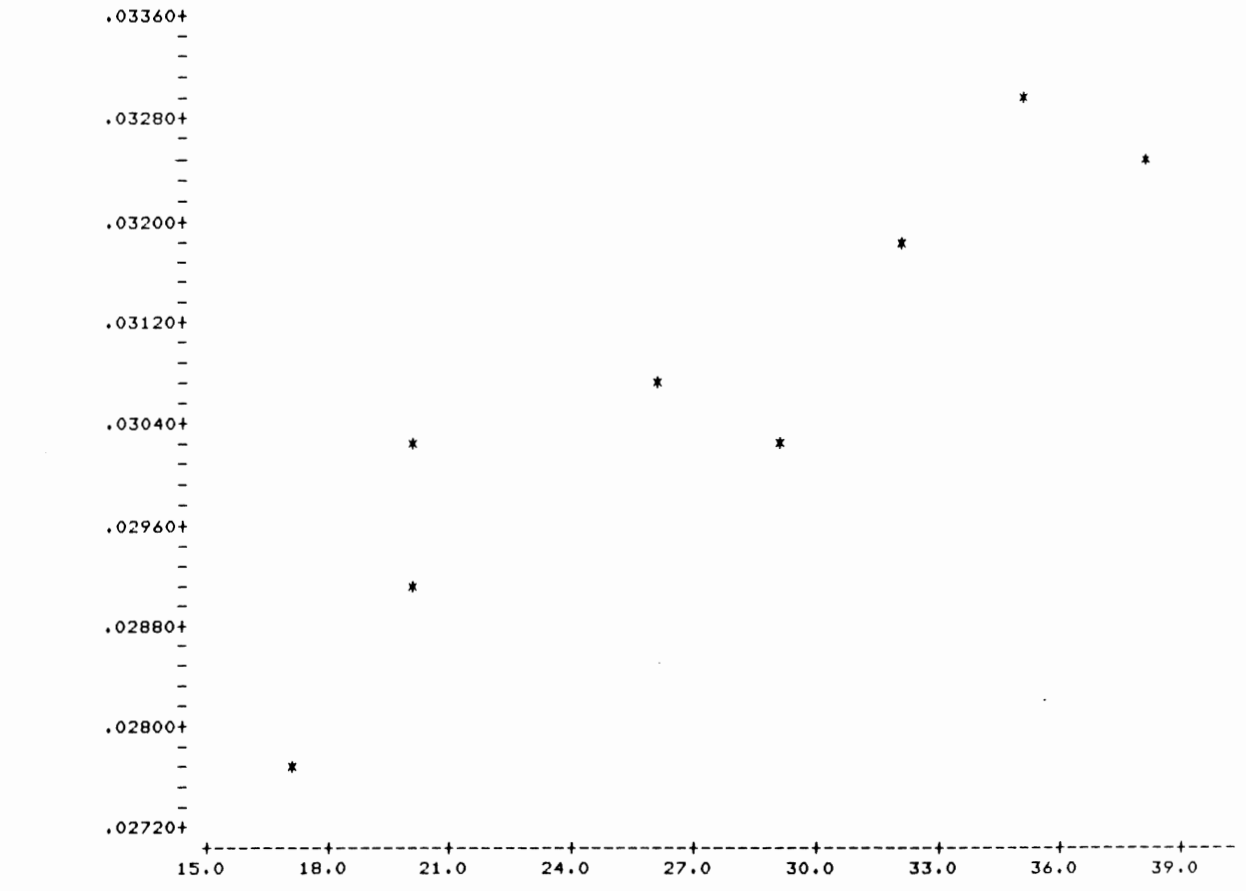
------3L06W----------
.03360+
.03280+
.03200+
.03120+
.03040+
.02960+
.02880+
.02800+
.02720+
15.0
18.0
21.0
24.0
27.0
30.0
33.0
36.0
39.0

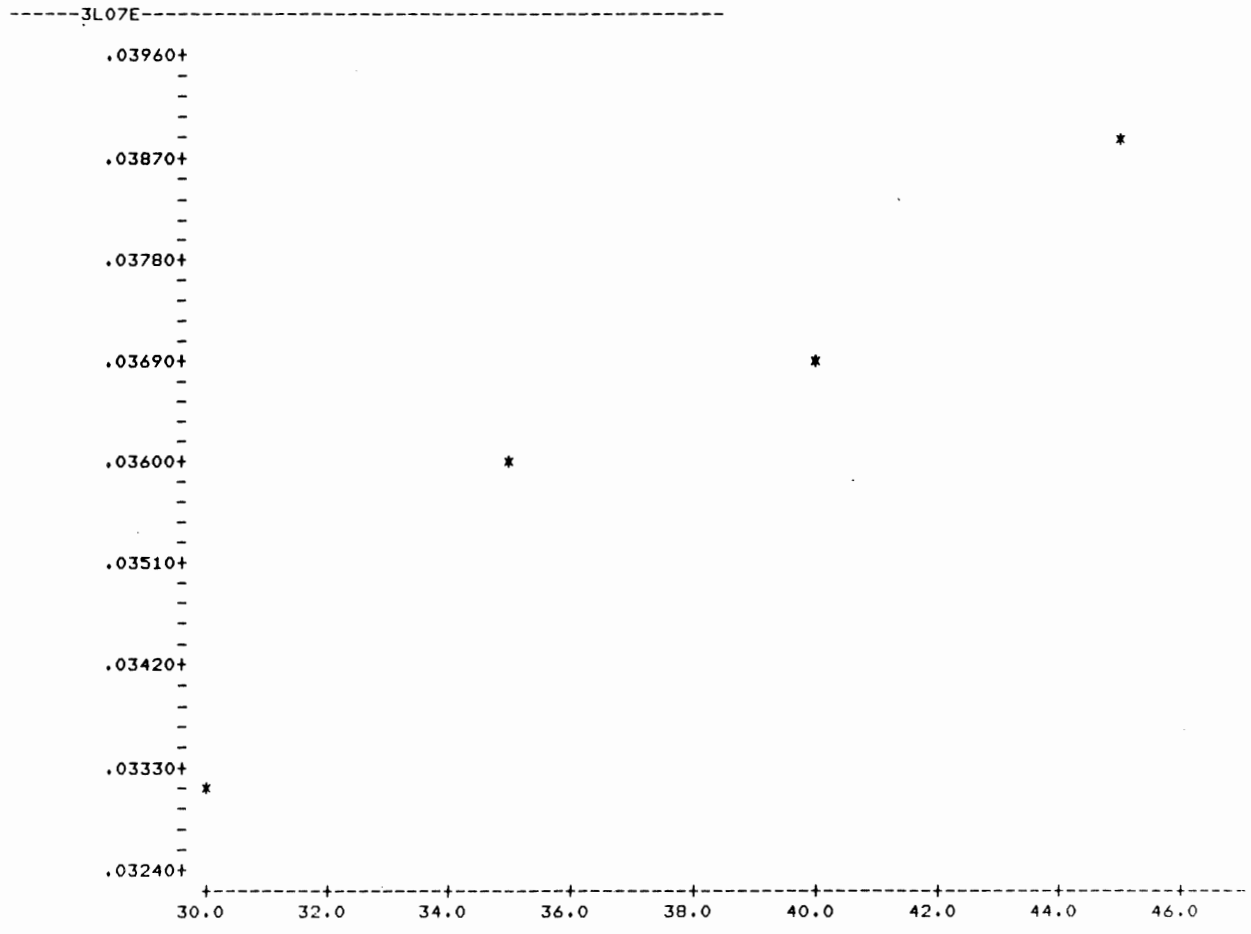
------3L07E----------
.03960+
.03870+
.03780+
.03690+
.03600+
.03510+
.03420+
.03330+
.03240+
30.0
32.0
34.0
36.0
38.0
40.0
42.0
44.0
46.0

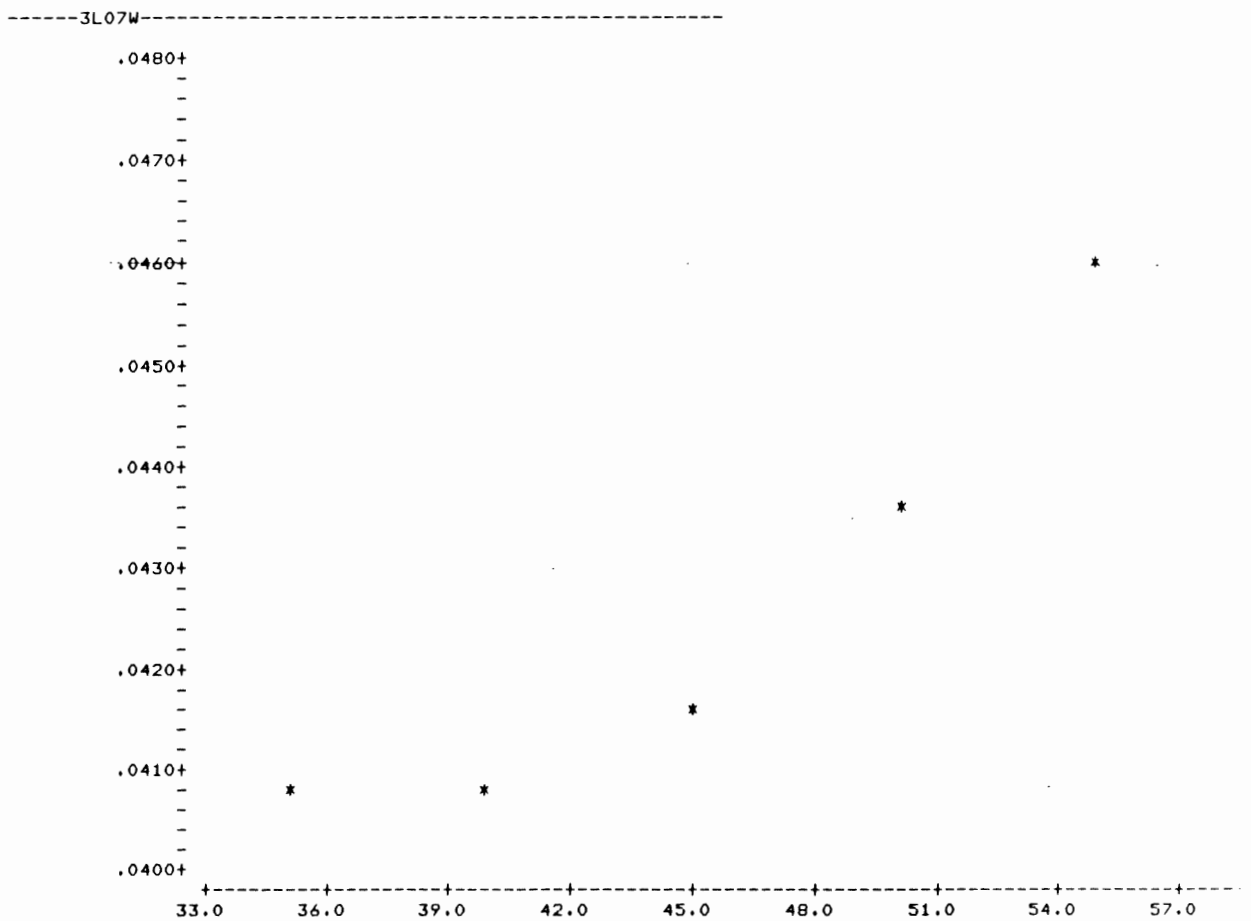
------3L07W----------
.0480+
.0470+
.0460+
.0450+
.0440+
.0430+
.0420+
.0410+
.0400+
33.0
36.0
39.0
42.0
45.0
48.0
51.0
54.0
57.0

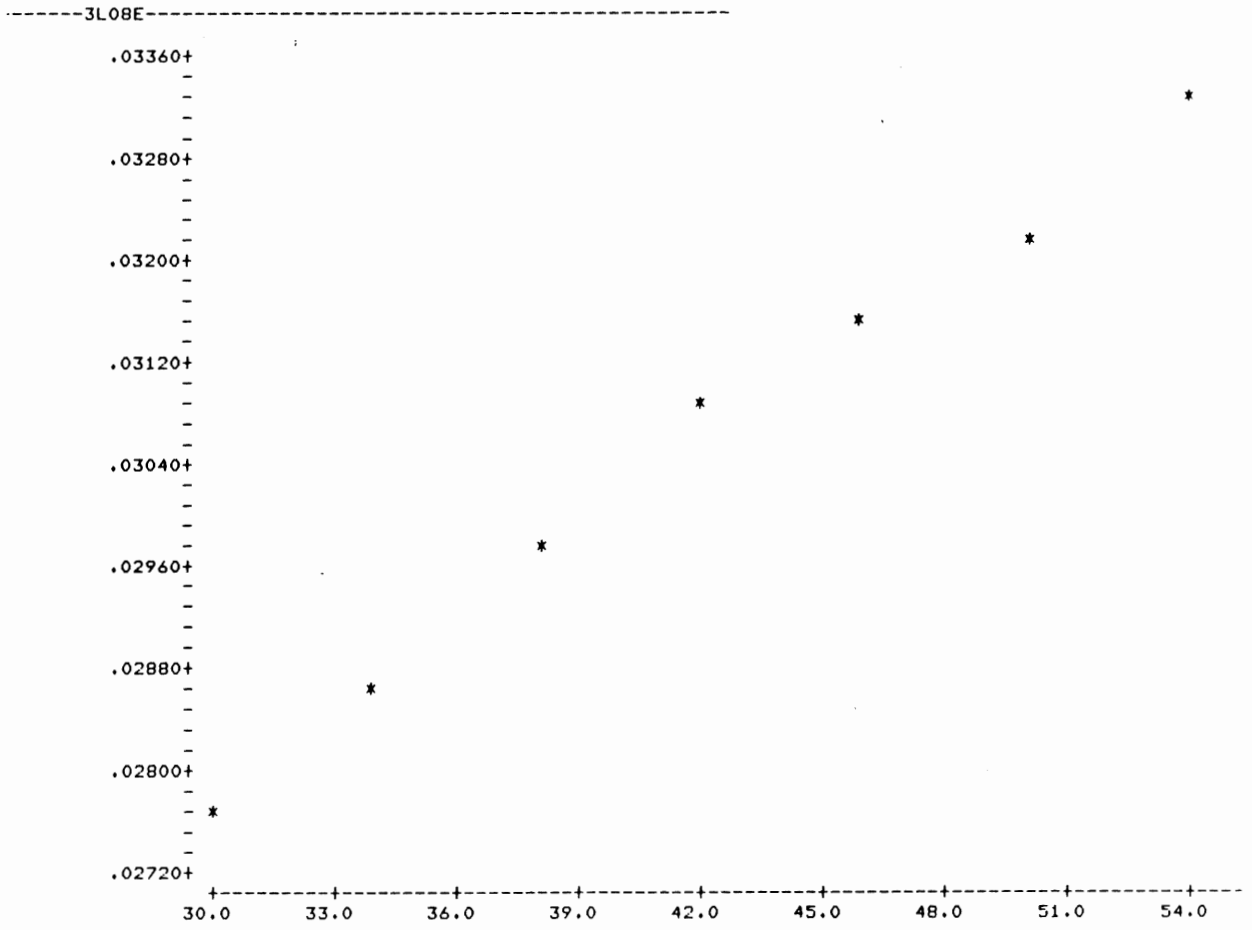
------3L08E----------
.03360+
.03280+
.03200+
.03120+
.03040+
.02960+
.02880+
.02800+
.02720+
30.0
33.0
36.0
39.0
42.0
45.0
48.0
51.0
54.0

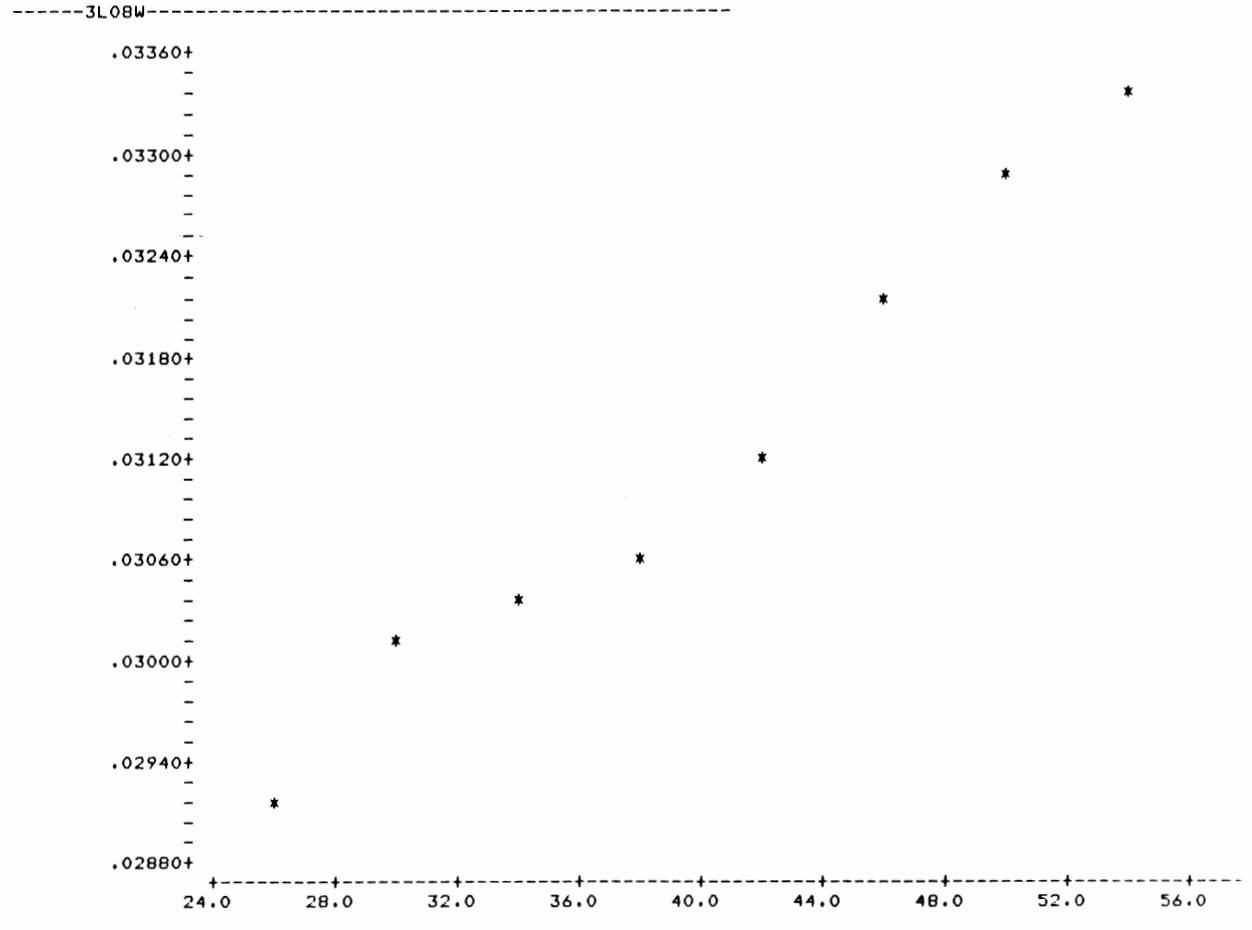
------3L08W----------
.03360+
.03300+
.03240+
.03180+
.03120+
.03060+
.03000+
.02940+
.02880+
24.0
28.0
32.0
36.0
40.0
44.0
48.0
52.0
56.0

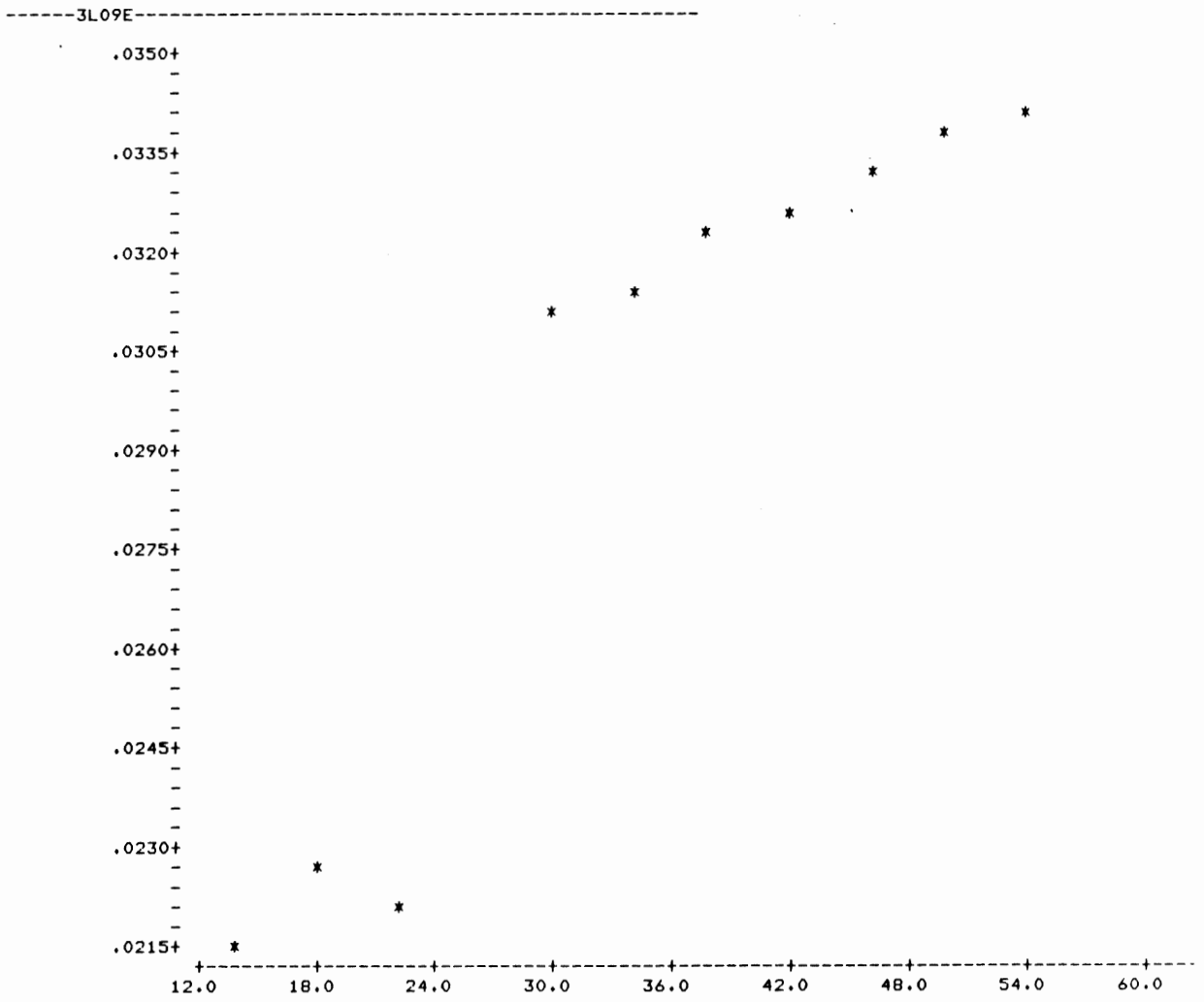
------3L09E----------
.0350+
.0335+
.0320+
.0305+
.0290+
.0275+
.0260+
.0245+
.0230+
.0215+
12.0
18.0
24.0
30.0
36.0
42.0
48.0
54.0
60.0

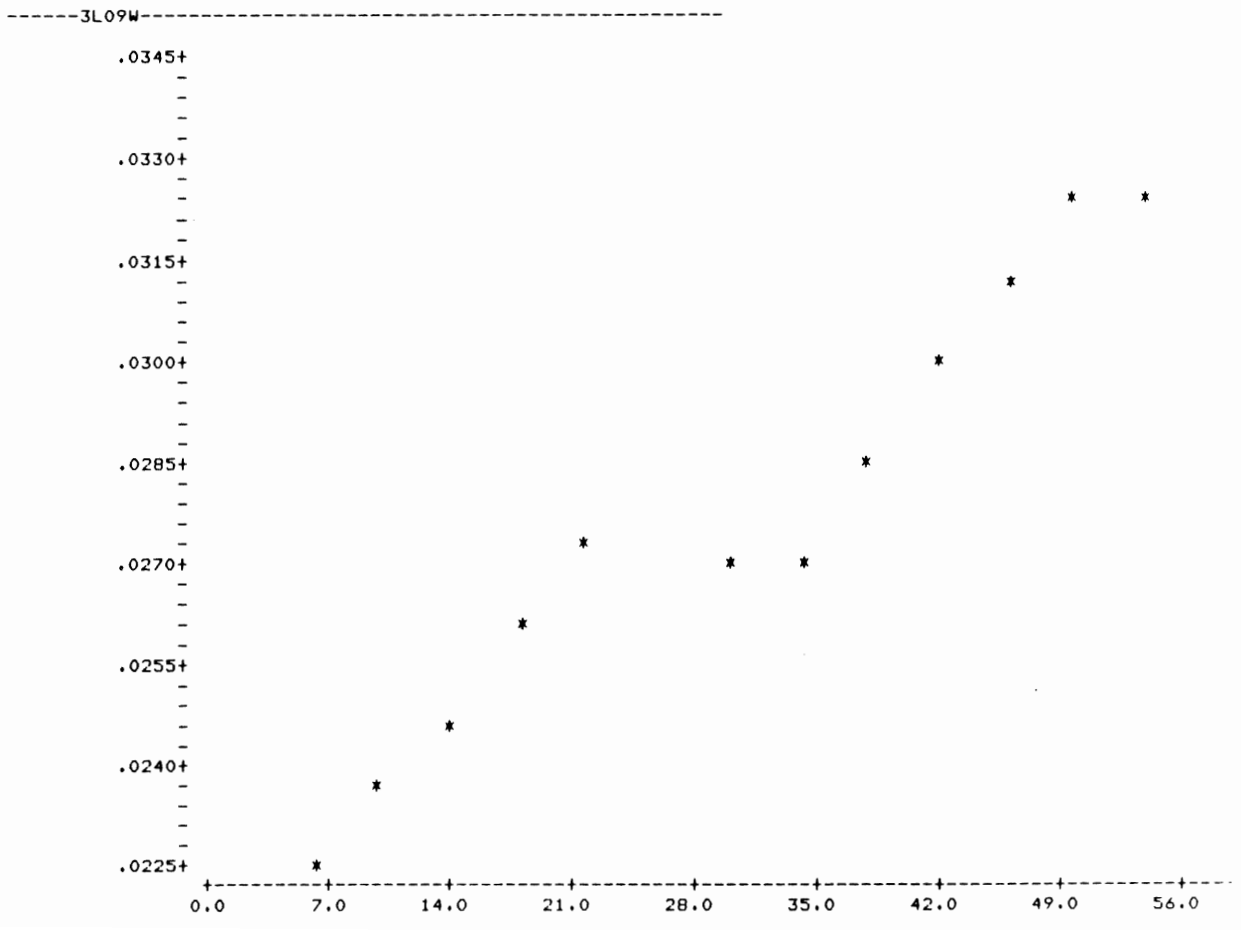
------3L09W----------
.0345+
.0330+
.0315+
.0300+
.0285+
.0270+
.0255+
.0240+
.0225+
0.0
7.0
14.0
21.0
28.0
35.0
42.0
49.0
56.0

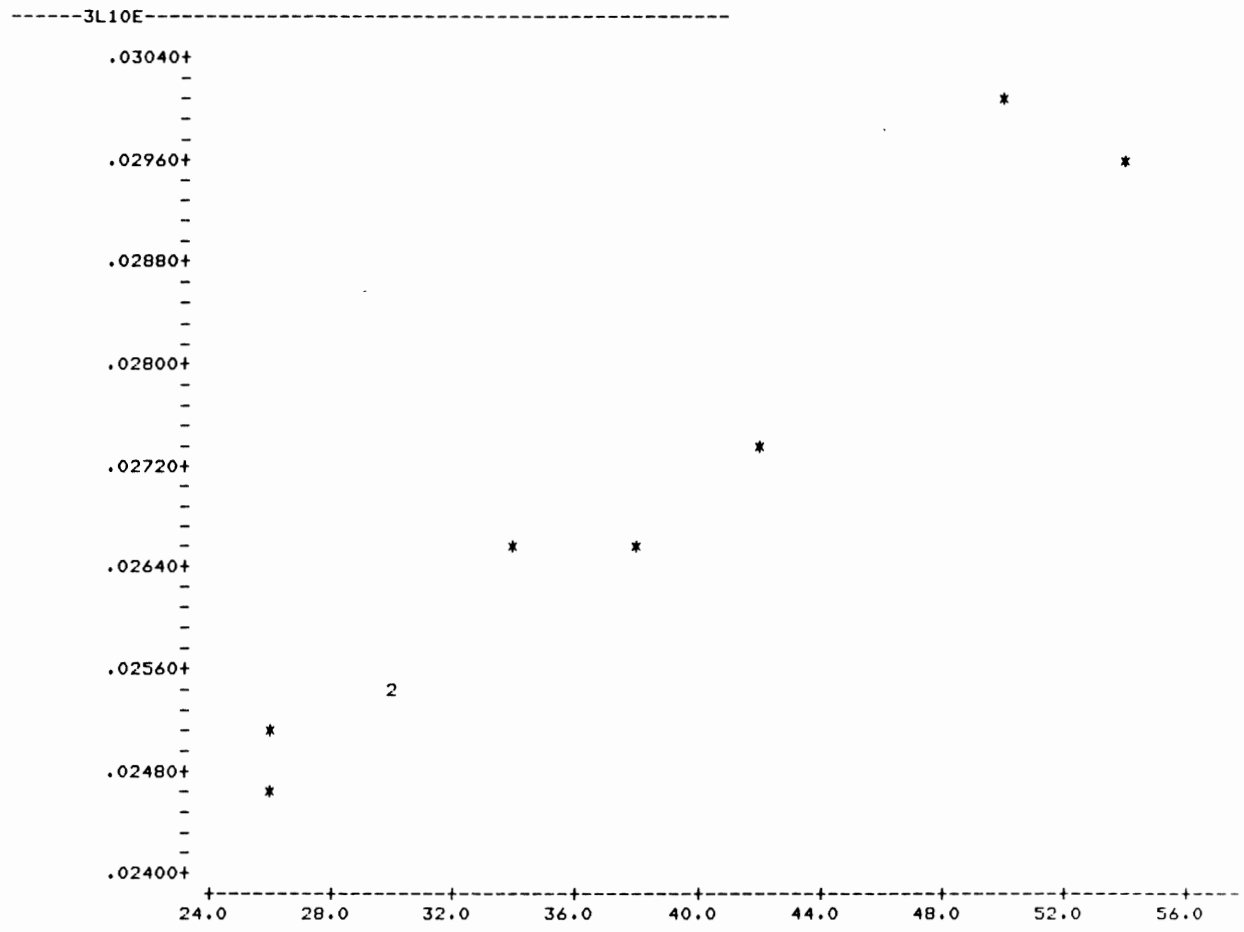
------3L10E----------
.03040+
.02960+
.02880+
.02800+
.02720+
.02640+
.02560+
.02480+
.02400+
24.0
28.0
32.0
36.0
40.0
44.0
48.0
52.0
56.0

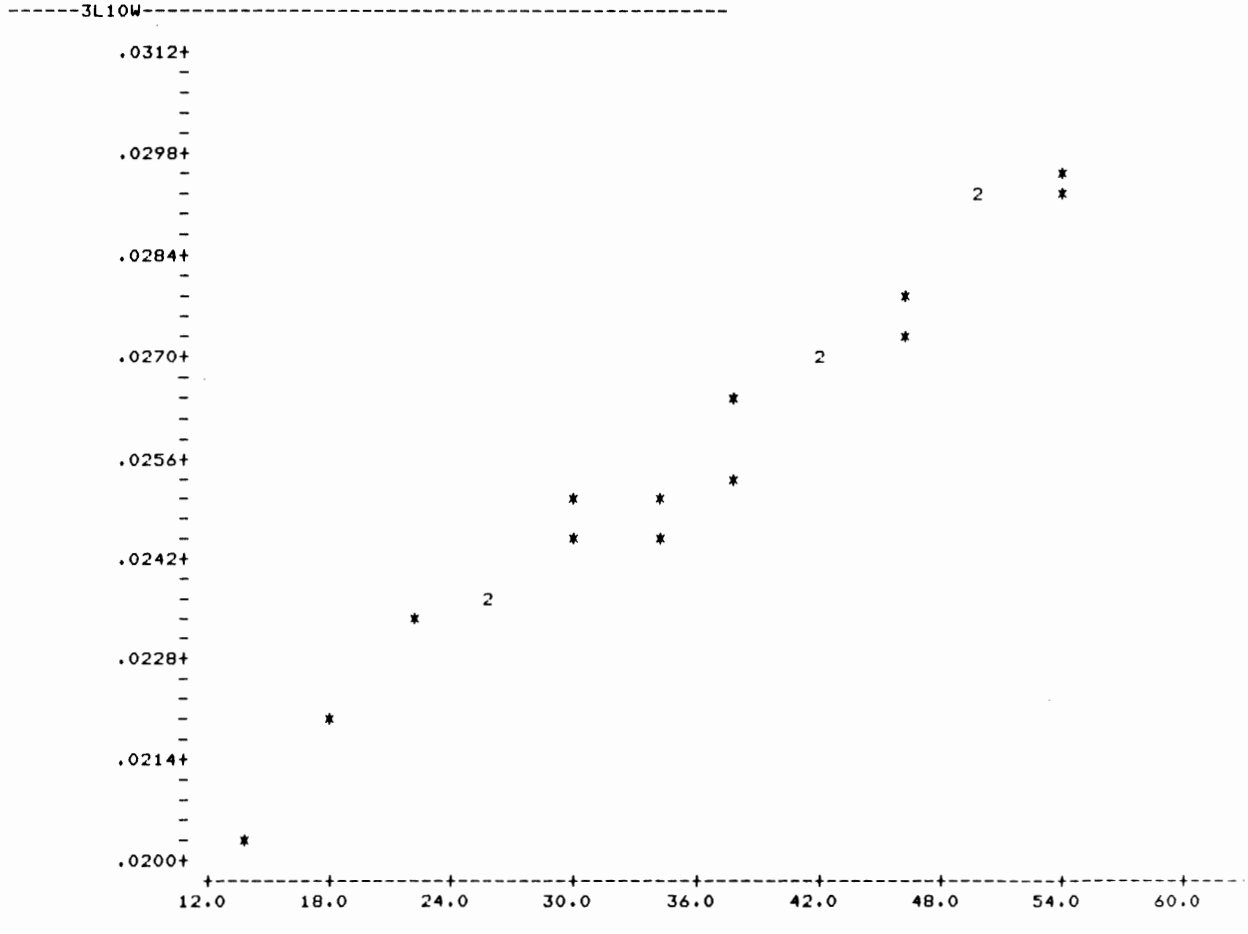
------3L10W----------
.0312+
.0298+
.0284+
.0270+
.0256+
.0242+
.0228+
.0214+
.0200+
12.0
18.0
24.0
30.0
36.0
42.0
48.0
54.0
60.0

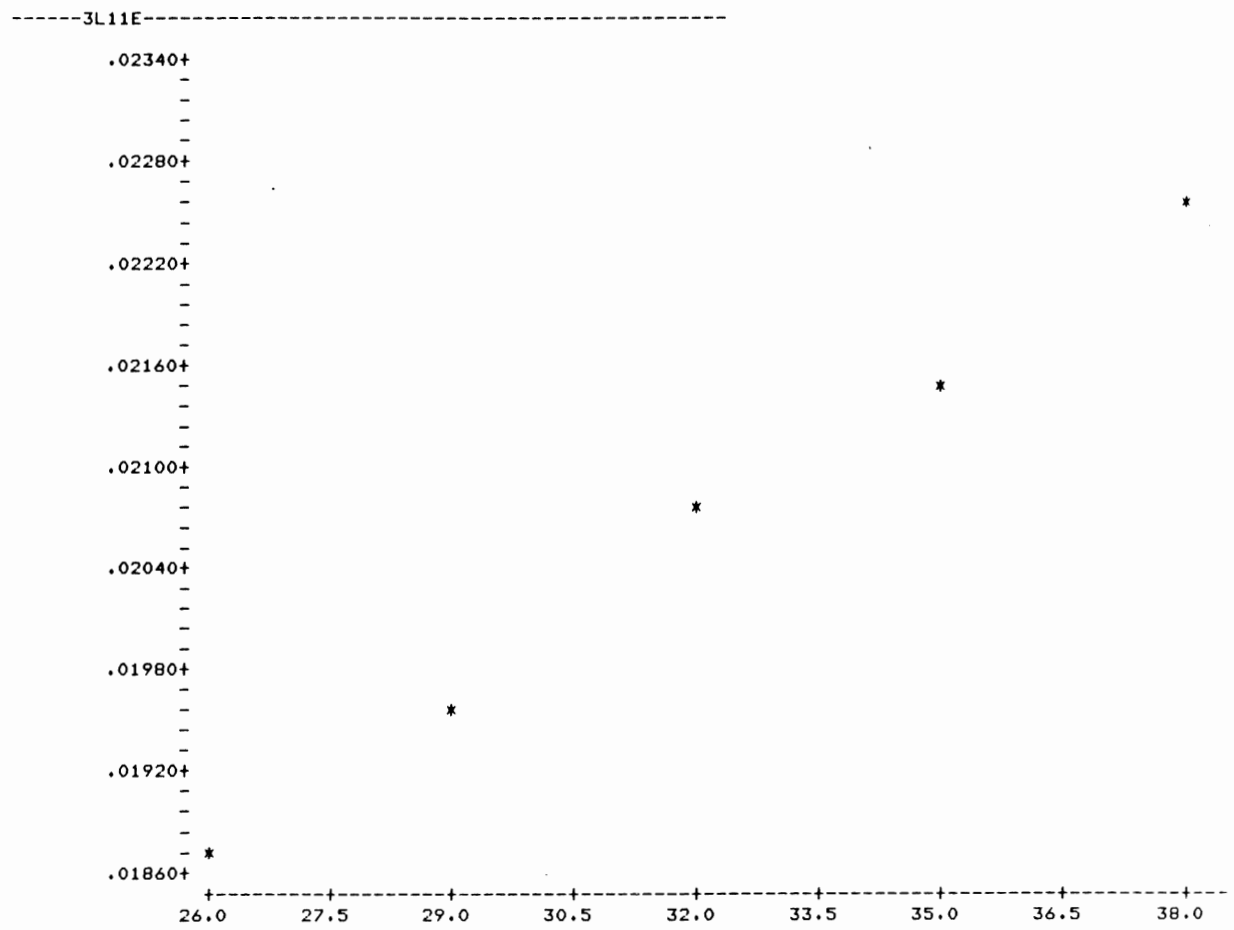
------3L11E----------
.02340+
.02280+
.02220+
.02160+
.02100+
.02040+
.01980+
.01920+
.01860+
26.0
27.5
29.0
30.5
32.0
33.5
35.0
36.5
38.0

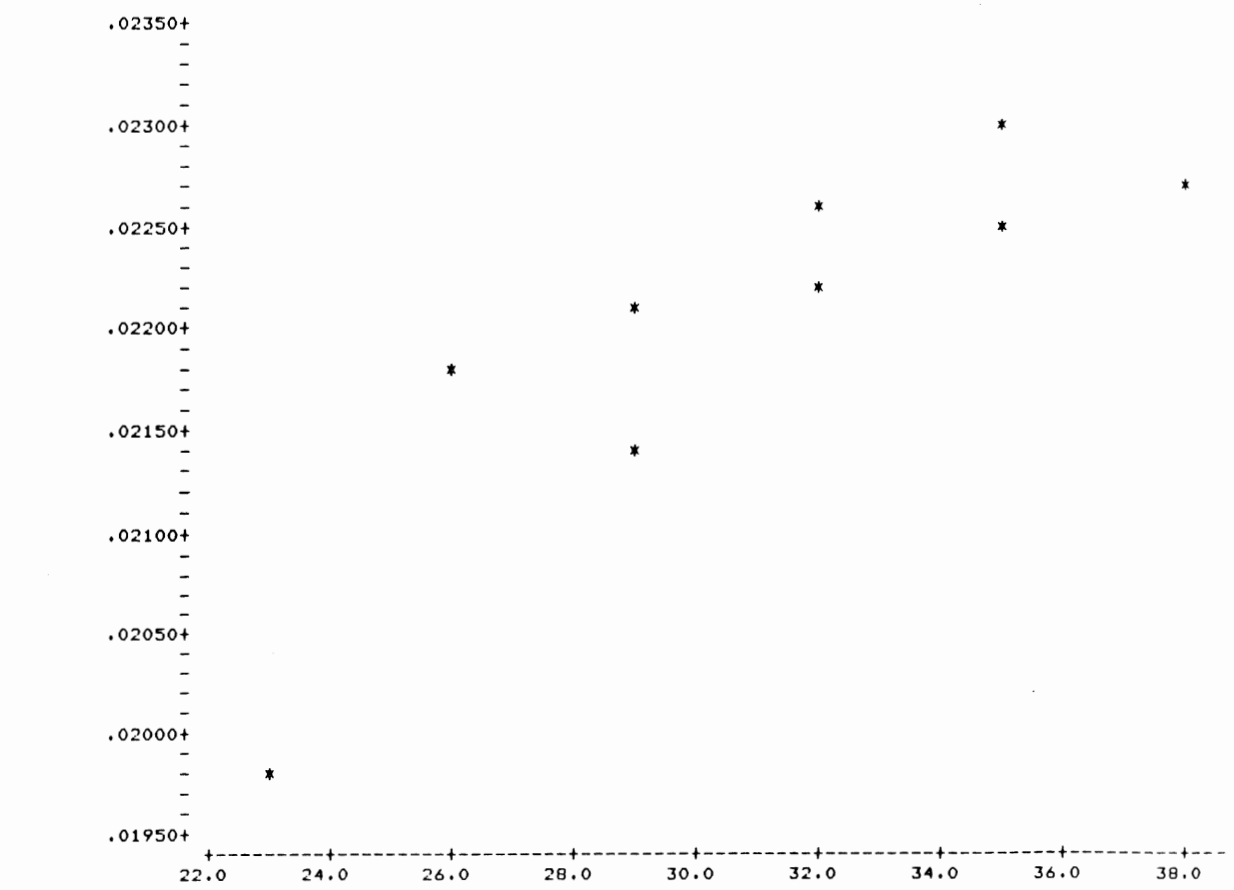
------3L11W----------
.02350+
.02300+
.02250+
.02200+
.02150+
.02100+
.02050+
.02000+
.01950+
22.0
24.0
26.0
28.0
30.0
32.0
34.0
36.0
38.0

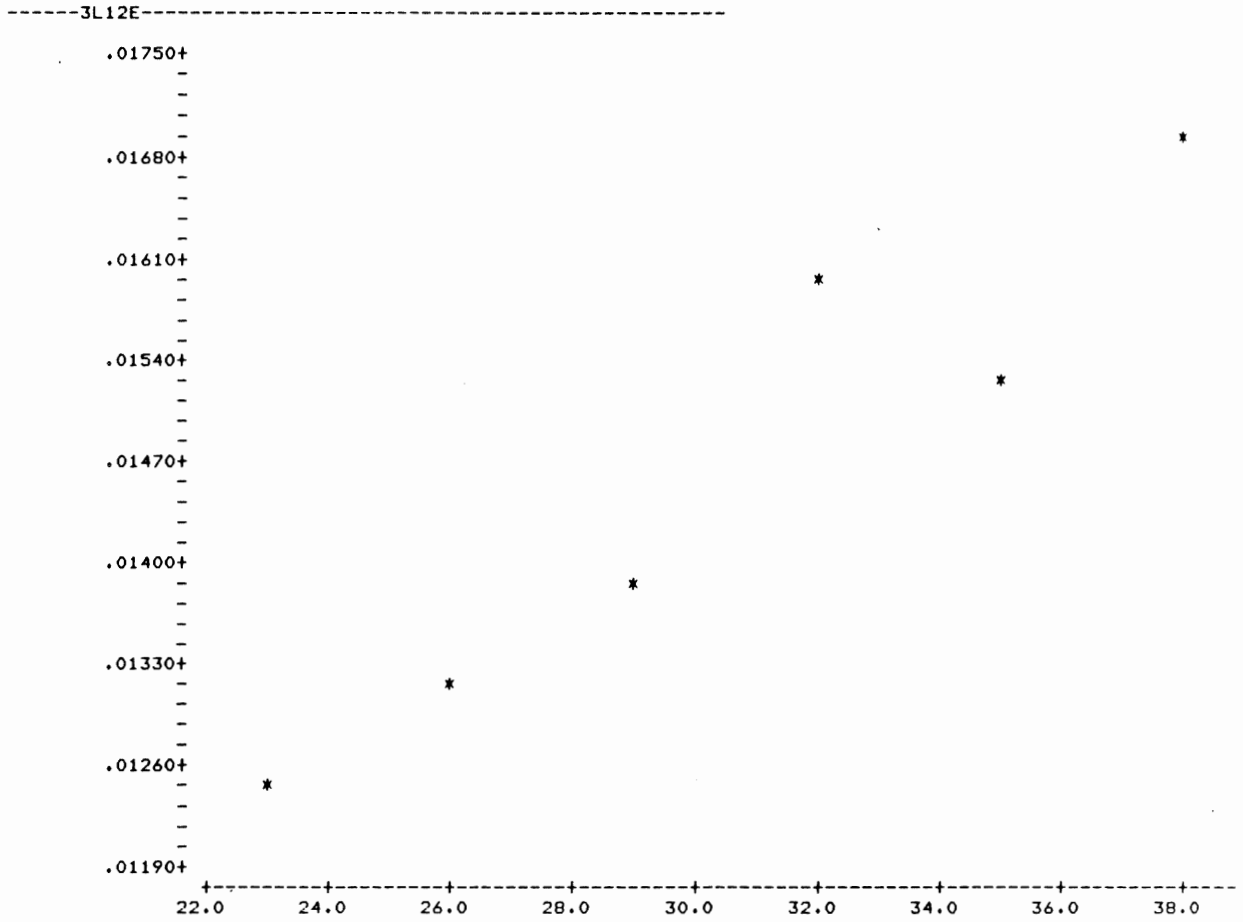
------3L12E----------
.01750+
.01680+
.01610+
.01540+
.01470+
.01400+
.01330+
.01260+
.01190+
22.0
24.0
26.0
28.0
30.0
32.0
34.0
36.0
38.0

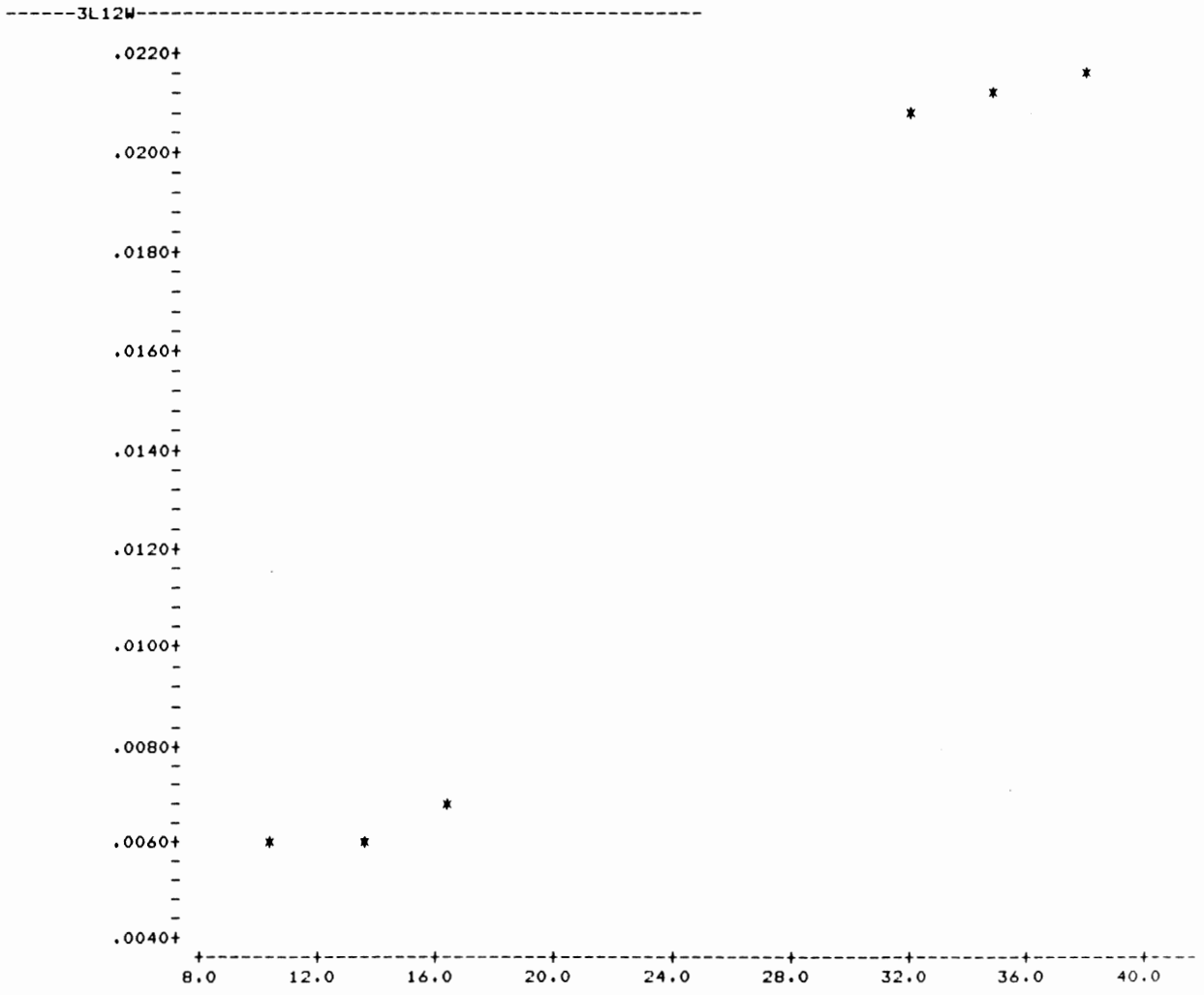
------3L12W----------
.0220+
.0200+
.0180+
.0160+
.0140+
.0120+
.0100+
.0080+
.0060+
.0040+
8.0
12.0
16.0
20.0
24.0
28.0
32.0
36.0
40.0

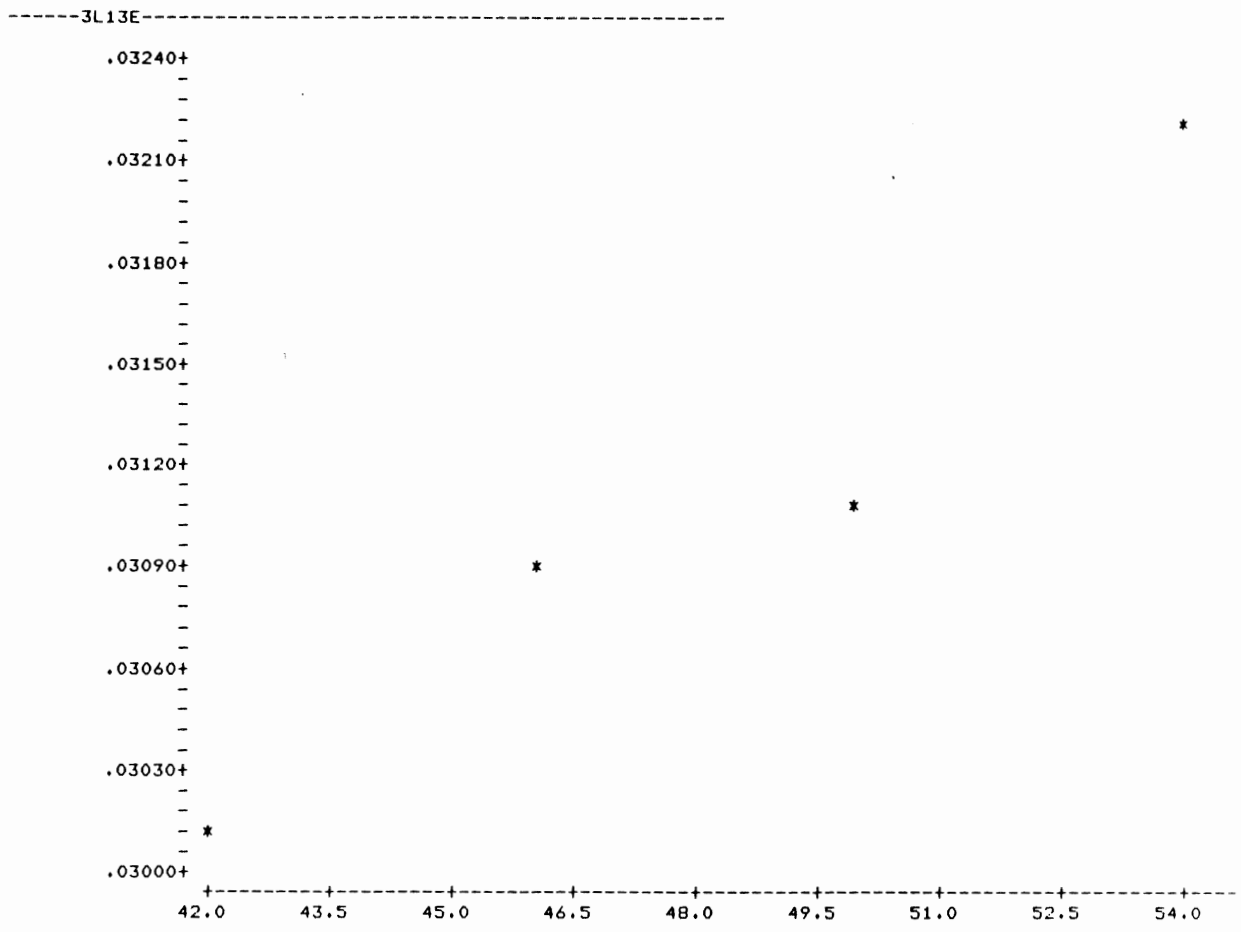
------3L13E----------
.03240+
.03210+
.03180+
.03150+
.03120+
.03090+
.03060+
.03030+
.03000+
42.0
43.5
45.0
46.5
48.0
49.5
51.0
52.5
54.0

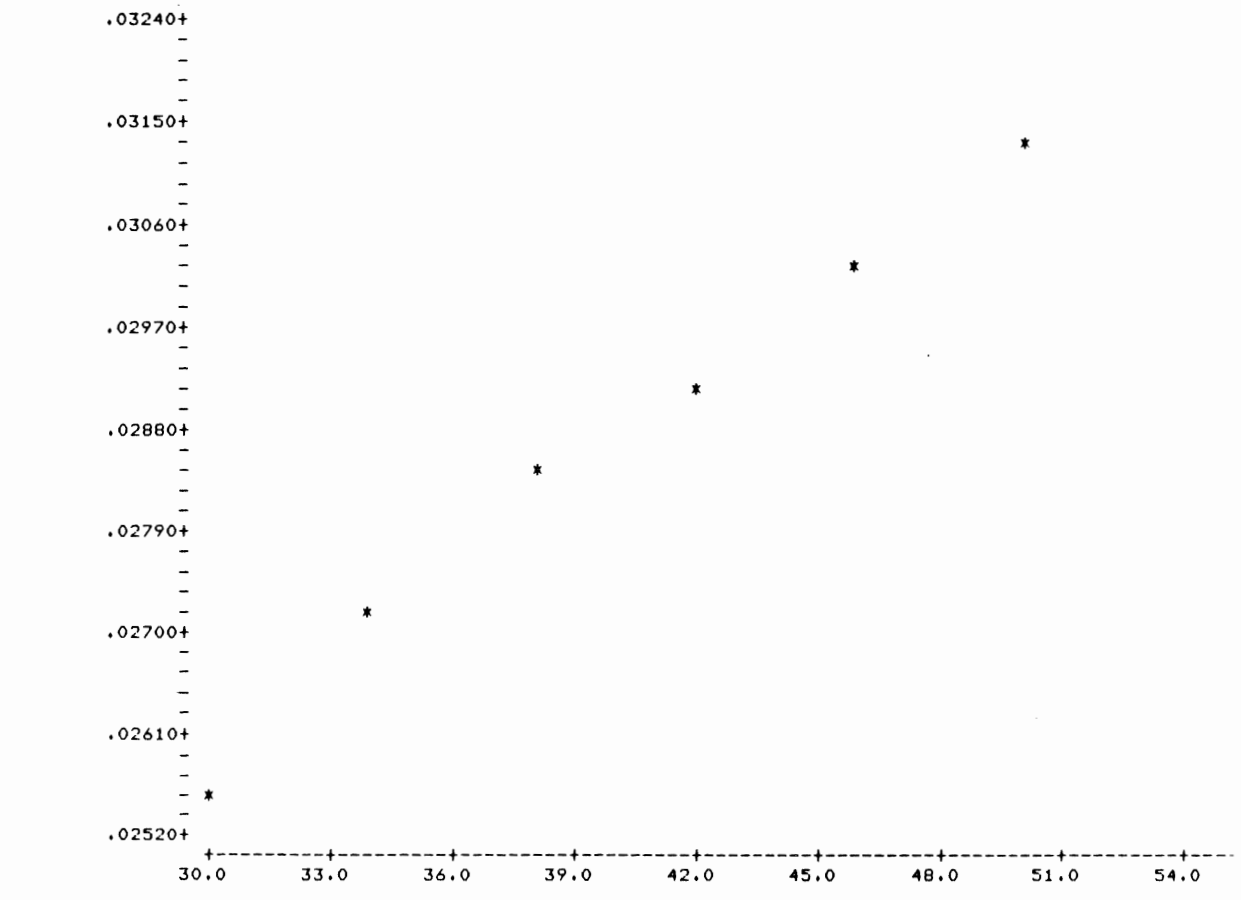
------3L13W----------
.03240+
.03150+
.03060+
.02970+
.02880+
.02790+
.02700+
.02610+
.02520+
30.0
33.0
36.0
39.0
42.0
45.0
48.0
51.0
54.0

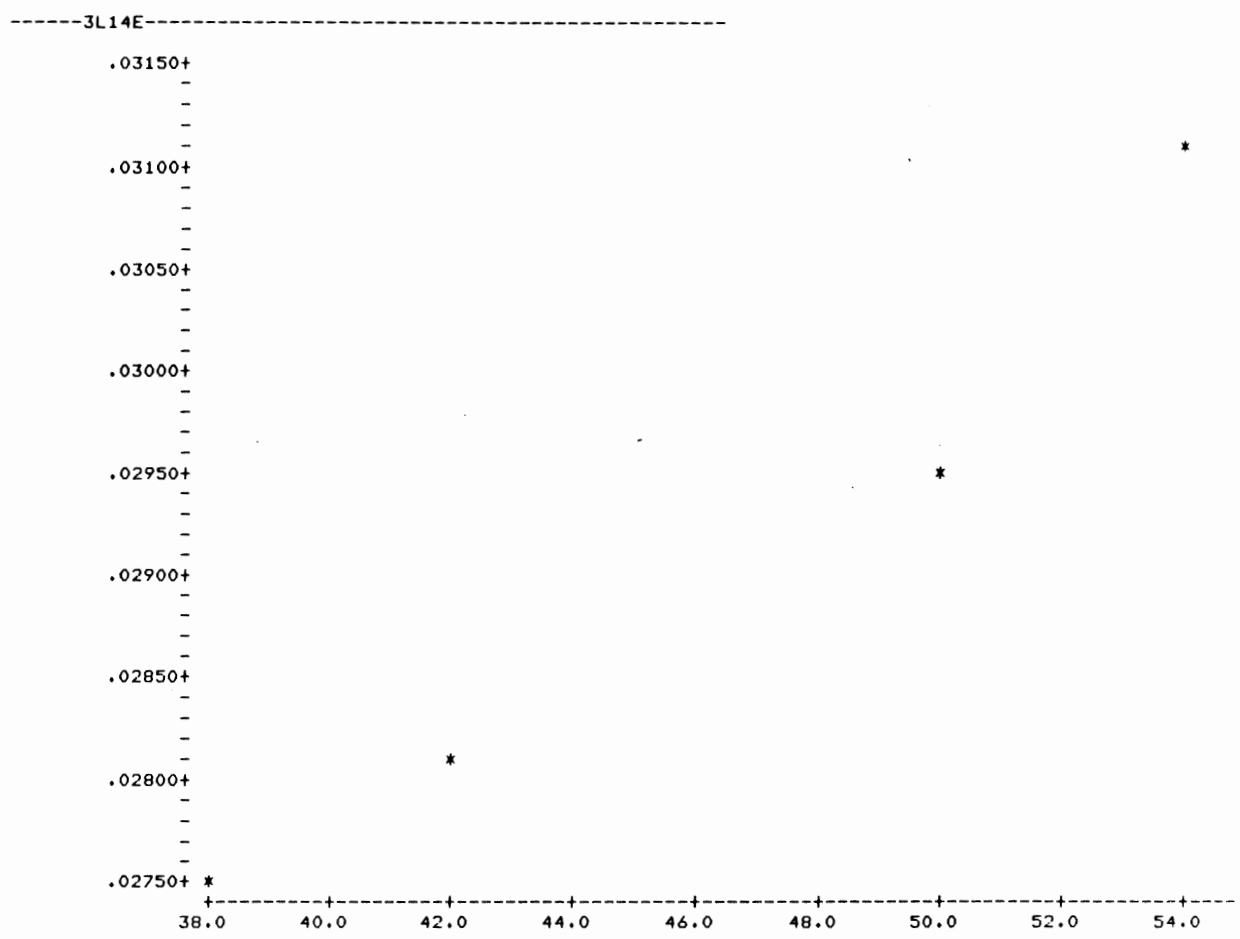
------3L14E----------
.03150+
.03100+
.03050+
.03000+
.02950+
.02900+
.02850+
.02800+
.02750+
38.0
40.0
42.0
44.0
46.0
48.0
50.0
52.0
54.0

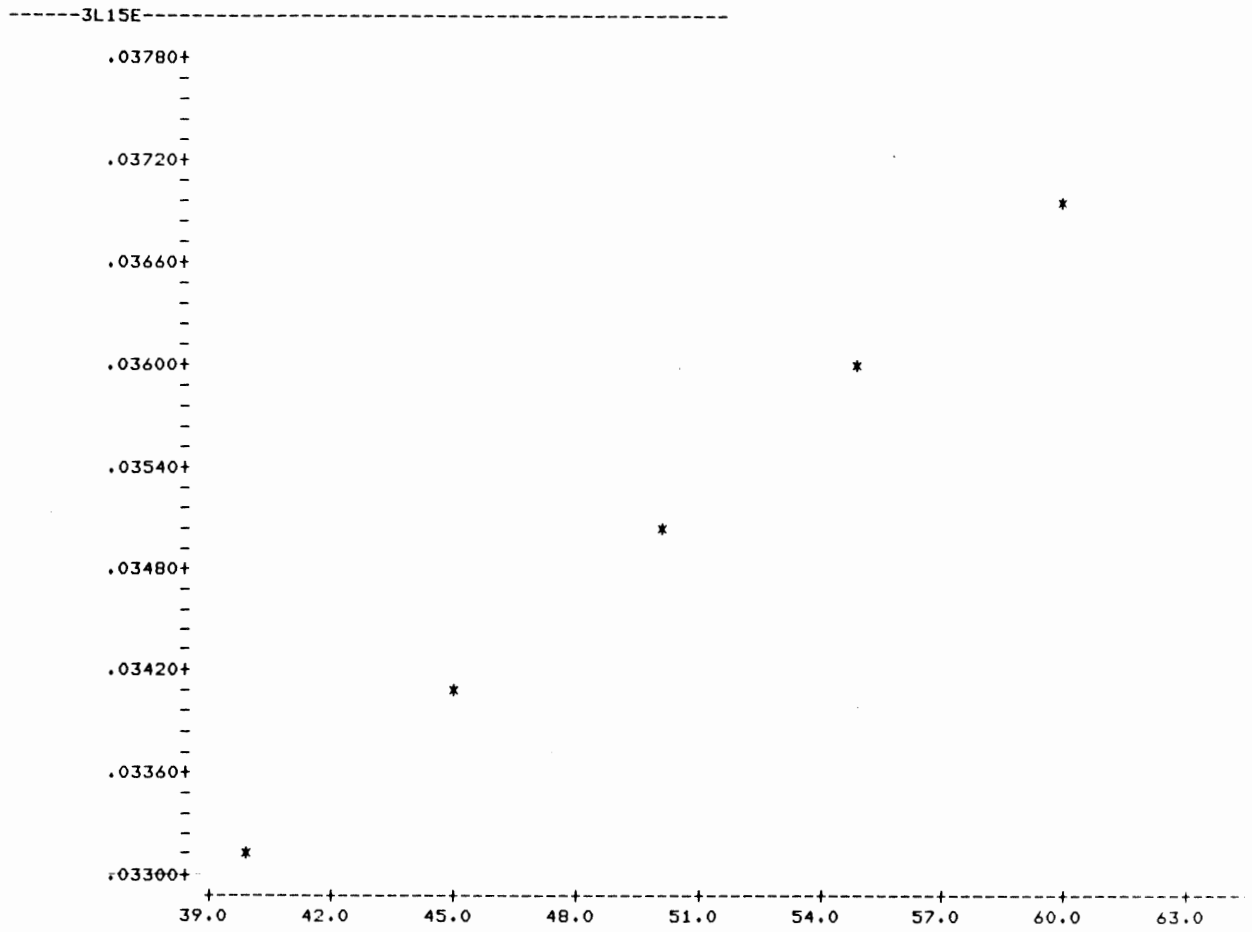
------3L15E----------
.03780+
.03720+
.03660+
.03600+
.03540+
.03480+
.03420+
.03360+
.03300+
39.0
42.0
45.0
48.0
51.0
54.0
57.0
60.0
63.0

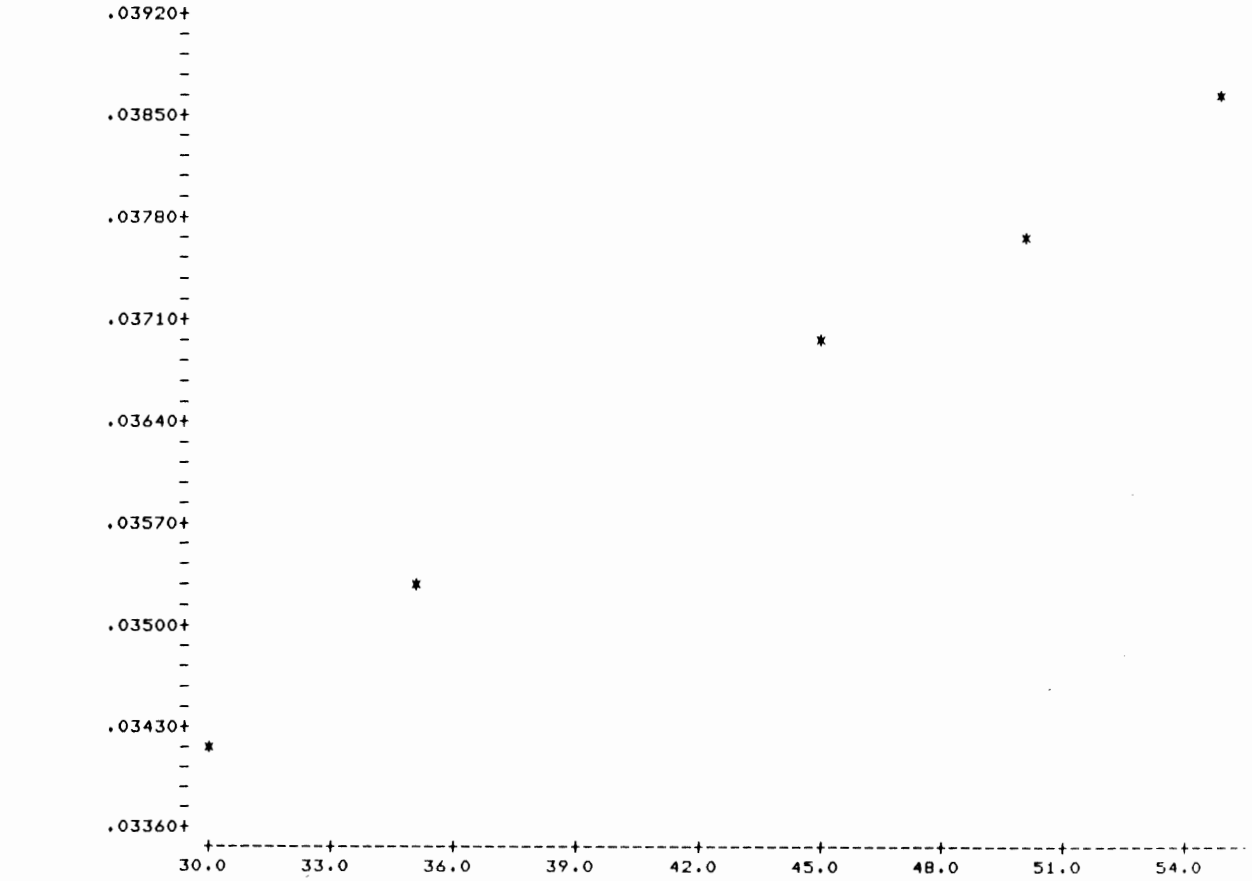
------3L15W----------
.03920+
.03850+
.03780+
.03710+
.03640+
.03570+
.03500+
.03430+
.03360+
30.0
33.0
36.0
39.0
42.0
45.0
48.0
51.0
54.0

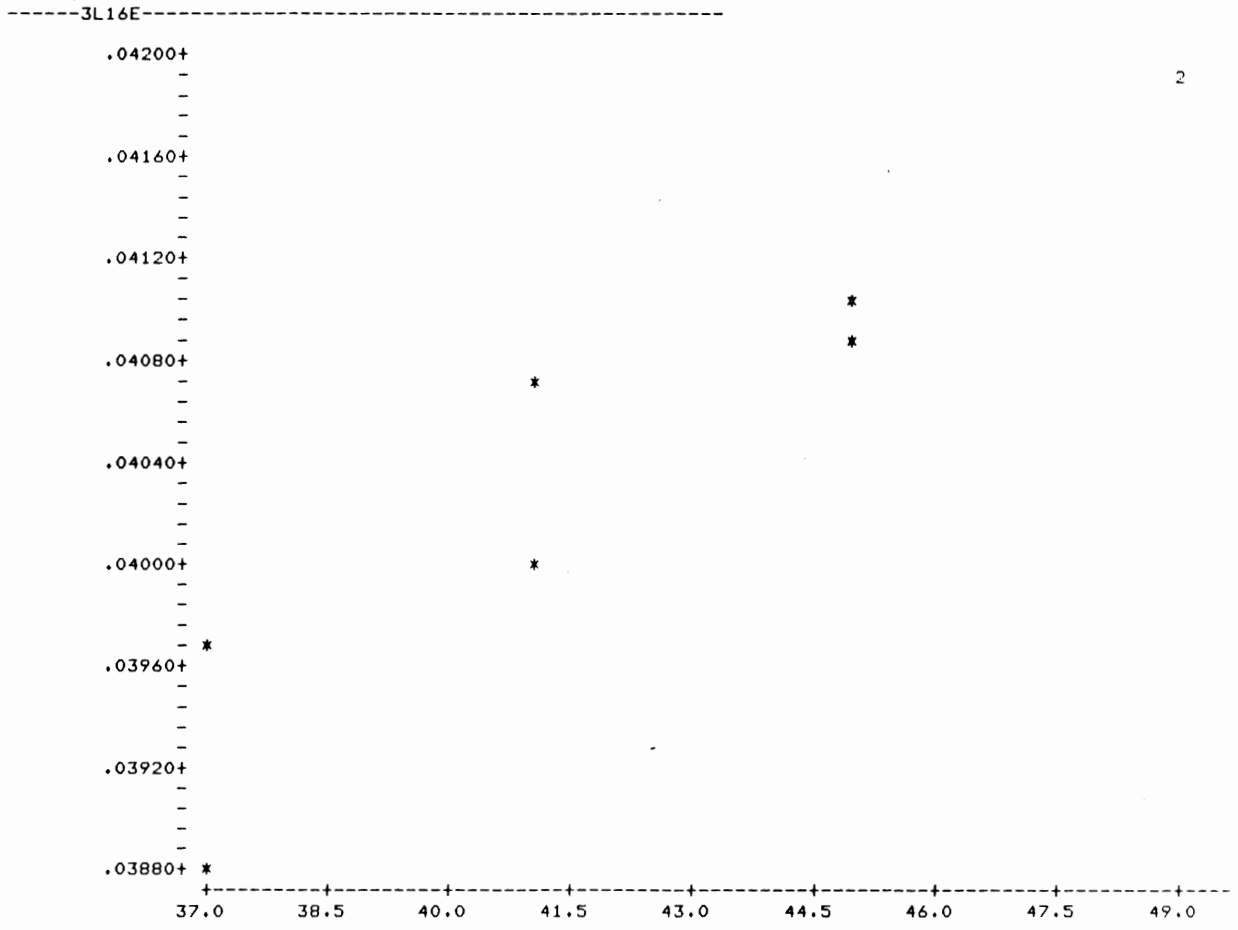
------3L16E----------
.04200+
.04160+
.04120+
.04080+
.04040+
.04000+
.03960+
.03920+
.03880+
37.0
38.5
40.0
41.5
43.0
44.5
46.0
47.5
49.0

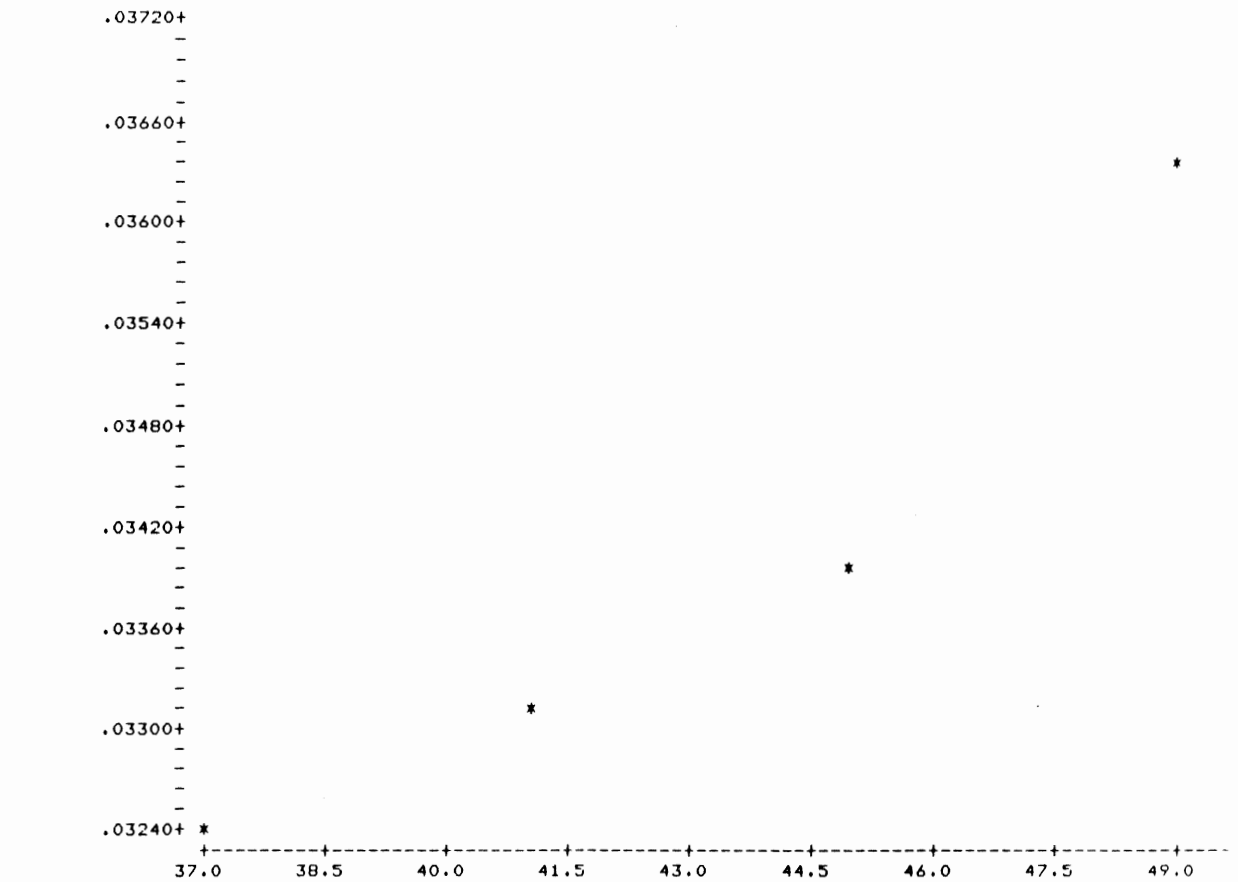
------3L16W----------
.03720+
.03660+
.03600+
.03540+
.03480+
.03420+
.03360+
.03300+
.03240+
37.0
38.5
40.0
41.5
43.0
44.5
46.0
47.5
49.0

APPENDIX 4

Program Listing

Purpose:
Used to calculate the true velocities, the dip of the interface, and the thickness of each layer.

Input:
Table 1.

Output:
Table 2.

Opperations:
-A line of data is read from table 2.
-The dip of the first interface is calculated and the true value for V_2 is determined.
-The thickness of layer ONE is calculated.
-The dip of the second interface is calculated and the true value for V_3 is determined.
-The thickness of layer TWO is calculated.
-The calculated values are output to tape2.
-The procedure is repeated.

```
      PROGRAM XPROGX(INPUT,OUTPUT,TAPE1,TAPE2)
      INTEGER STN,DIR
      REAL V2E,V2W,V2,V2U,V2D,D1,Z1E,Z1W,T2E,T2W
      REAL V3E,V3W,V3,V3U,V3D,D2,Z2E,Z2W,X,T3E,T3W
1     FORMAT (I2,1X,F5.0,1X,F5.0,1X,F5.0,1X,F5.0,1X,F6.5,1X
     ^,F6.5,1X,F6.5,1X,F6.5)
2     FORMAT (I2,1X,F5.0,1X,F5.0,1X,F4.1,1X,F4.1,1X,F4.1,1X
     ^,F4.1,1X,F4.1,1X,I1)
      V1=247.4
3     READ(1,1,END=4) STN,V2E,V2W,V3E,V3W,T2E,T2W,T3E,T3W
      IF(EOF(1).NE.0) GO TO 4
      IF (V2E.GT.V2W) THEN
      V2U=V2E
      V2D=V2W
      ELSE IF (V2E.LT.V2W) THEN
      V2U=V2W
      V2D=V2E
      END IF
      D1=(ASIN(V1/V2D)-ASIN(V1/V2U))/2
      V2=2*V2U*V2D*COS(D1)/(V2U+V2D)
      X=2*COS(ASIN(V1/V2))
      Z1E=T2E*V1/X
      Z1W=T2W*V1/X
      IF (V3E.GT.V3W) THEN
      V3U=V3E
      V3D=V3W
      DIR=2
      ELSE IF (V3E.LT.V3W) THEN
      V3U=V3W
      V3D=V3E
      DIR=1
      END IF
      D2=(ASIN(V2/V3D)-ASIN(V2/V3U))/2
      V3=2*V3U*V3D*COS(D2)/(V3U+V3D)
      Z2E=V2*(T3E-T2E*(COS(ASIN(V1/V3))/X))/2*COS(ASIN(V2/V3))
      Z2W=V2*(T3W-T2W*(COS(ASIN(V1/V3))/X))/2*COS(ASIN(V2/V3))
      WRITE(2,2) STN,V2,V3,Z1E,Z1W,Z2E,Z2W,D2,DIR
      GO TO 3
4     STOP
      END
```